LONG TERM PERFORMANCE MONITORING OF SHALLOW SLOPE STABILIZATION UTILIZING RECYCLED PLASTIC PINS

By

Cory Rauss

Presented to the Faculty of the Graduate School of

The University of Texas at Arlington in Partial Fulfillment

of the Requirements

for the Degree of

MASTER OF SCIENCE IN CIVIL ENGINEERING

THE UNIVERSITY OF TEXAS AT ARLIGNTON

May 2019

Acknowledgements

I want to first begin by giving thanks to my graduate supervisor, Dr. Sahadat Hossain, for giving me the opportunity to be a part of the SWIS group through both my undergraduate and graduate career. With his guidance and motivation, he encouraged me to excel in multiple facets of life, both academically and personally. With his support and the various opportunities he presented to me, I grew in terms of the work I produced, the way I observed problems, as well as how to communicate with a multitude of people.

Additionally, I want to express appreciation to Dr. Seyed Mohsen Shahandashti and Dr. Xinbao Yu for accepting to be on my examination committee.

To my slope site research team, notably Sachini Madanayake, Muhasina Dola, Prabesh Bhandari, Nur Basit Zaman, and Anuja Sapkota, I want to thank them for the multiple site visits and guidance in my thesis writing. To the rest of the members of the SWIS organization, I am thankful to have spent the time in my graduate career getting to know everyone better and share experiences in multiple site installations.

Lastly, I want to dedicate this accomplishment to my family and fiancé, Monica Araiza, for their unconditional support, love, encouragement, and advice through my graduate studies and throughout the thesis writing process. Their presence all along the way was a true blessing that I cannot repay.

Abstract

LONG TERM PERFORMANCE MONITORING OF SHALLOW SLOPE STABILIZATION UTILIZING RECYCLED PLASTIC PINS

Cory Rauss

The University of Texas at Arlington, 2019

Supervising Professor: MD Sahadat Hossain

Shallow slope failures are prevalent within the North Texas region. As highway slopes are underlain with high plastic clayey soils that experience cyclic shrinking and swelling, the soils shear strength generally decreases as the soil softens, making the soil more susceptible to sloughing and landslides. The Texas Department of Transportation (TxDOT) generally executes a rapid repair method as an economical option for repairing the slope. This method includes the failed soil removal, replacement, and recompaction to rectify the slope surface. While economical initially, this rapid repair technique may potentially prove to be costly with repeated repairs as the method does little to increase the soils shear strength. Recycled Plastic Pins (RPP), manufactured with recycled plastic and waste material, can potentially be utilized as a sustainable and cost effective alternative to stabilize surficial slope failures, in addition to alleviating the maintenance costs associated with continual repair.

The present study looks at the long-term performance of three slopes stabilized utilizing RPP. The three slopes are located at US-287 near the St. Paul overpass in Midlothian, the I-35 overpass at Mockingbird Lane, and SH-183 near the DFW airport. While previous studies have been conducted on the performance of RPP as a slope stabilization measure, the period of observation is limited. Additionally, both topographic surveys and inclinometer measurements

were performed to link both the vertical settlement and horizontal displacement. Based on the performance monitoring results, it was concluded that RPP provided adequate resistance against shallow slope failures. Moreover, near the location of each site during the monitoring period, several shallow slope failures were observed.

Table of Contents

ACKNOWLEDGEMENTS ..... **III**

ABSTRACT ..... **IV**

LIST OF ILLUSTRATIONS ..... **VIII**

LIST OF TABLES ..... **XI**

CHAPTER 1: INTRODUCTION **1**

1.1 BACKGROUND 1

1.2 PROBLEM STATEMENT 2

1.3 RESEARCH OBJECTIVES 3

1.4 THESIS ORGANIZATION 3

CHAPTER 2: LITERATURE REVIEW **5**

2.1 SLOPE FAILURE 5

2.2 SHALLOW SLOPE FAILURE 7

2.3 METHODS OF REPAIR FOR SURFICIAL SLOPE FAILURE 9

2.3.1 Rebuilding the Slope 10

2.3.2 Geogrid Repair 10

2.3.3 Soil Cement Repair 11

2.3.4 Earth Anchors 12

2.3.5 Stabilization Utilizing Geofoam 13

2.3.6 Launched Soil Nails 13

2.3.7 Micropiles 14

2.3.8 Plate Piles 14

2.3.9 Polypropylene (PP) Fibers 15

2.3.10 Retaining Wall 16

2.3.11 Soil Nail Wall 16

2.4 RECYCLED PLASTIC PINS 17

2.4.1 Manufacturing Process of RPP 18

2.4.2 Engineering Properties of RPP 19

2.4.3 Long Term Engineering Properties of RPP 22

2.4.4 Creep of RPP 26

CHAPTER 3: SITE INVESTIGATIONS **31**

3.1 PROJECT BACKGROUND (US-287) 31

3.1.1 GEOTECHNICAL BORINGS AND LABORATORY TESTING 32

3.1.2 RESISTIVITY IMAGING PROFILES 33

3.1.3 SLOPE STABILITY ANALYSES AND INSTALLATION OF RPP AT US-287 35

3.2 PROJECT BACKGROUND (I-35 AND MOCKINGBIRD SLOPE) 40

3.2.1 Geotechnical Borings and Laboratory Testing 41

3.2.2 Resistivity Imaging Profiles 44
3.2.3 Slope Stability Analysis and Installation of RPP at I-35 45
3.3 PROJECT BACKGROUND (SH-183) 47
3.3.2 Resistivity Imaging 50
3.3.3 Slope Stability Analysis and Installation of RPP at SH-183 52
CHAPTER 4: PERFORMANCE MONITORING RESULTS 54
4.1 PERFORMANCE MONITORING OF US-287 SLOPE 54
4.1.1 Topographic Survey 54
4.1.1.1 Control Section 1 57
4.1.2 Inclinometer 60
4.2 PERFORMANCE MONITORING OF I-35 SLOPE 64
4.2.1 Topographic Survey 64
4.2.2 Inclinometer 70
4.3 PERFORMANCE MONITORING OF SH-183 SLOPE 74
4.3.1 Topographic Survey 74
CHAPTER 5: COMPARISON OF SITE PERFORMANCE 76
5.1 COMPARISON OF US-287 SECTIONS 76
5.1.1 Cost Analysis of US-287 Sections 81
5.2 COMPARISON OF I-35 SECTIONS 84
5.2.1 Cost Analysis of I-35 Sections 87
5.3 COMPARISON BETWEEN US-287 AND I-35 SLOPES 89
5.4 COMPARISON OF SH-183 SECTIONS 93
5.4.1 Cost Analysis of SH-183 Section 95
5.5 COMPARISON BETWEEN US-287, I-35, AND SH-183 SLOPES 97
CHAPTER 6: CONCLUSIONS AND FUTURE RECOMMENDATIONS 101
6.1 SUMMARY AND CONCLUSION 101
6.2 RECOMMENDATION OF FUTURE RESEARCH 103
REFERENCES 105

List of Illustrations

Figure 2- 1 Clay Movement Types (Abramson et al., 2002).....6

Figure 2- 3 Geogrid Repair of Surficial Slope Failure (Day, R. W., 1996) 11

Figure 2- 4 Schematic of Soil Cement Repair (Day. R. W., 1996) 12

Figure 2- 5 Launched Soil Nail in Slope Stabilization (Titi and Helwany, 2007) 14

Figure 2- 6 Diagram of Plate Pile Stabilization (Short et al. 2005) 15

Figure 2- 7 Soil Nail Wall Construction (Source: HaywardBaker.com).....17

Figure 2- 8 Recycled Plastic Pin Slope Stabilization (Khan, 2013).....18

Figure 2- 9 Stress-Strain Response at different Loading Increments in Flexure for RPP.....21

Figure 2- 10 Flexural Variation of Stress-Strain with various Loading Rates (a) 0.5 kips/min (b) 2.7 kips/min (c) 4.9 kips/min (Ahmed, 2012) 22

Figure 2- 11 Compression modulus for both in-plane and cross-sectional dimensions for plastic lumber collected from West Meadow pier over a 24 month span (Breslin et al., 1998).....23

Figure 2- 12 Bending modulus for cross-sectional and in-plane directions for plastic lumber collected from West Meadow pier over a 24 month span (Breslin et al., 1998) 24

Figure 2- 13 RPP creep testing set up (Chen et al., 2007).....27

Figure 2- 14 Typical deflections under constant axial stress of RPP based on Batch B7 (Chen et al., 2007; Tamrakar, 2015) 28

Figure 2- 15 Method for estimating time to failure from the results of flexural creep (Chen et al., 2007).....30

Figure 3- 1 Location of US-287 Slope (Khan 2013) 31

Figure 3- 2 Shoulder cracks observed at crest of US 287 slope (Khan, 2013).....31

Figure 3- 3 Layout locations of RI lines and boreholes (Khan, 2013) 32

Figure 3- 4 Laboratory test results for US-287 samples, (a) Moisture variation with depth, (b) Plasticity Chart of soil borings (Khan, 2013; Tamrakar, 2015) 33

Figure 3- 5 Resistivity imaging (a) RI-1, (b) RI-2 at US 287 slope (Khan, 2013).....34

Figure 3- 6 Resistivity Imaging profile (a) Profile RI-1, (b) Profile RI-2 (Khan, 2013) 34

Figure 3- 7 RPP schematic at US-287 slope (Khan, 2013) 36

Figure 3- 8 Section view of slope stabilization on US-287 slope (a) Reinforced Section 1, (b) Reinforced Section 2, (c) Reinforced Section 3 (Khan, 2013).....38

Figure 3- 9 RPP installation plan for Control Section 1.....39

Figure 3- 10 Project location of I-35 slope....40
Figure 3- 11 Failure photos on shoulder of I-35 (Tamrakar, 2015) 40
Figure 3- 12 Failure condition schematic (a) Front elevation, (b) Cross-section 1-1 (Tamrakar, 2015)....41
Figure 3- 13 Location of Boring and Resistivity Imaging at I-35 (Tamrakar, 2015)....42
Figure 3- 14 Test results of I-35 (a) Moisture variation with depth, (b) Plasticity Chart of soil borings (Tamrakar, 2015)....44
Figure 3- 15 Resistivity Imaging profiles of I-35 slope (a) RI-1 and, (b) RI-2 (Tamrakar, 2015)45
Figure 3- 16 RPP reinforcement schematic at I-35 slope (Tamrakar, 2015)....46
Figure 3- 17 Location of the project for SH 183 slope....47
Figure 3- 18 Schematic of failure conditions on SH 183 slope (a) front elevation, (b) Section A-A (Tamrakar, 2015)....48
Figure 3- 19 Slope failure photos at SH-183 (Tamrakar, 2015)....48
Figure 3- 20 Test results of SH 183 (a) Moisture variation with depth, (b) Plasticity Chart of soil borings (Tamrakar, 2015)....50
Figure 3- 21 Resistivity Imaging line locations at SH-183 (Tamrakar, 2015)....51
Figure 3- 22 Resistivity Imaging Profiles of SH-183 (a) RI line 1, (b) RI line 2, (c) RI line 3 (Tamrakar 2015)....52
Figure 3- 23 RPP reinforcement schematic for SH-183 (Tamrakar, 2015)....53
Figure 4- 1 Settlement at the crest of US 287 55
Figure 4- 2 Layout of Inclinometer at US 287 slope (Tamrakar 2015)....60
Figure 4- 3 Displacement in Inclinometer I-1 at US 287 61
Figure 4- 4 Displacement in Inclinometer I-3 at US 287 62
Figure 4- 5 Comparison at 2.5 ft. depth of Inclinometers 1 and 3 63
Figure 4- 6 Settlement at the crest of I-35 Slope....64
Figure 4- 7 Gradual settlement experienced at the crest (a) August 2018, (b) September 2018 and (c) November 2018....66
Figure 4- 8 Settlement of shoulder in successive months (a) August 2018, (b) September 2018 and (c) November 2018....68
Figure 4- 9 Characteristics of crack on shoulder of I-35 (a) crack 2 ft. depth and (b) crack 1 ft. length....69

Figure 4- 10 Condition of slope on I-35 displaying (a) loss of contact between RPP, inclinometer and soil and (b) 1 ft. loss of contact soil on RPP 70

Figure 4- 11 Displacement in Inclinometer I-1 at I-35 71

Figure 4- 12 Condition of I-35 slope near Inclinometer 1 72

Figure 4- 13 Displacement in Inclinometer I-2 at I-35 73

Figure 4- 14 Displacement in Inclinometer I-3 at I-35 73

Figure 4- 15 Settlement at the crest of SH-183 slope 74

Figure 5- 1 Settlement along the crest of US-287 for Reinforced Section 1 (Distance along roadway from 0 ft. - 50 ft.) 77

Figure 5- 2 Settlement along the crest of US-287 for Reinforced Section 2 (Distance along roadway from 100 ft. – 150 ft.) 78

Figure 5- 3 Settlement along the crest of US-287 for Reinforced Section 3 (Distance along roadway from 200 ft. – 250 ft.) 79

Figure 5- 4 Incremental Settlement between Reinforced Sections of US-287 80

Figure 5- 5 Settlement at crest for I-35 slope Section S1 85

Figure 5- 6 Settlement at crest for I-35 slope Section S2 85

Figure 5- 7 Settlement at crest for I-35 slope Section S3 86

Figure 5- 8 I-35 Incremental Settlement 87

Figure 5- 9 Incremental Settlement of US-287 Slope Reinforced Sections 1, 2 and 3 and I-35 Slope 90

Figure 5- 10 Incremental Settlement Comparison of US-287 Reinforced Sections 1, 2 and 3 and I-35 Slope Reinforced Sections S1, S2, and S3 90

Figure 5- 11 Settlement at the Crest of SH-183 Slope (S1 Section) 94

Figure 5- 12 Settlement at the Crest of SH-183 Slope (S2 Section) 94

Figure 5- 13 SH-183 incremental settlement 95

Figure 5- 14 Comparison of Incremental Settlement between US-287, I-35 and SH-183 Reinforced Sections 98

Figure 5- 15 Precipitation data for Midlothian, Texas (US-287 Slope Site General Location) 98

Figure 5- 16 Precipitation data for Dallas/ Fort Worth Area, Texas (General Location of I-35 and SH-183) 99

List of Tables

Table 3- 1 Soil test results of I-35 (Tamrakar, 2015) 43

Table 3- 2 Test results of soil samples of SH-183 (Tamrakar, 2015) 49

Table 4- 1 Maximum total settlement on US-287 for reinforced sections and Control Section 2 56

Table 4- 2 Difference in maximum total settlement between 2012 and 2018 57

Table 4- 3 Maximum total settlement experienced at I-35 slope 65

Table 4- 4 Yearly precipitation for Dallas Area 69

Table 4- 5 Yearly incremental change in displacment Inclinometer I-1 71

Table 4- 6 Maximum total settlement for SH-183 slope 75

Table 5- 1 Incremental Settlement Values of Reinforced Sections of US-287 80

Table 5- 2 Total RPP and Cost per Reinforced Section 82

Table 5- 3 Average Driving Time of RPP at US-287 Slope (Khan, 2013) 82

Table 5- 4 Total Cost of Installment of RPP in each Reinforced Section 83

Table 5- 5 Cost per Square Foot of Reinforced for Three Slope Sections (US-287) 84

Table 5- 6 I-35 Incremental Settlement of Three Slope Sections 87

Table 5- 7 Total RPP and Material Cost for I-35 Slope 88

Table 5- 8 Total Cost of Installment of RPP in I-35 Slope 88

Table 5- 9 Comparison of Average Incremental Settlement between US-287 and I-35 Slope Sections 91

Table 5- 10: Cost per Square Foot of Reinforcement for Sections of US-287 and I-35 92

Table 5- 11 Cost per Square Foot of Reinforcement for Slopes US-287 and I-35 92

Table 5- 12 Total RPP and Material Cost for SH-183 Slope 96

Table 5- 13 Average RPP Driving Time (Tamrakar, 2015) 96

Table 5- 14 Total Cost of Installment of RPP in SH-183 Slope 97

Table 5- 15 Cost per Square Foot of Reinforcement for US-287, I-35 and SH-183 100

Chapter 1: Introduction

1.1 Background

The presence of high plastic clayey soil in highway embankments presents the possibility of routine maintenance work for various department of transportations (DOT). While highway fill slopes underlain by high plastic clayey soils display high factors of safety immediately after construction, with repeated wetting and drying, the factor of safety reduces. The reduction is caused by the behavior of the soil to shrink and swell in response to the seasonal climatic fluctuations. Over time, the soil tends to soften, reducing the effective shear strength of the soil and therefore reducing the factor of safety (McCormick and Short, 2006). Additionally, shrinkage cracks that develop on slopes act as a conduit for rainwater infiltration, providing a preferential flow path for the water into the slope. Due to the increase in hydrostatic pressure from the water saturating the surface of the slope, shallow slope failures can potentially occur (McCormick and Short, 2006; Khan et al., 2017). Despite not posing a direct threat to human life, shallow slope failures can cause damage in terms of guardrails, shoulders, drainage facilities, utility poles and even sections of the roadway (Titi and Helwany, 2007).

With the prevalence of expansive clayey soils in the North Texas region, along with the semi-arid climate, highway slopes are prone to shallow slope failures. These failures present the Texas Department of Transportation with a decision to make going forward on the means to remediate the slope. While the typical response to slope failures is recompacting the slope as part of routine maintenance work, it does not solve the problem of the slope instability and can potentially cost more in the long run than other stabilization measures. Typical slope stabilization methods include drilled shafts, geogrids, soil nails, retaining walls as well as the replacement of the poor soil. While the respective slope stabilization methods may work for a particular project,

they are generally more expensive and consume more resources when compared to a recent innovation in shallow slope failure stabilization utilizing recycled plastic pins (RPP) (Parra et al., 2003).

Primarily polymeric in composition, RPPs are comprised of recycled plastics with traces of additives such as fly ash and sawdust (Malcolm, 1995; Chen et al., 2007). In addition to the RPP's being lightweight, less susceptible to chemical and biological degradation, and resistant to moisture, the RPP's require little to no maintenance (Krishnaswamy and Francini, 2000). Installed to intercept the potential failure plane of the slope and add resistance for the long-term stability of the slope, RPP's provide a serious alternative as a slope stabilization method when considering environmental and life cycle cost analysis (LCCA) (Khan, 2014).

1.2 Problem Statement

In choosing the best stabilization measure for shallow slope failures, it is important to look at an economical and sustainable solution. The task of choosing a slope reinforcement method can be daunting as the location of the site as well as the experience of the engineer are gauged in the educated process. Previous studies have shown RPP to be beneficial after construction and continue to perform well after a short-term period of time, such as shown in Bowders and Loehr (2007), however, monitoring data beyond the short-term has not yet been presented.

- The present study looks at to evaluate the performance of RPP reinforcement on the long-term scale. Implemented in the field, the RPP are subjected to climatic conditions with repeated wetting and drying cycles that are prevalent in semi-arid regions.

Both the vertical settlement and horizontal displacement will be utilized for the performance of each of the three slopes investigated and a cost benefit analysis was conducted to determine the efficiency of the reinforced section in terms of economy. The study could contribute to various Department of Transportation (DOT) in their decision making process for surficial slope failures being a routine maintenance or stabilize the slope with RPP, which is economically, environmentally, and sustainably viable.

1.3 Research Objectives

The main objective of this study was to:

- Investigate the long-term performance and benefit of recycled plastic pins as a stabilization measure for highway embankment surficial slope failures.

In addition to this objective, the following tasks were additionally performed:

- Give a comparative analysis of performance between slopes of variable slope geometry's and slope reinforcement included in the study
- Conclude the overall performance of RPP and the effectiveness on the use of slope reinforcement long-term
- Compare the performance of the slope reinforcement scheme in terms of cost per square foot of reinforcement to establish an economic benefit to RPP as a reinforcement method.

1.4 Thesis Organization

The thesis is organized into five chapters that can be generalized below:

Chapter 1: Introductory section containing the background, problem statement, and the research objectives for the present study

Chapter 2: Literature review on different slope stabilization measures as well as the engineering properties of the recycled plastic pins.

Chapter 3: Background description, laboratory testing, and site layout of the three highway slopes that were investigated. The three highway slopes include US 287, I35, and SH 183.

Chapter 4: Analysis of the performance of the three slope sites stabilized with Recycled Plastic Pins. Analysis is performed on data collected from inclinometer data as well as topographic survey.

Chapter 5: Comparative analysis on the performance of the three investigated slope sites.

Chapter 6: Summarizes the conclusions drawn from the previous sections and gives insight into recommendations for future work and research.

Chapter 2: Literature Review

2.1 Slope Failure

Slope failures are common occurrences in regions where expansive soils are present. Generally, the slope failure occurs after a prolonged rainfall event, as the soil strength of the slope is reduced (Titi and Helwany, 2007). The failures that occur on slopes however, may or may not give signs of warning. Therefore the determination of a sufficient factor of safety for the design of the slope is a necessity.

Slope failures generally occur parallel to the slope. As described by Abramson et al. (2002), the slope instabilities are a result of the state of the slope changing from an unsaturated state to a saturated state after a prolonged rainfall event. When a heavy rainfall is experienced, the infiltration of the precipitation into the underlying soil has the potential to saturate the upper soil layers, if met with a soil that possesses a lower permeability. The lower permeability soil will act as a drainage barrier, allowing the water to perch, therefore potentially saturating the layers above while the lower permeability soil begins to expand due to the swelling behavior. As the soil changes from an unsaturated to saturated condition, the impact is observed in the pore water pressure the soil experiences. The pore water pressure changes from negative (soil suction) to positive. With the increase in positive pore water pressure in the soil, a decrease in effective stress on the potential plane occurs, subsequently decreasing the slopes soil strength. Pradel and Raad (1993) found that the intensity of the rainfall must be sufficient to exceed the infiltration rate that the soil possesses in order to saturate the slope. Once the resisting forces are decreased past the driving forces, therefore the slope is no longer in a state of equilibrium, the slope will fail with a constant total stress and an increase in pore water pressure (Abramson et al. 2002)

As the stability of the slope is governed by the balance between the driving and resisting forces, warning signs of slope failure may or may not occur, as previously stated. According to Titi and Helwany (2007), the movement of the soil as well as the depth of the failure slip surface is dependent on factors such as the type of soil, soil stratification, the slopes geometry, as well as the presence of water. Abramson et al. (2002) described the various slides that are typical in clayey soils, such as (1) translational, (2) plane or wedge surface, (3) circular, (4) noncircular, and (5) a combination of those previously described. Presented in Figure 2-1 are the illustrations of the typical types of slope failure.

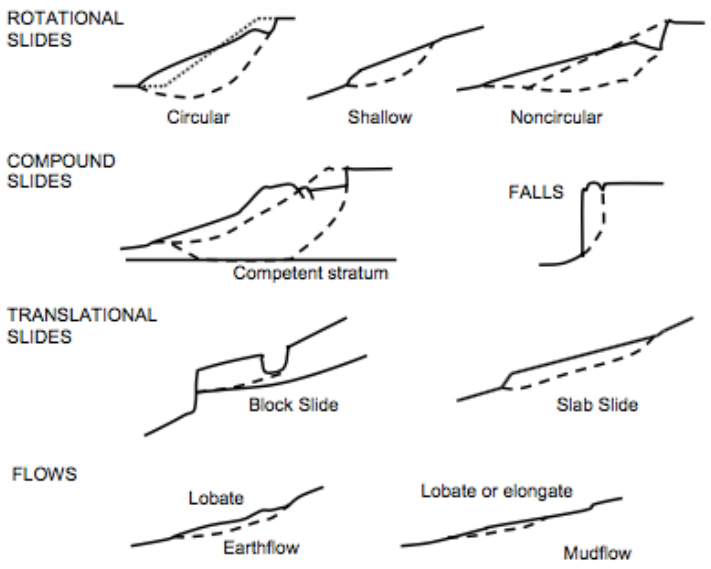

Figure 2- 1 Clay movement types (Abramson et al., 2002)

Slope designs experience various uncertainties in the pursuit of stability. Uncertainties in such a design include the determination of soil strength, distribution of pore pressures, and the soil stratification. Such factors influence the selection of a rational factor of safety that is required for the slope. Moreover, minimal engineering experience along with low quality site investigation of the subsurface condition call for a higher factor of safety for slope construction (Abramson et al., 2002).

The factor of safety that is necessary to maintain a just-stable slope is calculated by the comparison of available shear strength along a potential sliding surface with the equilibrium shear stress. Along the potential slip surface, the factor of safety is considered constant and can be characterized in terms of stresses (total and effective), forces, and moments. Several factors, such as accuracy and extent of the soil data, experience of the designing engineer, level of construction monitoring, and the potential risk level of the associated slope, are influential in the selection of the factor of safety that will be utilized in the slope design (Titi and Helwany, 2007). For a typical design of a slope, the factor of safety required will generally fall between 1.25 and 1.5 (Abramson et al. 2002).

2.2 Shallow Slope Failure

Surficial slope failures can occur anywhere in the world, however, attract additional attention in the world that possess semi-arid climates. This, in part, is due to the upper layers of soil generally drying out during the warmer years, followed by a year in which heavy rainfall occurs, saturating the supper layers and causing a number of surficial slope failures (Lade, 2010). Throughout the United States surficial failures are common. According to Titi and Helwany (2007), shallow slope failures is generally associated with surficial slope instabilities along highway cut and fill slopes, as well as highway embankments. Various literatures define shallow slope failures in terms of depth. While some observe that shallow slope failures typically occur at a depth of or less than 4 ft., others classify the failure as a depth less than 10 ft. (Evans, 1972; Day, R. W., 1989; Loehr et al., 2000).

While there are no serious implications on the well being of human life, surficial slope failures can affect surrounding infrastructures. Such infrastructures include damaging guardrails, highway shoulders, road surface, drainage facilities, and others. Additionally, if the debris flow

were to reach the highway, it could have an impact on the flow of traffic. According to Titi and Helwany (2007), the size of the failure zone affected by the shallow slope failure can be attributed to factors such as the geometry of the slope, the soil type, the degree of saturation, and seepage. In addition, the depth of the failure can be attributed to the type of soil, the slope geometry, and climatic conditions. With the repairs of the slope generally being performed by district and local levels of Department of Transportations as routine maintenance work, more often than not, the temporary repairing of the slope failures will occur again after a year or two with a prolonged rainfall.

In the semi-arid region of North Texas, the expansive soil experiences shrinking and swelling behavior. The level of shrinkage that can be experienced by the soil is dependent upon factors such as temperature and humidity, the plat root systems moisture extraction, along with the overall plasticity of the clay itself (Day and Axten, 1989). As part of the process of shrinkage and drying, the presence of desiccation cracking can appear due to the decrease level of liquid pressure in the soil and an increase in the level of suction caused by evaporation (Peron et al. 2009). With the presence of desiccation cracks, preceded by heavy rainfalls, the cracks can act as preferential conduits for the water to further infiltrate the slope. If the soil infiltration rate is less than that of the rainfall intensity experienced, the buildup of excess pore water pressure as previously described can lead to saturation at a particular depth and lead to its eventual failure (Abramson et al., 2002). Figure 2-2 displays the failure surface of a slope failure after heavy and prolonged rainfall in September and October 2018.

Figure 2- 2 Slope Failure off I-20 east bound near Clark Rd.

2.3 Methods of Repair for Surficial Slope Failure

Several slope stabilization methods for repair of surficial slope failures exist. When choosing a method for implementation, certain considerations for the selection process must be evaluated. The availability of construction equipment, experienced contractors, site accessibility, steepness of the slope to be repaired, time restrictions and the availability of funds for the project are all influential factors for analysis of which stabilization technique will suffice. An economical solution commonly employed by department of transportations for shallow slope repair is rebuilding the slope. While cost effective initially, the shear strength of the soil is not significantly altered, therefore, the slope could potentially fail after another prolonged rainfall event (Day, R. W., 1997).

Many additional stabilization techniques involve the reshaping of the slopes surface by benching the slope, or flattening the steepness of the slope. Recorded below are various surficial slope repair methods that can be utilized during the design phase.

2.3.1 Rebuilding the Slope

Rebuilding the slope consists simply of taking the soil that was part of the surficial failure and using it again to backfill the failed area. For this method, the soil that will be utilized again is often air dried and recompacted to specification within the failure area (Day, R. W., 1997). Performed as routine maintenance work for failed slopes throughout the country, the rebuilding of slopes is an economical quick fix solution. However, with clayey soils, it is typically an inefficient solution for the failure area due to the general behavior of clay. As rainfall infiltrates the soil, the clay will swell, meaning that the benefit of recompaction that was performed on the soil previously is lost. Additionally, the soils shear strength is not significantly increased by the recompaction leading to the possibility of repeated failures with time (Titi and Helwany, 2007).

2.3.2 Geogrid Repair

Geogrids are fabricated from high-density polyethylene resins, and are designed to improve the slope by increasing the shear strength of the soil. The open structure of the geogrids allow for the interlocking of granular materials to improve the stability of the soil. Day, R. W., (1996) investigated the use of geogrids as a potential surficial slope repair technique. As part of the installation, it was recommended that the failed soil from the surficial failure zone be disposed of completely rather than reused. Once excavated, benches would be cut into the undisturbed soil as to provide frictional contact between the fill mass and the horizontal cut of the bench. After excavation of the bench, in order to dispose of water infiltration off-site, vertical and horizontal drains are constructed and implemented. Lastly, the slope is reconstructed utilizing layers of geogrids and compacted granular material. Often, additional geosynthetics can be used for erosion control on the slope face and the slope can be replanted to allow for the

development of root structures. The general schematic for the implementation of geogrids is displayed in Figure 2-3.

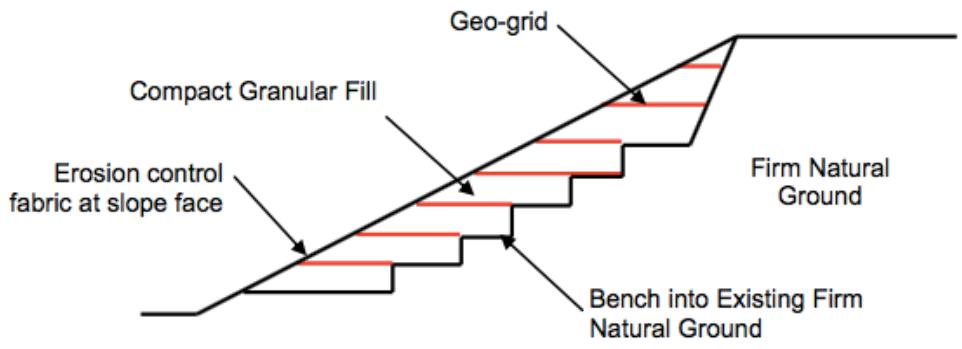

Figure 2- 3 Geogrid repair of surficial slope failure (Day, R. W., 1996)

2.3.3 Soil Cement Repair

Compacted soil-cement fill has been utilized previously in several infrastructure projects to meet certain engineering needs such as improvement of unsuitable subgrades or modifying the properties of soft soils (Bergado et al. 1996; PCA 2016). Similar to the repair technique for geogrids, the failed soil is excavated and removed off site for the benching into the existing soil on the slope. After implementation of drains, rather than placing the geogrid with the granular soil on the constructed bench's, the granular imported soil is mixed, typically, with 6% cement and compacted to a minimum of 90% of the laboratory tested maximum dry density (modified proctor) (Day, R. W., 1996). While the repair's use of cement in the soil mixture can increase the shear strength of the granular soil, preventing future surficial failures, if not properly mixed in the construction phase, uncemented zones can appear, potentially leading to erosion and slope failure. Displayed in Figure 2-4 is the schematic of the repair method for soil cement.

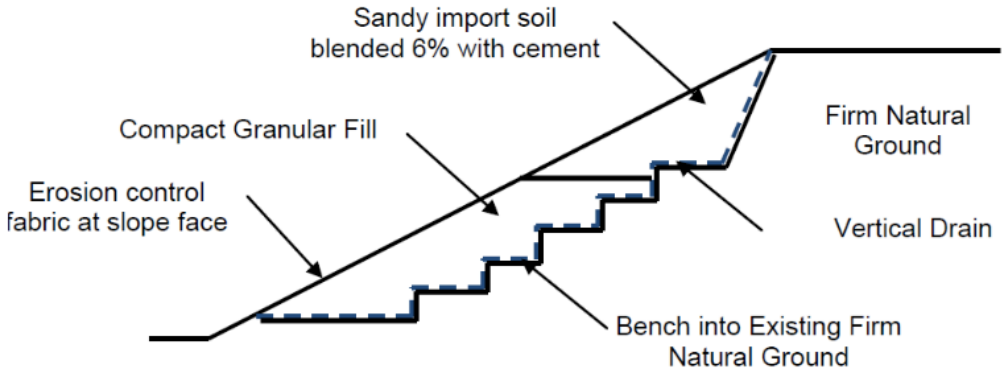

Figure 2- 4 Schematic of Soil Cement repair (Day. R. W., 1996)

2.3.4 Earth Anchors

Earth anchoring systems are comprised of three main components consisting of mechanical earth anchors, wire rope/rod, and an end plate. The construction practice for implementing earth anchors begins with the grading of the failed slope using either the failed soil or imported granular fill. After grading, the slope is seeded and erosion control fabric is placed on the slope face. The earth anchors are then installed by pushing the anchors below the depth of the failure area (Titi and Helwany, 2007). The wire tendons of the anchors are then pulled into place so that the anchors are in its full working position. The wire tendons are then locked against the end plate for the system to be tightened.

It is important that the quality of the design and the construction process is adequately carried out for proper slope stabilization. In addition, periodical inspections and routine maintenance should be performed to ensure quality control on the earth anchor system. According to Jeng and Chen (2013), general problems that affect the performance of earth anchors are failure of the anchor head and the integrity of the systems components, especially the tendon wires against corrosion.

2.3.5 Stabilization Utilizing Geofoam

With the multitude of difficult sub soil conditions that are prevalent around the world, geofoam is a geotechnical application that is often used. Formed with low-density cellular plastic solids, geofoams are lightweight, chemically stable, and environmentally safe. In addition, geofoam has mechanical and thermal properties that are favorable in design such as its compressive strength and thermal insulation characteristics (BASF, 2006). The typical unit weight range for goefoam ranged between 0.7 to 1.8 pcf and possessed a compressive strength between 13 to 18 psi. Along with its lightweight design, geofoam is chemically inactive with the presence of soil or water and inherently non-biodegradable (Horvath, 1994).

2.3.6 Launched Soil Nails

Soil nails, either hollowed or solid, are shot into the face of the slope at high speeds with the use of high-pressure compressed air. The launched soil nails should penetrate through the soil beyond the failure surface as to utilize the bond between the soil-nail (tensile resistance of nails) and the shear resistance of the launched nail against the driving forces of the slope (Titi and Helwany, 2007). Installed in a staggered pattern, the schematic of the use of soil nails is presented in Figure 2-5. The typical dimensions for hollow steel bar soil nails include a length of 20 feet, an outer diameter of 1.5 inch, and recommended minimum yield strength of the bar to be 36 ksi according to Titi and Helwany (2007). After installation of the soil nails, it is typical to treat the slope surface with an erosion mat, steel mesh, or shotcrete. The effectiveness of the soil nail, however, can be attributed to achieving the proper penetration length of the nail. With the soil type and the compressed air pressure governing the depth of the nail penetration depth, it can sometimes be difficult to control.

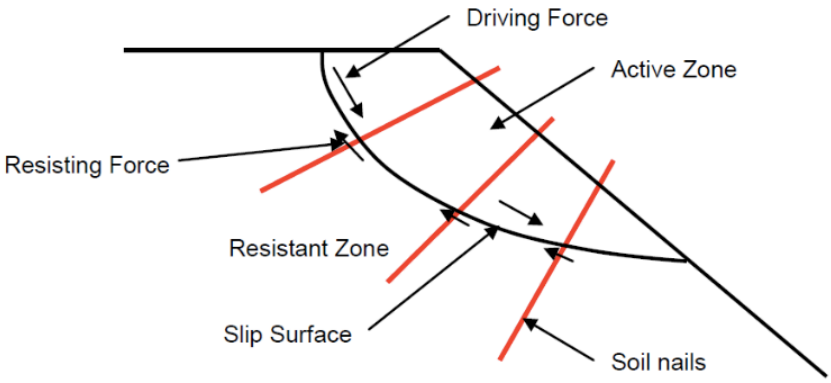

Figure 2- 5 Launched Soil Nail in slope stabilization (Titi and Helwany, 2007)

2.3.7 Micropiles

More commonly used for foundation, micropiles (also known as pin piles or mini piles) may also offer potential utilization in the stabilization of slopes (Taquino and Pearlman, 1999). Micropiles, as defined by Bruce and Juran (1997), are small diameter (often less than 300 mm), drilled and grouted piles that are generally reinforced. Micropiles are constructed by drilling a borehole, placing reinforcement, and using grout to fill the hole (Sun et al., 2013). The benefits of the use of micropiles for slope stabilization are for areas with limited equipment access. Landslides that have occurred on hilly, steep, or mountainous areas can benefit in the use of micropile application.

2.3.8 Plate Piles

A study conducted in California by Short et al., (2005) investigated the use of plate piles as a slope stabilization measure. The use of plate piles in slope stabilization increases the slopes resistance to sliding by the application of the vertical members to resist shear stresses. Generally having a length of 6 – 6.5 feet long, the plate piles have a 2.5 inch x 2.5 inch galvanized steel angle section with a 2 ft. x 1 ft. rectangular steel plate welded to one end (Short et al., 2005). The plate plies are driven into the potential slide area, typically a depth of 2 to 3 feet of the residual

soil, over a stiffer soil or bedrock. Figure 2-6 displays the installment of plate piles. The plate transfers the load to the stiffer soil, reducing the driving forces on the upper soil mass.

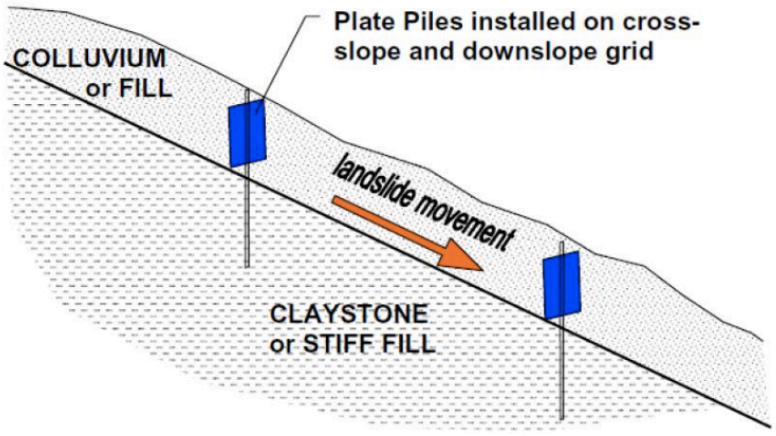

Figure 2- 6 Diagram of Plate Pile stabilization (Short et al. 2005)

2.3.9 Polypropylene (PP) Fibers

Widely used in the laboratory for soil reinforcement, PP fibers currently are utilized in the enhancement of soil strength properties, reduction in shrinkage properties, and overcoming chemical and biological degradation (Musenda, C., 1999, Puppala and Musenda.,2000). Conducted by Puppala and Musenda (2000), PP fibers increased the unconfined compressive strength of the soil while reducing the volumetric shrinkage strains and swell pressures of the tested expansive clays.

While advantages were seen in lab scale studies, there is a lack of scientific standards for field projects. Additionally, if not properly spread during construction, the fibers could clump together, meaning that the soil unreinforced would not experience a significant change. The PP fibers have also not seen any results in slope stabilization.

2.3.10 Retaining Wall

Utilized when retaining material at a steep angle and/or a limitation in space (right of way), retaining walls can be used. Retaining walls are low retaining structures constructed at the toe of the slope to make possible grading the slope to a stable angle without loss of land at the crest (USDA 1992). According to Gray and Sotir (1996), the retaining wall can also protect the toe of the slope against scouring as well as prevent undermining of the cut slope. The retaining structure is capable of being built externally of the slope (concrete or masonry wall), or utilize reinforced soil (Fay et al, 2012). In addition to retaining structures being able to stabilize shallow slope instabilities, larger failures, such as deep-seated failures, can also be stabilized.

2.3.11 Soil Nail Wall

Soil nailing has frequently been discussed as a slope stabilization method (Abramson et al. 1996). The earth retention system is comprised of three main components. (1) The reinforced mass of soil with nails, (2) the structural facing, and (3) the unreinforced soil behind the wall (Turner and Jensen, 2005). The nails are generally spaced closely, either one grouted nail per 10 to 55 ft^2 (1 to 5 m^2) of the facing or one driven nail per 2.7 ft^2 (0.25 m^2). The facing of the wall is generally 4 to 8 inches thick shotcrete with wire mesh for reinforcement (Turner and Jensen, 2005).

The walls are generally constructed downwards under normal circumstances. Over the exposed soil cut, a drainage system is installed in order to collect and release the accumulation of groundwater behind the wall. The steel bars inside the ground are restrained by steel plates and nuts, thereby providing a passive resistance (Hayward Baker, 2013). Figure 2-7 displays construction of a soil nail wall.

Figure 2- 7 Soil Nail wall construction (Source: HaywardBaker.com)

2.4 Recycled Plastic Pins

Recycled plastic pins (RPP), also commercially known as recycled plastic lumber, are a post-consumer waste plastic manufactured for the acceptable use in the construction of docks, piers and bulkheads (Khan, 2013). The recycled plastic pins are also marketed as being an environmentally preferable material based on environmental and life cycle cost analyses (Khan, 2013). Resistant to moisture, corrosion, rotting, insects and requires no maintenance, it is under serious consideration as a structural material for marine and waterfront application. In addition to the material properties listed previously, being comprised of post-consumer recycled materials helps in the reduction of plastics disposed in landfills. The composition of the RPP generally consists of 50% or more of polyolefin in terms of high-density polyethylene (HDPE), low-density polyethylene (LDPE), as well as polypropylene (Khan, 2013). It is the polyolefin that acts as an adhesive in the manufacturing process to combine high melt plastics and additives such fiberglass, wood fibers within a rigid structure. The general schematic in the slope stabilization scheme utilizing RPP is depicted in Figure 2-8.

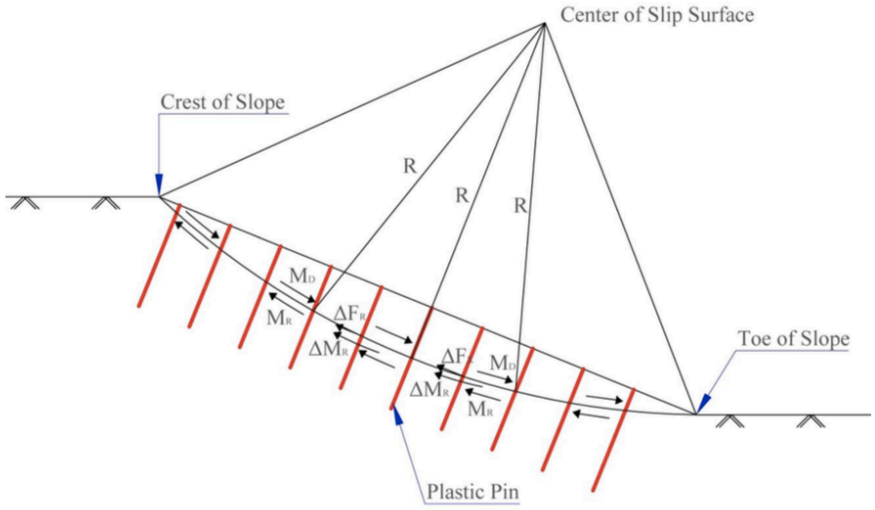

Figure 2- 8 Recycled Plastic Pin slope stabilization (Khan, 2013)

2.4.1 Manufacturing Process of RPP

To manufacture plastic lumber, raw materials are collected, cleaned, and pulverized. The resulting confetti of plastic is taken to the production site for melting in an extrusion machine. According to Bowders et al., (2003), two common practices are used for creating the plastic lumber are compression molding and extrusion forming. In the compression molding practice, the waste stream is pulverized, blended together, heated till the material is partially melted, and then compress in a mold of specific shape and dimension. For extrusion forming, the steps are moderately similar, rather than compressed into a mold, the melt is forced through a die of desired cross section (Bowders et al., 2003). The benefit of the extrusion process is the ability to manufacture different lengths without having to change molds. It can be also noted that the continuous extrusion process requires a considerable investment in comparison to the molding process (Khan, 2013).

2.4.2 Engineering Properties of RPP

As described previously, the use of the stabilization method is to drive the RPP's past the failure surface and "pin" the slope. In order for the RPP's to be efficient in its design, engineering properties such as compressive, tensile, and flexural strength must be adequate as they will dictate the design and construction practice. Bowders et al., (2003) investigated the engineering properties of RPP on the stabilization of slopes. Included in the study are the results attributed to Uni-axial compression tests and four point flexure test performed on members from three different manufactures to see the variance in results. The results of the two performed tests are provided in Table 2-1 and Table 2-2 below.

Table 2- 1 Results of uniaxial compression tests (Bowders et al., 2003)

Specimen Batch	No. of Specimen tested	Nom. Strain Rate (%/min)	Uniaxial Compressive Strength (ksi)		Young's Modulus, $E_{1\%}$ (ksi)		Young's Modulus $E_{5\%}$ (ksi)	
			Avg.	Std. Dev.	Avg.	Std. Dev.	Avg.	Std. Dev.
A1	10	-	2.76	0.13	133.7	7.7	56.6	3.9
A2	7	0.005	2.9	0.12	186.4	10	54.8	2.2
A3	6	0.006	2.9	0.13	176.9	15.7	52.6	3.9
A4	3	0.004	2.9	0.13	199.7	23.9	52.6	3.6
A5	4	0.006	1.74	0.15	93.5	23.1	32.6	2.5
A6	4	0.006	1.89	0.13	114	15.4	34.5	4.9
B7	2	0.007	2.03	0.07	78.5	5.2	38.9	0.4
B8	2	0.006	2.32	0.06	93.3	0.1	44.7	0.1
C9	3	0.0085	2.47	0.16	77.3	12.2	56.1	5.8

Table 2- 2 Four-point bending test results (Bowders et al., 2003)

Specimen Batch	No. of Specimens Tested	Nom. Def. Rate (in/min)	Flexural Strength	Secant Flexural Modulus $E_{1\%}$ (ksi)	Secant Flexural Modulus $E_{5\%}$ (ksi)
A1	13	-	1.6	113	96
A4	3	0.168	2.6	201.3	-
A5	3	0.226	1.6	103.1	73.1
A6	4	0.143	1.5	92	64.3
B7	1	0.159	1.3	78.9	61.6
B8	1	0.223	-	118.4	-
C9	2	0.126	1.7	100.2	80.2

Ahmed (2012) investigated the response of RPP, wood, and bamboo under flexure. Performed utilizing the three-point bending test, the test specimen for the RPP was 68 in. in length. Presented in Tables 2-3 is the loading rates for the flexural test, along with the number of samples that were conducted in the study.

Table 2- 3 Flexural loading rates and number of samples (Ahmed, 2012)

Loading Rate (kips/min)	Recycled Plastic Pin	Bamboo	Wood	Total
0.5	3	3	3	9
2.7	3	3	3	9
4.9	3	3	3	9

Based to the three-point bending test of the RPP, it was observed that a similar trend had developed in the three different loadings in the elastic region. Moreover, it was observed that though the peak strength of the RPP saw an inversely proportional relationship with loading increment (lower loading witnessed a higher peak strength), the modulus of elasticity remained relatively constant for the three loading increments. Figure 2-9 presents the observed stress-strain relationship for RPP.

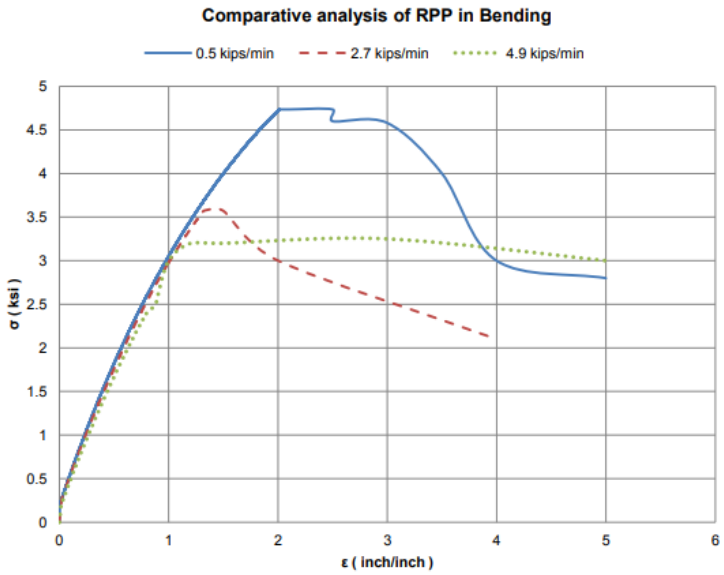

Figure 2- 9 Stress-strain response at different loading increments in flexure for RPP (Ahmed, 2012)

Based on the three-point bending test for the different test specimens, the failure strain for RPP was measured around 1-2%, whereas the failure strain of both wood and bamboo was approximately 0.5%. Therefore, in flexure, it was observed that RPP exhibited a more elastic behavior in comparison to bamboo and wood. The results of the three testing materials under flexure are presented in Figure 2-10 (a) through (c).

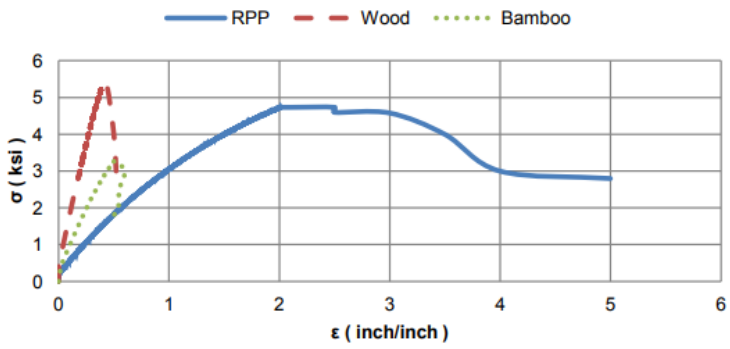

(a)

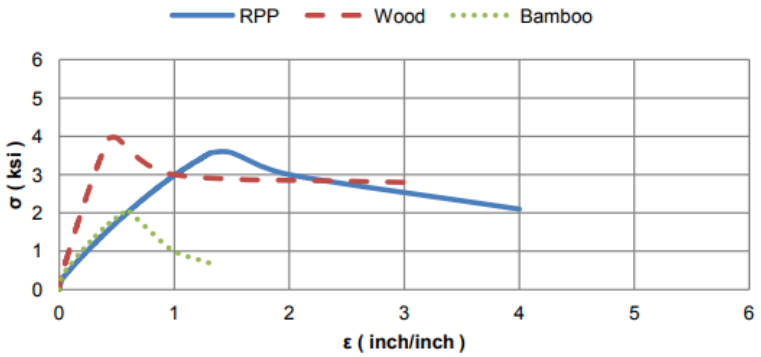

(b)

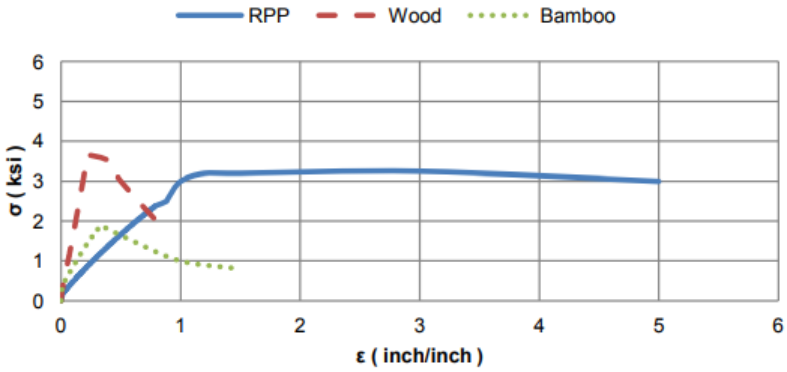

(c)

Figure 2- 10 Flexural variation of stress-strain with various loading rates (a) 0.5 kips/min (b) 2.7 kips/min (c) 4.9 kips/min (Ahmed, 2012)

2.4.3 Long Term Engineering Properties of RPP

Breslin et al., (1998) investigated the long term engineering properties of recycled plastic lumber. As part of the study, plastic lumber samples were removed from the deck of a pier periodically over a two-year span and tested in the laboratory. The tests that were performed on the plastic lumber included Shore D hardness, compression modulus, and modulus of elasticity. The recycled plastic lumber that was tested were produced using a continuous extrusion process and were not under severe traffic loading. The lumber was subjected to two summer cycles, where the highest temperatures and UV intensities occurred. Breslin et al., (1998) did not observe any noticeable change in the plastic lumber such as warping, discoloration, or cracking.

Testing the compression modulus, 3.3 cm diameter cylinders with a thickness of 3.3 cm. samples were taken from the plastic lumber. Taking measurements in both the in-plane axis and cross-sectional axis, Figure 2-11 presents the results of the study.

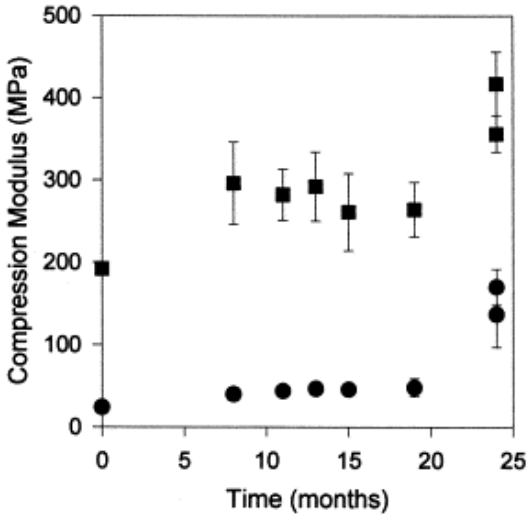

Figure 2- 11 Compression modulus for both in-plane and cross-sectional dimensions for plastic lumber collected from West Meadow pier over a 24-month span (Breslin et al., 1998)

From the results, the in-plane compression modulus (192 MPa) was approximately six to eight times greater, on average, than the measured compression modulus (24 MPa) in the cross-sectional axis. Significant increases in the compression modulus for both the in plane (417 MPa) and cross-sectional (170 MPa) axes samples were witnessed after 24 months. While the samples compression modulus remained relatively constant, even after a 19 month period, the change after the 24 month period may be attributed to variability in the material properties of the lumber profiles.

Breslin et al. (1998) additionally presented a study on the modulus of elasticity based on the various compositions of plastic lumber. Similar to the compression modulus, the test was performed on the in plane direction as well as the cross-sectional direction. From the data collected in the study, the modulus of elasticity variations are presented in Figure 2-12.

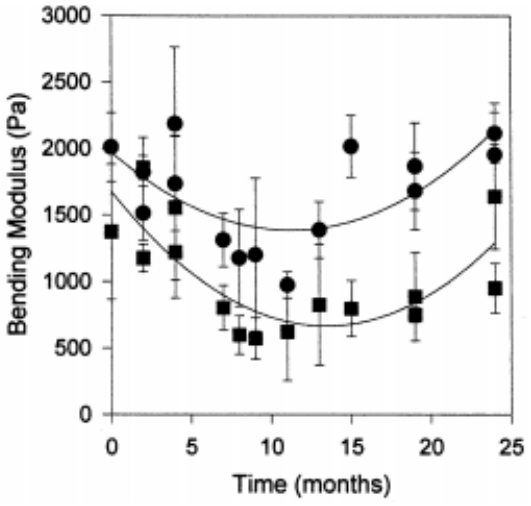

Figure 2- 12 Bending modulus for cross-sectional and in-plane directions for plastic lumber collected from West Meadow pier over a 24-month span (Breslin et al., 1998)

Based on the testing results, it was observed that initial bending modulus was higher in the cross-sectional direction in comparison to the in-plane direction. Over time, the bending modulus taken from the in-plane direction continuously decreased. The bending modulus taken from the cross-sectional direction showed no significant differences over time for the span of 0 to 19 months. While the bending modulus either decreased or remained generally constant, after testing for 24 months, both the in-plane and cross-sectional directions experienced significant increases. From the data, no clear trend could be made however it was reasoned that the variation in measurements could be attributed to heterogeneity of the material, rather than changes in the initial properties of the plastic lumber due to weathering (Khan, 2013).

In addition to the research conducted by Breslin et al. (1998), the weathering effects on the mechanical behavior of recycled HDPE based plastic lumber was investigated by Lynch et al. (2001). The plastic lumber that was investigated was part of a deck built at Rutgers University that had experienced eleven years of continuous exposure to the environment before being removed and replaced. The flexural properties of the weathered recycled plastic lumber deck

boards were tested by performing flexural tests in three-point loading. The results of the three point loading test would allow for a comparison of the original flexural properties according to ASTM D 796. The results obtained from the three-point loading tests on the weathered samples are presented in Tables 2-4 and 2-5.

Table 2-4 presents the flexural properties of the side of the recycled plastic lumber exposed in tension while Table 2-5 presents the flexural properties of the side of the recycled plastic lumber that was not exposed was tested in tension. Based on the results of the test it can be seen that the modulus increased by 28 percent and 25 percent from the original when comparing the exposed and unexposed side testing in tension, respectively.

Table 2- 4 Three point bending results of recycled plastic lumber samples after weathering (exposed side tested in tension) (Lynch et al., 2001)

Sample	Modulus (ksi)	Strength at 3% strain (ksi)	Ultimate Strength (ksi)
1A	240.47	2.77	3.43
2A	213.79	2.48	3.12
3A	200.88	2.44	2.86
4A	214.22	2.55	3.32
5A	227.42	2.73	3.31
Average	219.3	2.59	3.21

Table 2- 5 Three point bending results of recycled plastic lumber after weathering (unexposed side tested in tension) (Lynch et al., 2001)

Sample	Modulus (ksi)	Strength at 3% strain (ksi)	Ultimate Strength (ksi)
1B	217.56	2.77	3.49
2B	201.5	2.47	3.05
3B	190.29	2.45	3.05
4B	219.3	2.43	3.11
5B	234.67	2.76	3.25
Average	213.21	2.58	3.19

2.4.4 Creep of RPP

Recycled plastic pins are manufactured from a combination of industrial wastes, typically polymeric materials (high or low density polyethylene), as well as varying amounts of saw dust, fly ash, and other by-product additives. Though economically and environmentally beneficial, polymeric material can experience higher rates of creep in comparison to other stabilization materials such as timber, concrete, or steel (Cheng et al., 2007). Chen et al., (2007) performed an analysis on the creep behavior of RPP on multiple samples from three manufactures. Variability of the engineering properties of the commercially available materials was seen due in part to the difference in manufacturer as well as the difference in which the RPP was developed (compressive molding or extruding).

Testing the compressive creep of the RPP, Chen et al., (2007) cut test specimens from the full sized RPP, with nominal dimensions of 3.5 X 3.5 in. cross section and 7 in. length. Utilizing a spring as the compressive load sustained, the spring possessed a spring constant of 800 lb/in. Additionally, the test specimens were all tested at a room temperature of 21°C. In addition to the compressive creep test, Chen et al., (2007) also tested the flexural creep response for RPP. In contrast to the previous testing method, the flexural test were performed on test specimens of the RPP that were 2 X 2 in. in cross section with a length of 24 in. For the flexural creep testing, five varying temperatures were used to utilizing a temperature controlled environmental room (21, 35, 56, 68 and 80°C). While the temperature was continually monitored, there was no monitoring on the humidity levels that were experienced during testing. The testing set up for both the compressive and flexural creep is displayed in Figure 2-13.

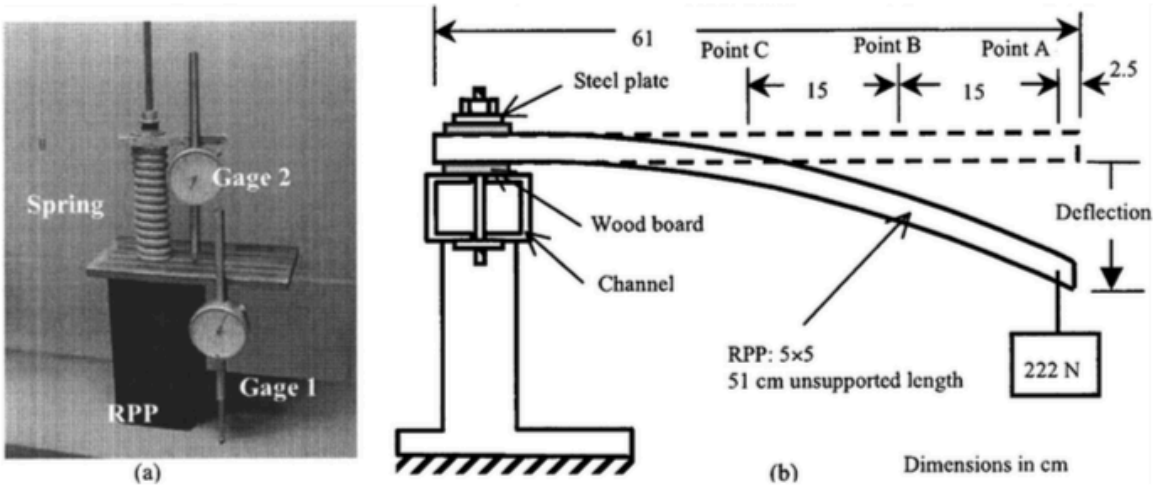

Figure 2- 13 RPP creep testing set up (Chen et al., 2007)

The results of the flexural creep test performed on the various manufacturing specimens in Chen et al. (2007) study is presented in Table 2-6. Additionally, the plot for the deflection vs. time for the compression creep tests is also shown in Figure 2-14. Based off of the plot, it can be seen that primary creep was concluded after approximately one day, while secondary creep continued for a year at a steady rate.

Table 2- 6 Summary results of compressive creep test (Chen et al., 2007)

Manufacturing	Number of Specimens	Creep Stress (psi)	Ratio of Creep stress to compressive strength (%)	Maximum Creep Strain (%)
A3	2	105	3.7	0.1
A6	2	100	6.3	0.1
B7	1	110	5.3	0.4
C9	1	120	5.1	0.4

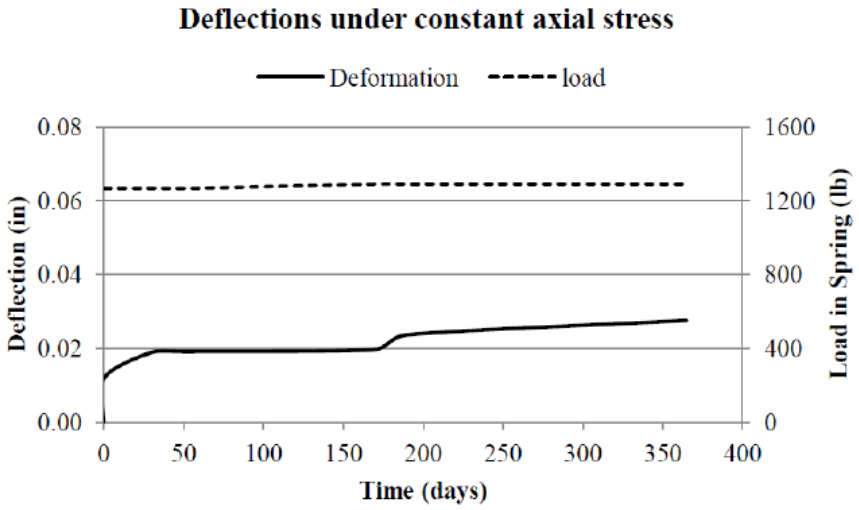

Figure 2- 14 Typical deflections under constant axial stress of RPP based on Batch B7 (Chen et al., 2007; Tamrakar, 2015)

Table 2-7 presents the summary of the flexural creep tests under a variety of loading conditions, as performed by Chen et al. (2007). From the results presented, it was observed that at higher temperatures, the average time for the specimen to reach failure decreased at the same loading condition. It was determined in the study that both the loading level and the temperature affect the creep performance of the recycled plastic specimens. Additionally, Chen et al. (2007) noted that as the load levels increased, closer to the ultimate strength of the material, the creep rate increased, decreasing the time needed to achieve failure.

Table 2- 7 Summary of flexural creep test (Chen et al., 2007)

Loading Conditions	Temperature (◦C)	Number of Specimens tested	Average time to reach failure (days)	Comments
44-N at 5 points	21	2	1185[a]	Not Failed
	56	2	195	Failed
	68	2	3.5	Failed
	80	2	0.8	Failed
93-N single load	21	2	1185[a]	Not Failed
	56	2	574	Failed
	68	2	17.5	Failed
	80	2	8.5	Failed
156-N single load	21	2	1185[a]	Not Failed
	56	2	71.5	Failed
	68	2	0.6	Failed
	80	2	0.8	Failed
222-N single load	21	2	1185[a]	Not Failed
	35	4	200	Failed
	56	2	3.1	Failed
	68	2	0.4	Failed
	80	2	0.8	Failed

[a] Last day of testing: specimen not ruptured

From the study, the author presented an investigative method for estimating the design life of RPP based on the load mobilization, as shown in Figure 2-15. Based on the analysis, it can be observed that the higher the mobilized load on the RPP, the more likely the design life of the RPP is to creep failure. In order to reduce the stress levels felt on the RPP, the author suggested increasing the amount of RPP in the design, changing the constituent blend of the RPP to reduce the susceptibility of creep, or changing the cross-section of the RPP in order to increase their moment of inertia.

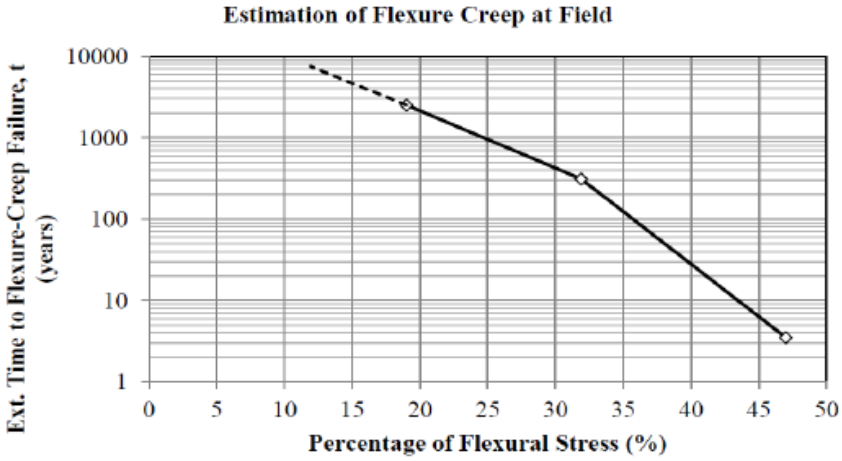

Figure 2- 15 Method for estimating time to failure from the results of flexural creep (Chen et al., 2007)

Chapter 3: Site Investigations

3.1 Project Background (US-287)

Located over the highway US-287, near the St. Paul overpass in Midlothian, Texas, the US-287 slope site was a slope reinforcement study performed by Khan (2013). Constructed in 2003-2004 from fill soil in the general vicinity of the project, the slope possesses a maximum height of approximately 30 – 35 ft. and a slope geometry of 3 (H): 1 (V). In 2010, it was observed that cracks had developed on the shoulder of the highway, near the crest of the slope. Figures 3-1 and 3-2 presents the location of the site and the preliminary investigation of the cracks on the crest of the slope, respectively.

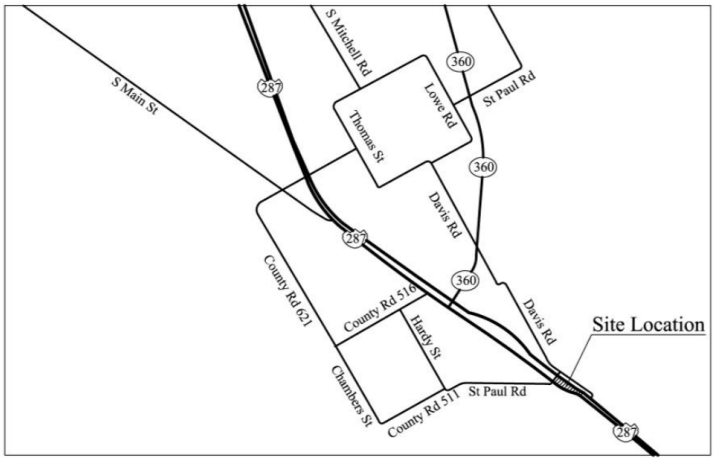

Figure 3- 1 Location of US-287 slope (Khan 2013)

Figure 3- 2 Shoulder cracks observed at crest of US 287 slope (Khan, 2013)

The subsurface condition of the slope was investigated in October 2010, utilizing two lines of Resistivity Imaging (RI) as well as three soil borings. The layout of the geotechnical and geophysical exploration is presented in Figure 3-3.

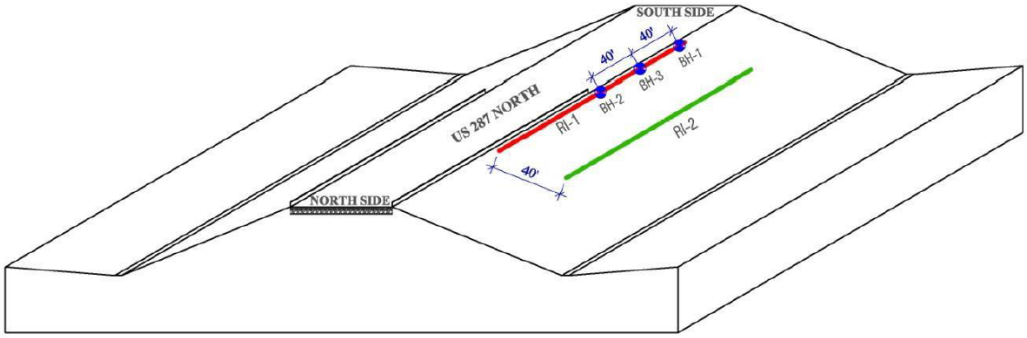

Figure 3- 3 Layout locations of RI lines and boreholes (Khan, 2013)

3.1.1 Geotechnical Borings and Laboratory Testing

Three soil borings were performed near the crest of the slope as displayed in Figure 3-3. Both disturbed and undisturbed soil samples were collected from the three soil borings, which attained depths in the range of 20 – 25 ft. The soil samples collected at different depths were utilized in the determination of the geotechnical properties of the subsoil of the slope.

It was concluded, through laboratory investigation, that the soil samples collected were classified as high plastic clay (CH) based on the Unified Soil Classification System. Additionally, it was determined that the liquid limits and plasticity indexes for the soil samples were in the range of 48-79 and 25-51, respectively. The moisture variation profiles with increasing depth along with the plasticity chart of the three boreholes are presented in Figures 3-4(a) and 3-4(b).

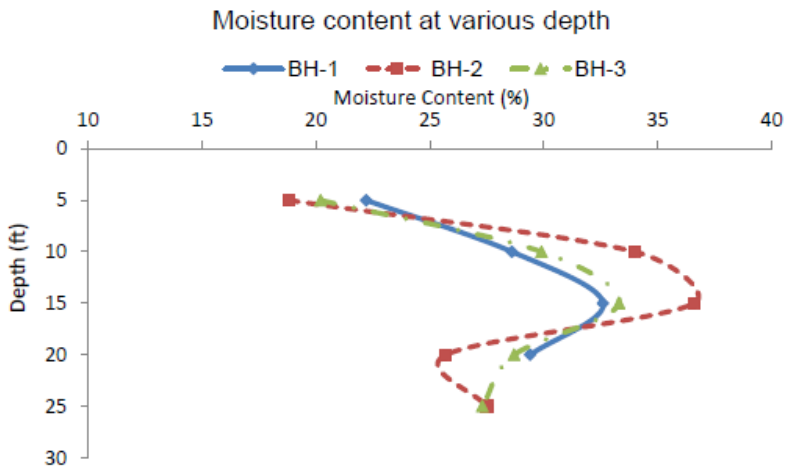

(a)

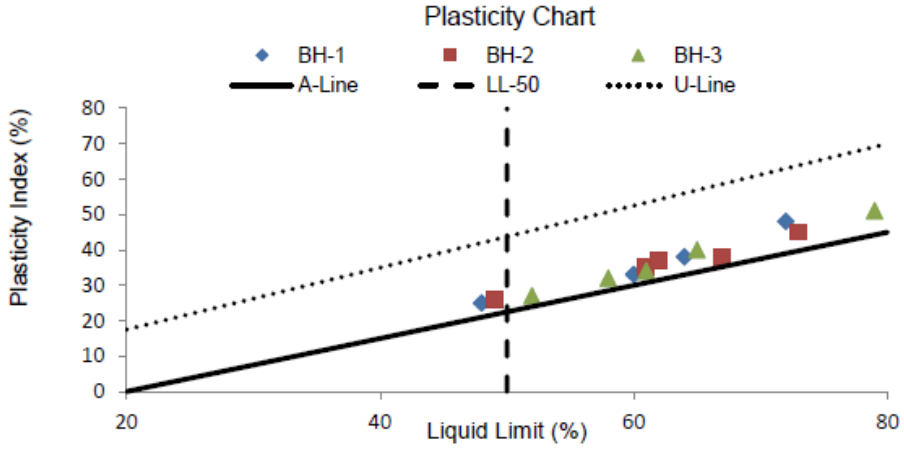

(b)

Figure 3- 4 Laboratory test results for US-287 samples, (a) Moisture variation with depth, (b) Plasticity Chart of soil borings (Khan, 2013; Tamrakar, 2015)

3.1.2 Resistivity Imaging Profiles

While investigating shallow geophysical investigations and geo-hazards, 2D resistivity imaging (RI) was heavily used (Hossain et al., 2010). As performed by Tamrakar (2015), two RI lines were utilized in the investigation of the subsurface condition for the US-287 slope. RI-1 and RI-2 were the two lines that were conducted on the slope face. RI-1 was performed near the crest

of the slope as presented in 3-5(a) while RI-2 was conducted at the middle of the slope, approximately 40 ft. from RI-1, as presented in 3-5(b).

(a) (b)

Figure 3- 5 Resistivity imaging (a) RI-1, (b) RI-2 at US 287 slope (Khan, 2013)

While performing the geophysical investigation, an 8-channel Super String equipment was used, which relayed results relatively quicker than that of a conventional single channel unit. The resistivity lines each consisted of 56 electrodes, spanning a distance of approximately 275 ft., with the spacing between electrodes at 5 ft. c/c.

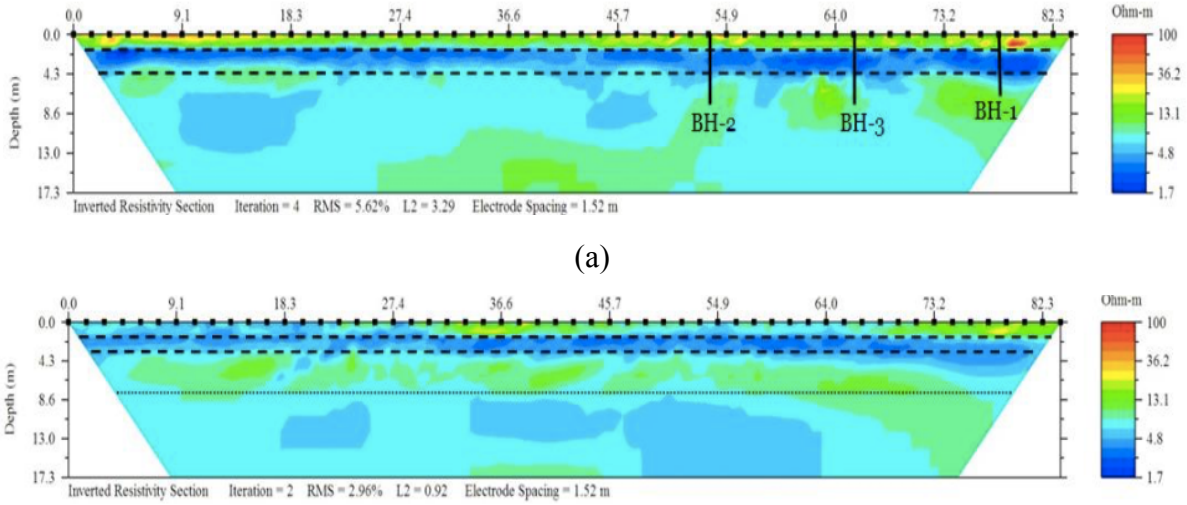

(a)

(b)

Figure 3- 6 Resistivity Imaging profile (a) Profile RI-1, (b) Profile RI-2 (Khan, 2013)

After analyzing the resistivity profiles, shown in Figure 3-6(a) and (b), it was observed that a zone of lower resistivity was present. For both RI-1 and RI-2, the topsoil of the slope showed the lower resistivity zone, decreasing approximately 16.4 ohm-ft. at depths of 5 – 14 ft. The presence of high moisture in the soil could be related to the low resistivity zone.

3.1.3 Slope Stability Analyses and Installation of RPP at US-287

Based on the subsoil investigation, it was determined that the underlying soil for the slope on US-287 was high plastic clay, with a dominant mineral of the soil being montmorillonite (Tamrakar, 2015). The high plastic clay, paired with the presence of montmorillonite, makes the soil highly susceptible to shrinking and swelling behavior due to the seasonal wetting and drying cycles. It is believed that after constant exposure to repetitive climatic conditions (i.e. shrinking and swelling, wetting and drying cycles), high plastic clays will eventually attain fully softened strength. The fully softened strength is what provides the governing strength for first-time slides in both fill and excavated slopes (Saleh and Wright, 1997). In the fully softened state, it is not the friction angle of the soil that is significantly influenced by the cyclic wetting and drying of the soil, but rather a near disappearance in the cohesion of the soil (Saleh and Wright, 1997). Therefore, it is probable that due to the surface soil attaining a softened state, due to the shrinking and swelling nature of the soil, it potentially initiated the movement of the slope and the resulting cracks on the shoulder of US-287.

As the cracks on the shoulder developed, a conduit was provided for rainfall into the slope, a preferential flow path, leading to the saturation of the soil near the crest. As a result of the rainwater infiltration, the driving forces increased, reducing the factor of safety of the slope. While the US-287 slope did not experience a slope failure during the time of investigation, the movement at the crest can be taken as an indication of the initiation of failure.

Khan (2013) modeled the US-287 slope utilizing PLAXIS 2D, an elasto-plastic finite element method (FEM) software, to determine the slope stabilization analysis. For the analysis, the shear strength reduction method (phi-C reduction analysis) was used in the determination of the factor of safety (FS) for the slope. From the FEM analysis conducted, it was concluded that with the soils present in the slope, and the top 7 ft. of soil considered as the failure zone in a fully softened state, remedial action was necessary to ensure that the slope did not fail. Therefore, three sections on the US-287 slope were reinforced and were designated as Reinforced Section 1, Reinforced Section 2, and Reinforced Section 3.

In addition to the three reinforced sections, two control sections were unreinforced, designated as Control Section 1 and Control Section 2, in order to evaluate the performance of the reinforced sections. The width of each section was 50 ft. as shown in the layout and cross section displayed in Figures 3-7 and 3-8, respectively.

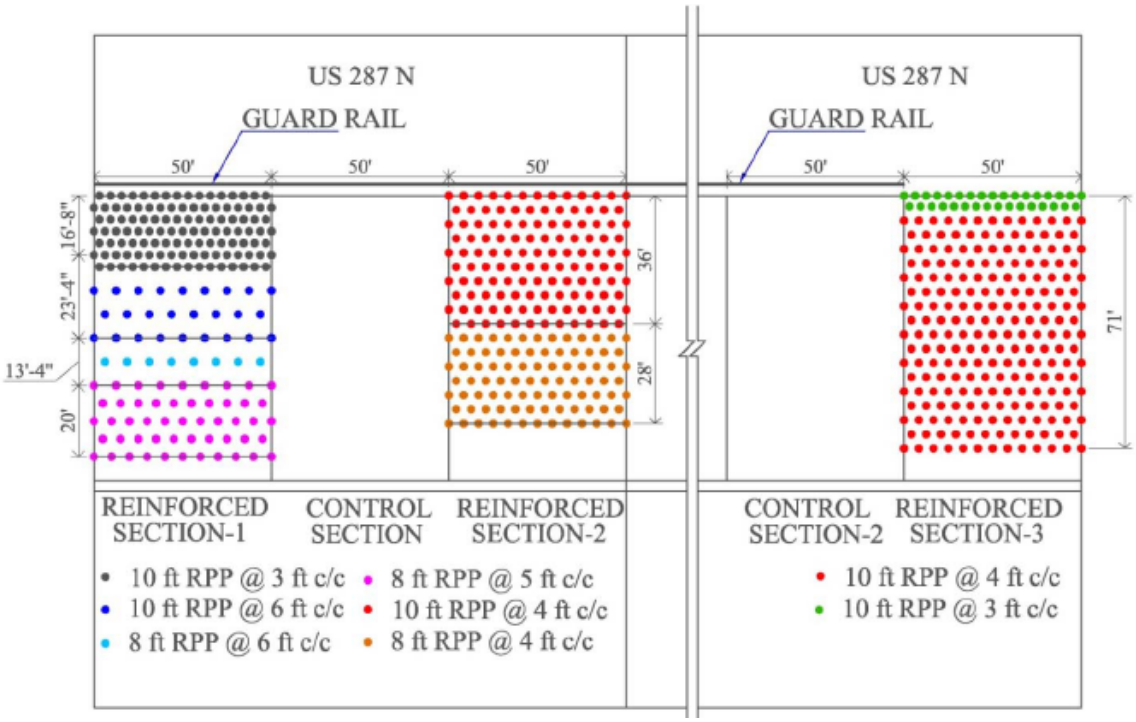

Figure 3- 7 RPP schematic at US-287 slope (Khan, 2013)

From the figure, varying lengths and spacing's of the RPP were more prevalent in the design schematic for Reinforced Section 1 in comparison to Reinforced Sections 2 and 3. With respect to Reinforced Section 1, four variations were present in the design. The top 17 ft., approximately, utilized 10 ft. RPP at a spacing of 3 ft. c/c. At the middle of the slope, the reinforcement became less as the 10 ft. RPP were spaced at 6 ft. c/c. Furthermore, at the toe of the slope for Reinforced Section 1, the length of the RPP was reduced to 8 ft. and spaced closer at 5 ft. c/c.

With respect to Reinforced Section 2, the spacing of the RPP remains at 4 ft. c/c but changes in length are observed near the middle of the slope from 10 ft. to 8 ft. Reinforced Section 3, similar to Reinforced Section 1, utilized 10 ft. RPP spaced at 3ft. c/c, however it was only implemented at the crest of the slope (i.e. the first 2 rows). Soon after, the reinforcement is held constant with 10 ft. RPP at 4 ft. c/c spacing. It should be noted that the first two rows were to be installed at a depth 2 ft. below that of the surface of the existing slope. The RPP was designed to be in a staggered grid pattern over the reinforced sections.

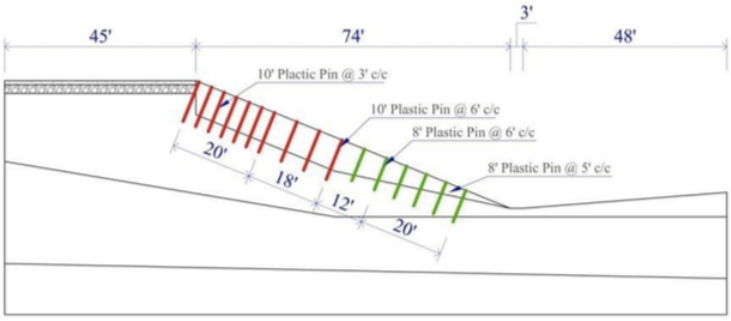

(a)

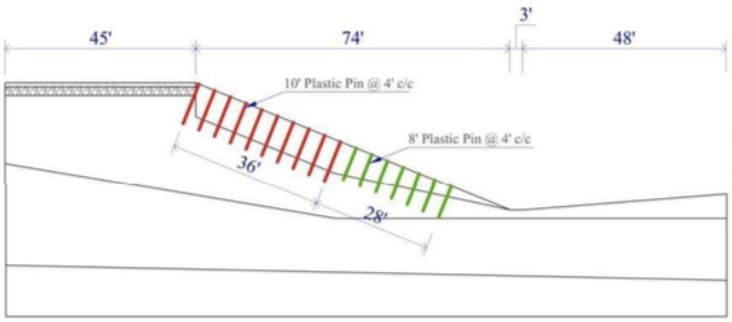

(b)

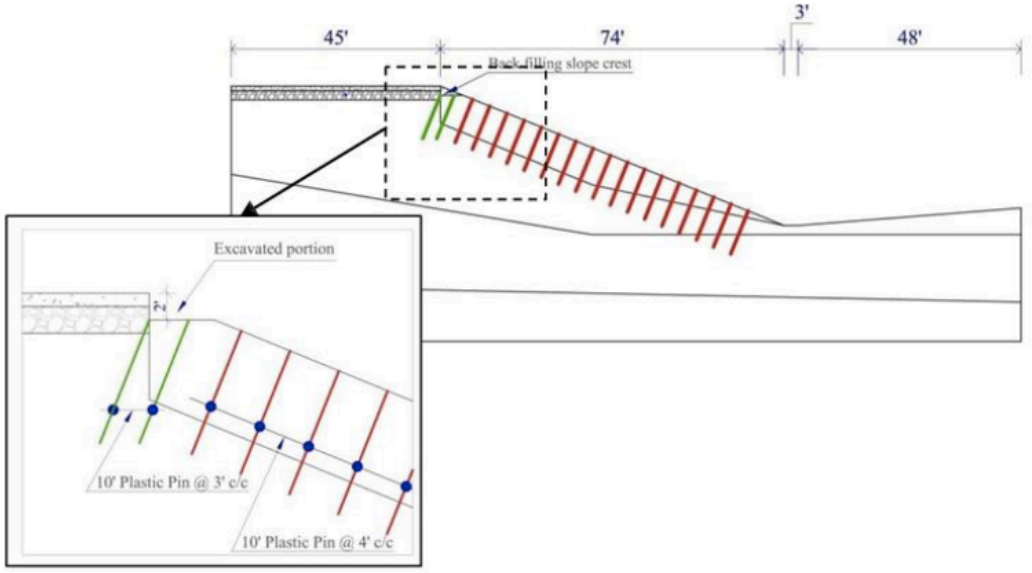

(c)

Figure 3- 8 Section view of slope stabilization on US-287 slope (a) Reinforced Section 1, (b) Reinforced Section 2, (c) Reinforced Section 3 (Khan, 2013)

From the proposed grid design scheme, Khan (2013) further analyzed the stability of slope by evaluating the factory of safety of each of the reinforced sections. Based off of the results, the factor of safety was observed as 1.43, 1.48 and 1.54 for Reinforced Section 1, Reinforced Section 2, and Reinforced Section 3, respectively.

It should be noted that during August 2017, after a dry summer in which most of Texas experienced drought conditions, Control Section 1 was reinforced with the design schematic present in Figure 3-9. It was determined that with the excessive cracks that had developed on the

shoulder of the highway, during rainfall events, water could easily penetrate into the slope and saturate the soil near the crest. With an increase of water present within the slope, the pore water pressure at the saturated zone would increase, resulting in the decrease of the shear strength of the soil. In order to resist further movement of the slope, it was determined that additional support was necessary.

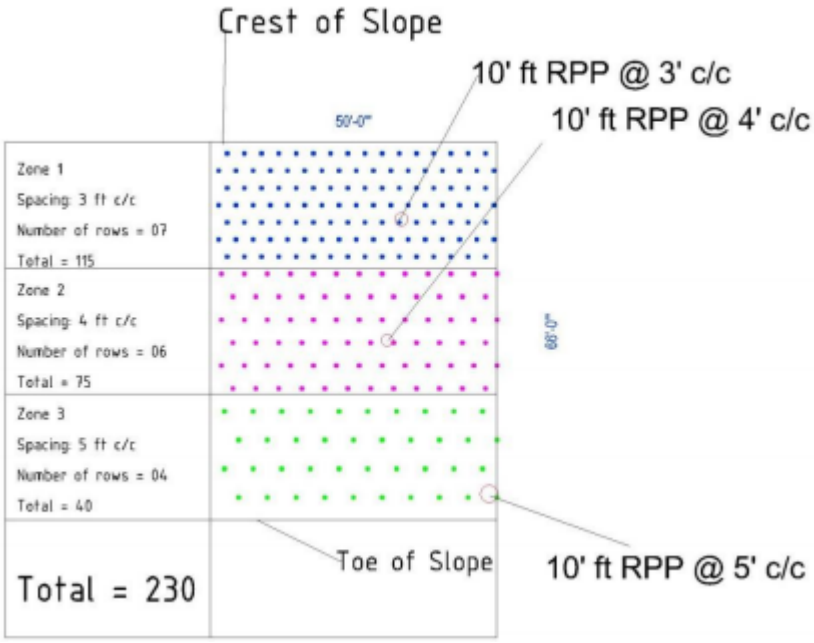

Figure 3- 9 RPP installation plan for Control Section 1

The 50 ft. control section possess three varying patterns, with the crest utilizing 10 ft. RPP at 3 ft. c/c spacing, followed by 10 ft. RPP at 4 ft. c/c spacing in the middle of the slope, and concluding at the toe of the slope using 10 ft. RPP at 5 ft. c/c spacing.

3.2 Project Background (I-35 and Mockingbird Slope)

The I-35 slope is located along the northbound I-35E near the south of the Mockingbird Lane overpass, shown in Figure 3-10. In addition to the site location, Tamrakar (2015) collected photos of the shoulder cracks at the crest of the slope as part of the preliminary site investigation shown in Figure 3-11. The cracks on the shoulder can be attributed to the surficial movement of the slope. The schematic of the failure condition is presented in Figure 3-12.

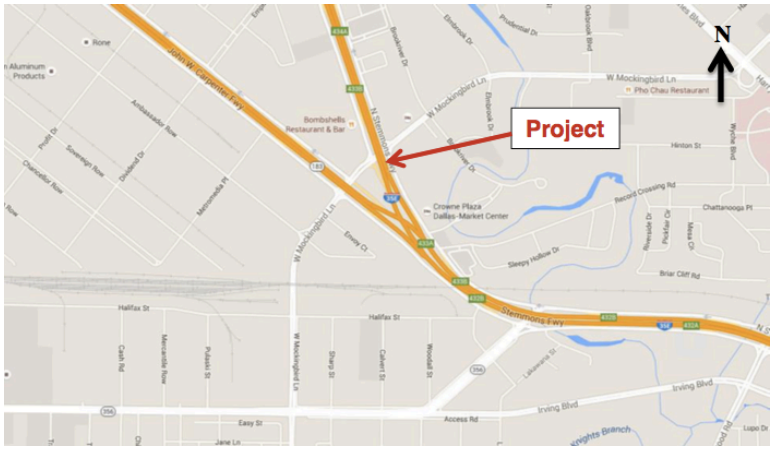

Figure 3- 10 Project location of I-35 slope

Figure 3- 11 Failure photos on shoulder of I-35 (Tamrakar, 2015)

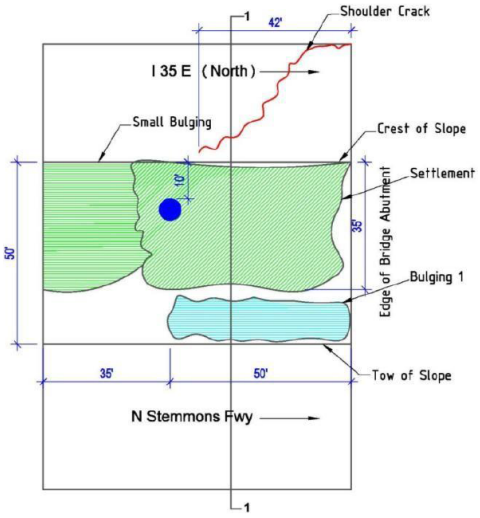

(a)

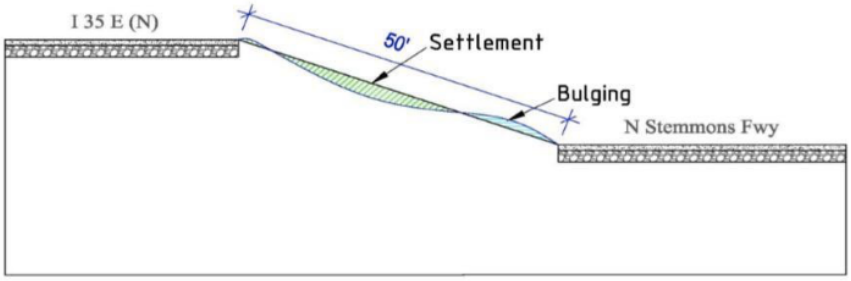

(b)

Figure 3- 12 Failure condition schematic (a) Front elevation, (b) Cross-section 1-1 (Tamrakar, 2015)

Performed in February 2014, the site investigation included geophysical testing (resistivity imaging) as well as soil test borings.

3.2.1 Geotechnical Borings and Laboratory Testing

Three boring log tests were conducted in February 2014 on the I-35 slope, with locations presented in Figure 3-12. Soil boring BH-1 was located on the crest of the slope, while both boring BH-2 and BH-3 were located near the toe of the slope. Each borehole that was performed was conducted to a depth of 30 ft., collecting both disturbed and undisturbed samples for further

laboratory testing. The disturbed samples that were collected were done so by collection at the time of the auger boring.

Figure 3- 13 Location of Boring and Resistivity Imaging at I-35 (Tamrakar, 2015)

The results of the soil boring and laboratory testing are presented in Table 3-1 and plotted in Figure 3-14(a) and (b). Samples collected from BH-1 indicated a high moisture zone at a depth between 10 and 30 feet after laboratory testing. The high moisture zone from BH-1 was similarly found in the resistivity profiles below the failed zone.

Table 3- 1 Soil test results of I-35 (Tamrakar, 2015)

Boring	Depth (ft)	Liquid Limit (%)	Plasticity Index (%)	Moisture Content (%)	Soil Type
	4	-	-	10.2	-
	7	51	27	3.1	CH
	9	-	-	27.4	-
	10	62	30	29.7	CH
	12	-	-	32.3	-
	17	68	39	27.1	CH
	21	-	-	32.8	-
BH-1	27	70	45	25.3	CH
	2	52	28	23.2	CH
	8	58	29	19.7	CH
	17	-	-	22.3	-
	21	59	28	22.1	CH
BH-2	27	59	33	27.3	CH
	3	68	36	26.4	CH
	12	64	39	23.1	CH
	15	-	-	22.3	-
	21	48	26	21.8	CL
BH-3	27	56	28	12.6	CH

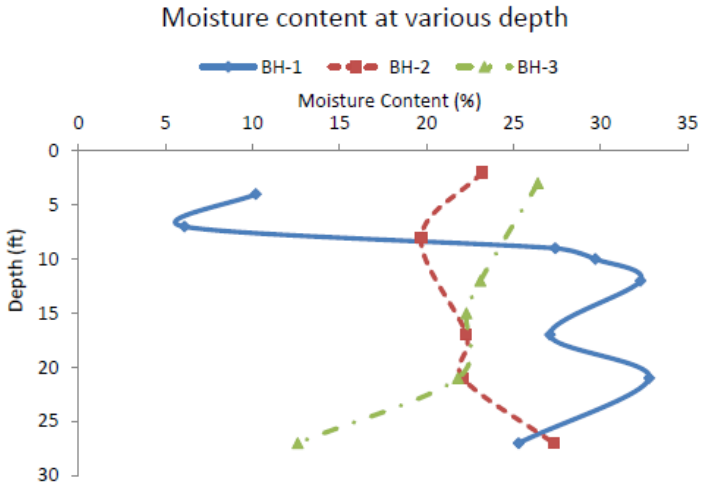

(a)

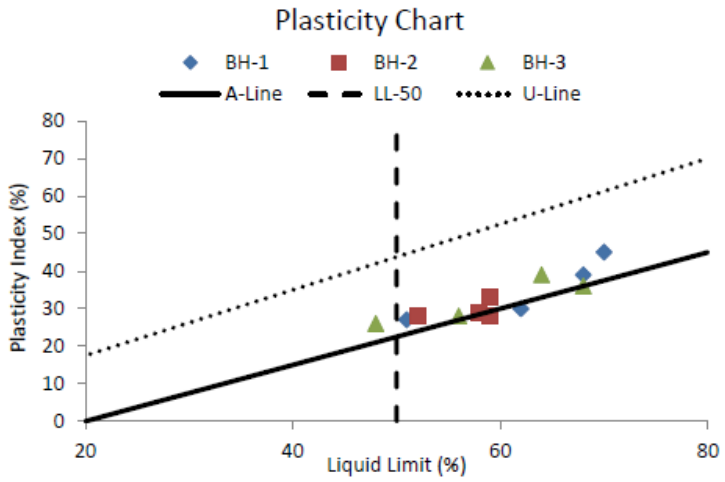

(b)

Figure 3- 14 Test results of I-35 (a) Moisture variation with depth, (b) Plasticity Chart of soil borings (Tamrakar, 2015)

Based on the soil boring laboratory testing, it was determined that the slope consisted primarily of high plastic clayey soil. Typically, due to the behavior of the soil to shrink and swell, within the first few years after construction the shear strength of the highly plastic clay soil will soften. Additionally, cracks caused by the shrinking behavior act as conduits for further rainwater infiltration, potentially saturating the crest of the slope. The potential saturation of the crest due to the additional influx of rainwater might lead to the failure of the slope.

3.2.2 Resistivity Imaging Profiles

A total of two 2D resistivity imaging lines were utilized in the subsurface investigation at the site. Identified as RI-1 and RI-2, the 2D imaging sections are shown in Figure 3-15. Resistivity line RI-1 was located near the crest of the slope while resistivity line RI-2 was located near the toe of the slope.

Based on the resistivity profile, RI-1 displayed a high resistivity zone around a depth of 7 ft., at the surface of the slope of the failure area. There is potential that the high resistivity zone was a result of the surficial movement loosening and/or disturbing the soil. Therefore, the depth

of failure due to the surficial movement could be as much as 7 ft. Immediately after the high resistivity zone was a zone of low resistivity below the failure zone. The low resistivity zone might signify the presence of a high moisture zone.

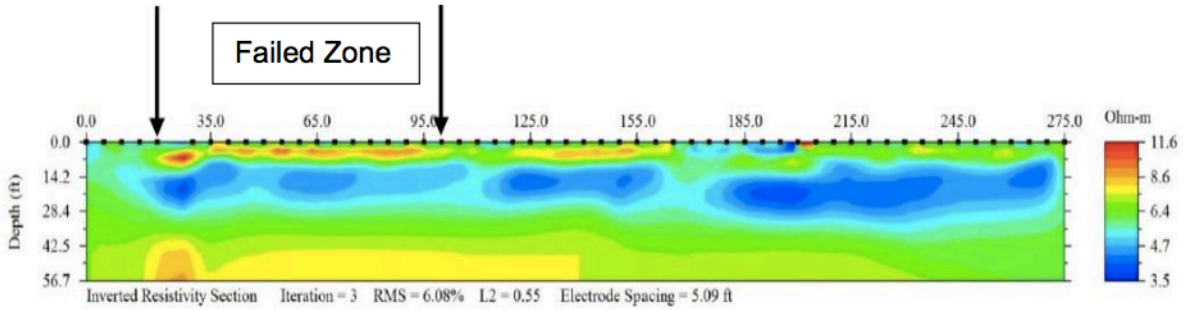

(a)

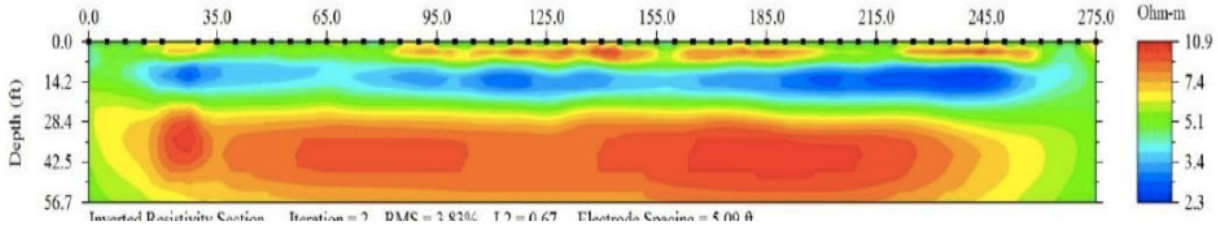

(b)

Figure 3- 15 Resistivity Imaging profiles of I-35 slope (a) RI-1 and, (b) RI-2 (Tamrakar, 2015)

3.2.3 Slope Stability Analysis and Installation of RPP at I-35

PLAXIS, the finite element program, was used in the analysis of the slope study. Tamrakar (2015) utilized the general Mohr-Coulomb soil model for the modeling of the I-35 slope. Based off of the results from the model, it was concluded that the factor of safety of the unreinforced slope was 1.03, nearing the threshold of failure. Therefore it was determined that the slope would benefit from the reinforcement of RPP.

An eighty-five foot section of the I-35 slope was considered for the installment of RPP as a slope stabilization measure. The cross-section used in the install was a 4 inch x 4 inch rectangular fiber reinforced RPP with a length of 10 feet. The top 6 rows of RPP near the crest of

the slope were spaced at 3 ft. c/c. The 5 rows of RPP after were spaced at 5 ft. c/c nearing the toe of the slope. The design grid schematic of the layout of RPP on the I-35 slope is presented in Figure 3-16. From the PLAXIS 2D model, it was determined that the factor of safety, with the RPP reinforcement, increased to 1.74 (Tamrakar, 2015).

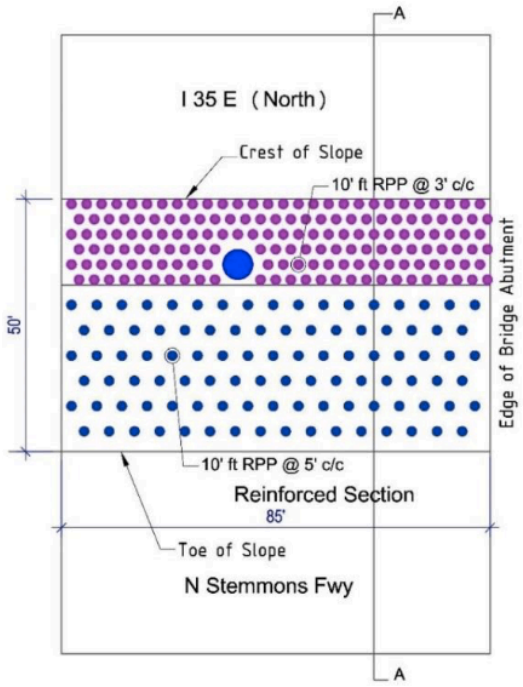

Figure 3- 16 RPP reinforcement schematic at I-35 slope (Tamrakar, 2015)

3.3 Project Background (SH-183)

The SH-183 site is located to the east of the exit ramp from eastbound SH-183 heading toward northbound SH-360, in the northeastern corner of TxDOT's Fort Worth District, shown in Figure 3-17. Near the crest of the existing slope, surficial failure as well as bulging was observed. Tamrakar (2015) developed the schematics of the condition of the failure on the slope shown in Figure 3-18 as well as the failure photos that were taken at the time of the site investigation displayed in Figure 3-19.

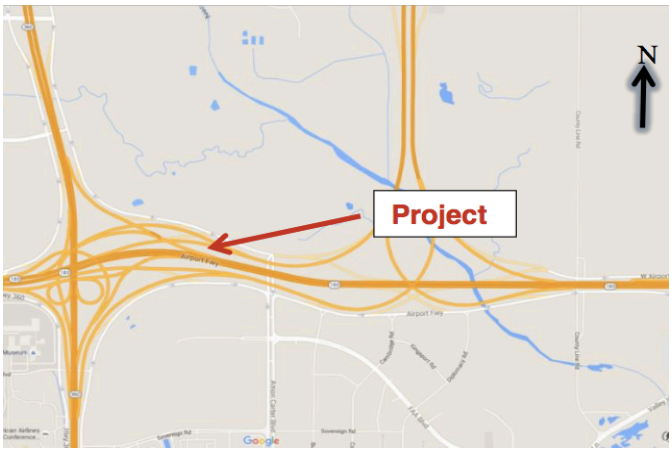

Figure 3- 17 Location of the project for SH 183 slope

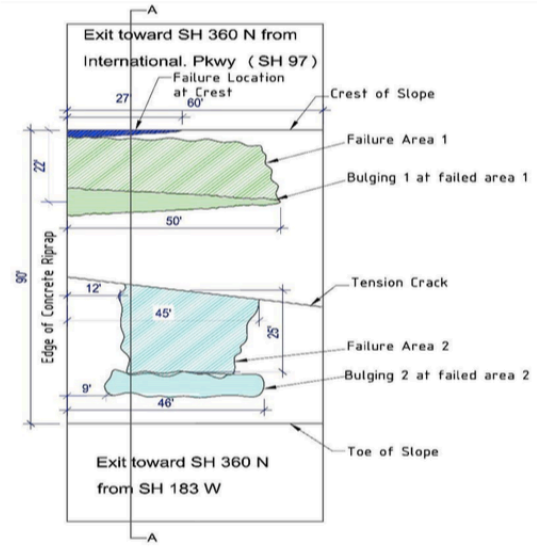

(a)

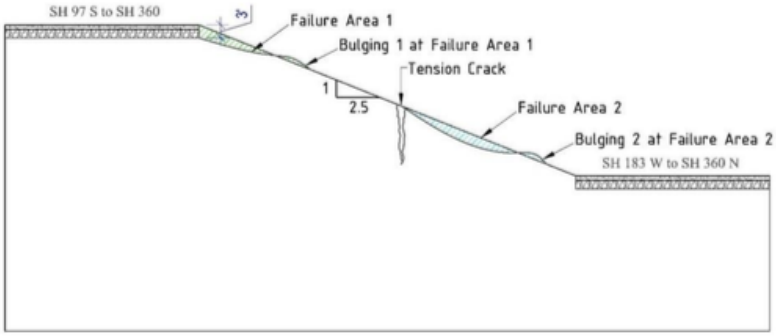

(b)

Figure 3- 18 Schematic of failure conditions on SH 183 slope (a) Front elevation, (b) Section A-A (Tamrakar, 2015)

Figure 3- 19 Slope failure photos at SH-183 (Tamrakar, 2015)

3.3.1 Geotechnical Borings and Laboratory Testing

Summarized in Table 3-2, the results of the liquid limit and plasticity index are presented based on the samples obtained from the borehole testing. From the results of the laboratory testing, it was determined that the soil samples, classified using the Unified Soil Classification System (USCS), were low to highly plastic clay. Soil collected from the top layer of Boreholes BH-1 and BH-2 were both classified as low plastic clay (CL) while the top soil layer collected for Borehole BH-3 was classified as high plastic clay (CH). A potential reason as to why the soil changes at a depth of approximately 8-12 ft. could be due to the construction of the pavement

subgrade soil (Tamrakar, 2015). Both boreholes BH-1 and BH-2 were drilled through the pavement along the roadway along the shoulder near the crest where one of the failures had occurred.

Table 3- 2 Test results of soil samples of SH-183 (Tamrakar, 2015)

Boring	Depth (ft.)	Liquid Limit (%)	Plasticity Index (%)	Moisture Content (%)	Soil Type
	7	39	17	20	CL
	123	51	31	23	CH
	17	58	39	21	CH
	24	52	31	22	CH
BH-1	29	54	34	20	CH
	3	43	23	21	CL
	8	48	24	17	CL
	13	66	42	20	CH
	17	56	31	21	CH
	22	54	33	20	CH
BH-2	27	48	21	18	CL
	3	60	26	19	CH
	8	64	39	22	CH
	12	48	30	19	CL
	22	46	28	12	CL
BH-3	28	37	22	11	CL

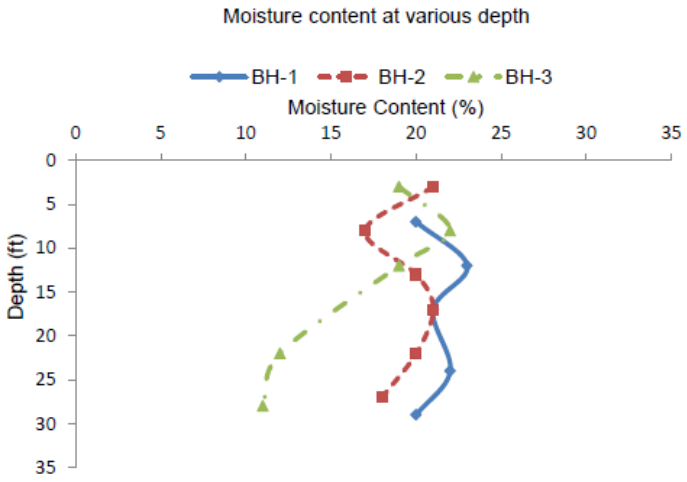

(a)

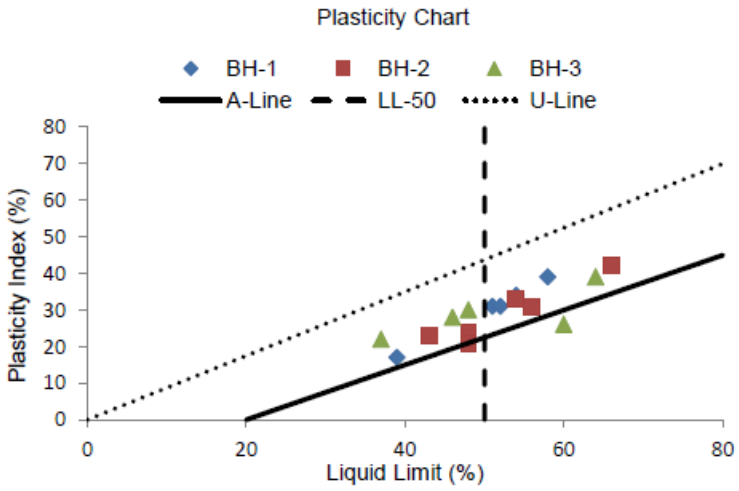

(b)

Figure 3- 20 Test results of SH 183 (a) Moisture variation with depth, (b) Plasticity Chart of soil borings (Tamrakar, 2015)

Shown in Figure 3-20 (a) and (b), the moisture variation and plasticity chart is plotted for the three boreholes, respectively. It was observed from the moisture variation plot that for Borehole BH-1, the moisture content fluctuated between the range of 20% and 23% after a depth of 5 ft. For Borehole BH-2, the moisture content ranged from 17% to 21% after a depth of 5 ft. Borehole BH-3 saw a wider range for the moisture content from 11% to 18% after a depth of 5 ft. The higher observed moisture content for Boreholes BH-1 and BH-2 could be attributed to shoulder cracks that were observed near the crest of the slope during a preliminary site visit. The cracks can potentially act as a conduit for the infiltration of rainwater. Once the rainwater has infiltrated into the slope, it will perch unless it otherwise dries up or percolates deeper into the slopes soil layers. However, percolation into the clay soil usually is a long process due to the low permeability of the soil.

3.3.2 Resistivity Imaging

Three total lines of 2D resistivity imaging (RI) were conducted on the site location. Denoted as “Resistivity Line 1”, “Resistivity Line 2”, and “Resistivity Line 3”, the location of

the 2D imaging sections are presented in Figure 3-21. Resistivity Line 1 was located at the crest of the slope while Resistivity Line 2 and Resistivity Line 3 were located at the mid-slope, over the tension crack, and near the toe of the slope, respectively.

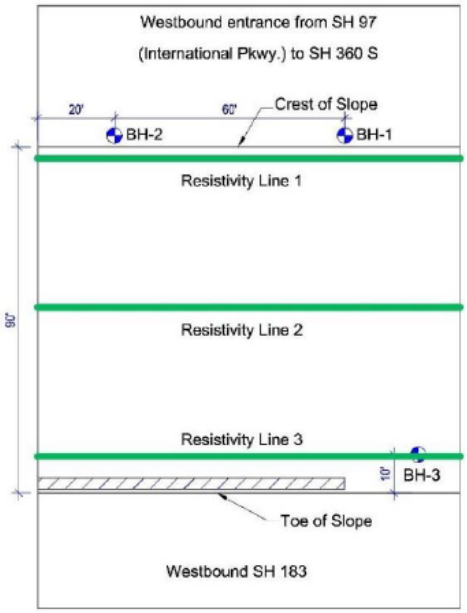

Figure 3- 21 Resistivity Imaging line locations at SH-183 (Tamrakar, 2015)

Similar to previous investigations, the RI investigation utilized an 8-channel Super Sting resistivity meter. The lines were comprised of 56 electrodes at a spacing of 5 feet to develop each of the lines profiles. The profiles that were obtained from the three lines are presented in Figure 3-22.

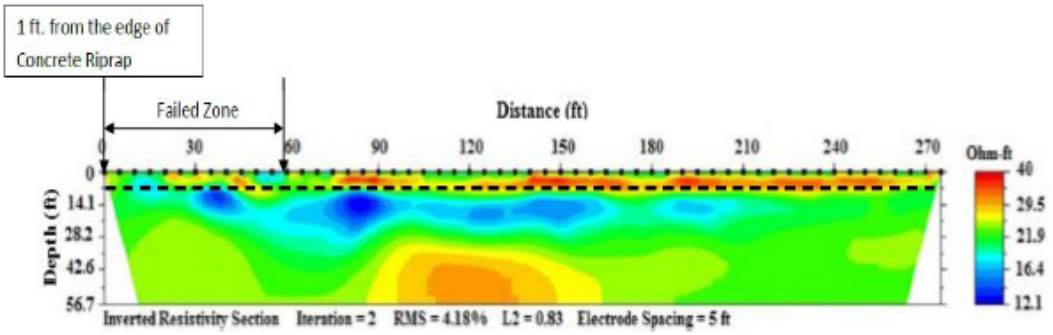

(a)

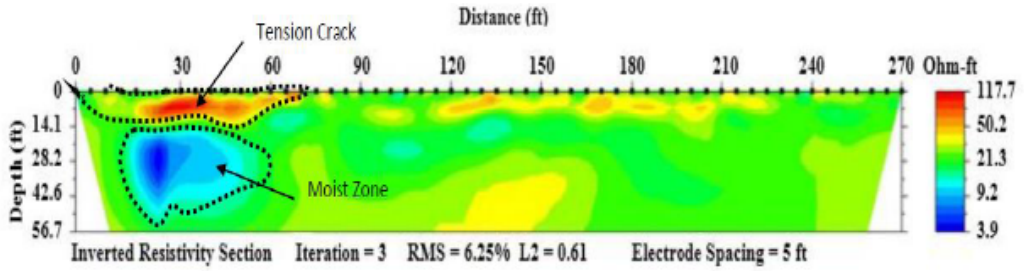

(b)

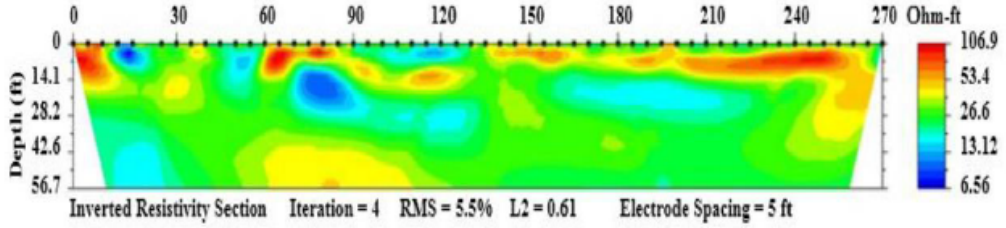

(c)

Figure 3- 22 Resistivity Imaging Profiles of SH-183 (a) RI line 1, (b) RI line 2, (c) RI line 3 (Tamrakar 2015)

From the resistivity profiles, it can be observed that a high resistivity zone, at a depth of approximately 7 ft., is present near the crest of the slope. The zone could be attributed to the disturbance previously caused during the slope failure or being in the presence of an active zone (Tamrakar, 2015). As the resistivity measured is dependent upon the moisture conditions and void ratio of the soil under investigation, the slope movement could have loosened the surrounding soil creating an area with higher void ratio and the resulting high resistivity.

3.3.3 Slope Stability Analysis and Installation of RPP at SH-183

Tamrakar (2015) analyzed the stability of the slope using PLAXIS 2D, a finite element modeling program. It was theorized in the creation of the model that the behavior of the high plastic CH clay present in the slope would affect the slopes performance. As the clay would shrink and swell due to the seasonal wet-dry cycles, once the clay contracted, pathways for further water intrusion from rainfall would create a perched water zone due to the low permeability of the soil present. Assuming that the water intrusion would saturate the upper 5 ft.,

temporarily creating a perched water zone (fully moistened zone), the factor of safety (FOS) obtained from the model was approximately 1.09.

Based on the analyses conducted, a 60 ft. x 90 ft. section of the SH 183 slope was to be stabilized using RPP. The upper 30 feet of the slope near the crest was reinforced with 10 ft. RPP at spacing 3 ft. c/c, and the remaining slope was spaced at 4 ft. c/c. All pins used were 10 ft. in length. The schematic of the grid pattern for the RPP is displayed in Figure 3-23. With the stabilized pattern shown, the PLAXIS 2D software predicted a factor of safety of the slope to be 1.74.

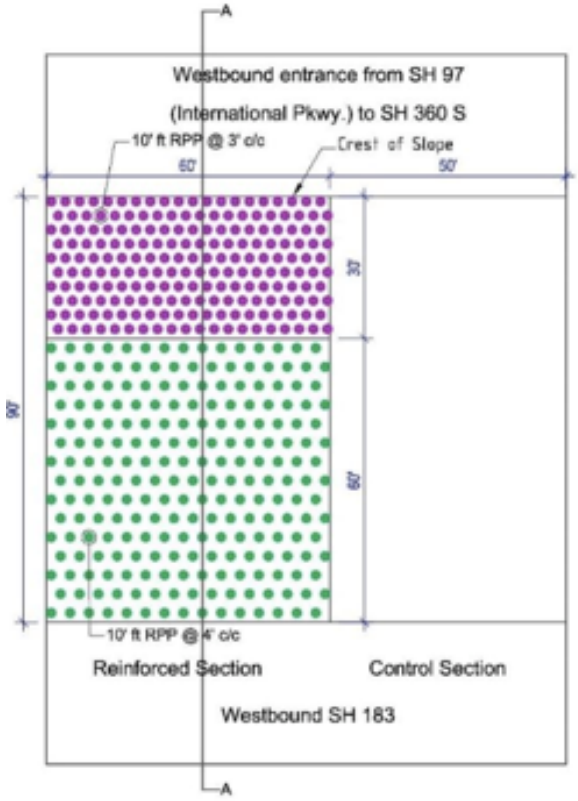

Figure 3- 23 RPP reinforcement schematic for SH-183 (Tamrakar, 2015)

Chapter 4: Performance Monitoring Results

4.1 Performance Monitoring of US-287 Slope

The performance monitoring of the US-287 slope included a monthly site visit utilizing a total station for the topographic survey for measurement of the vertical deformation and an inclinometer to measure the displacement. The results obtained are summarized in the subsequent sections.

4.1.1 Topographic Survey

The reference points for the topographic survey were conducted on the location of the crack on the shoulder at the crest of the slope. The marked, fixed points were taken monthly to observe the performance of the RPP to resist further surficial movement of the slope. Figure 4-1 presents the location of the survey line with respect to the installed RPP.

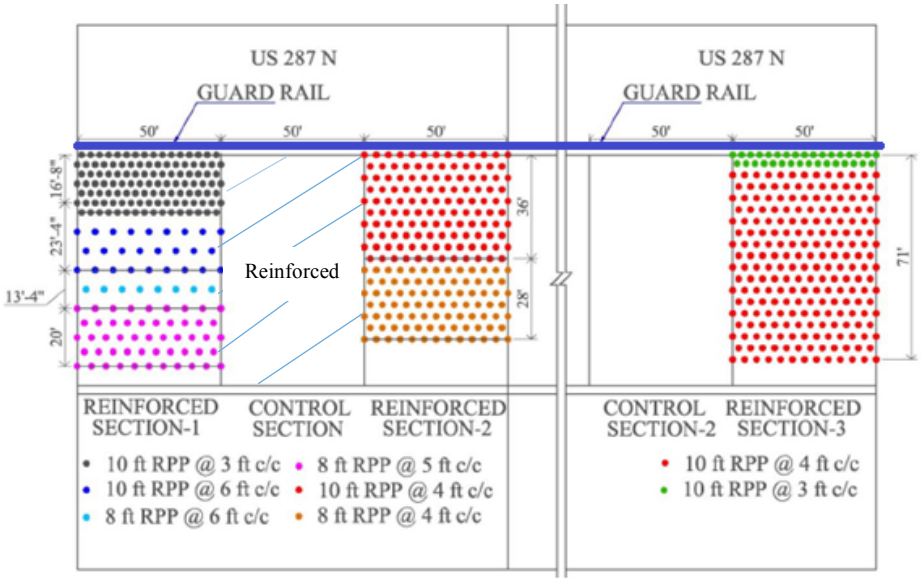

Figure 4- 1 US-287 reinforcement design scheme with location of survey line

The readings for the topographic survey began in May 2012 after the completion of the RPP installation in Reinforced Section 3. Performed monthly thereafter, the results obtained presents a continuous measurement plot used in the evaluation of the performance of the slope in

terms of vertical deformation, or settlement. Presented in previous sections, during the investigation of the US-287 site, cracks were observed along the shoulder of the highway slope section. To better analyze the performance of the RPP to resist surficial movement of the slope, the cracks were left unsealed, therefore allowing for repeated wetting and drying cycles with the potential of an increase in rainfall infiltration into the slope. The results of the monthly topographic survey measurements are presented in Figure 4-2

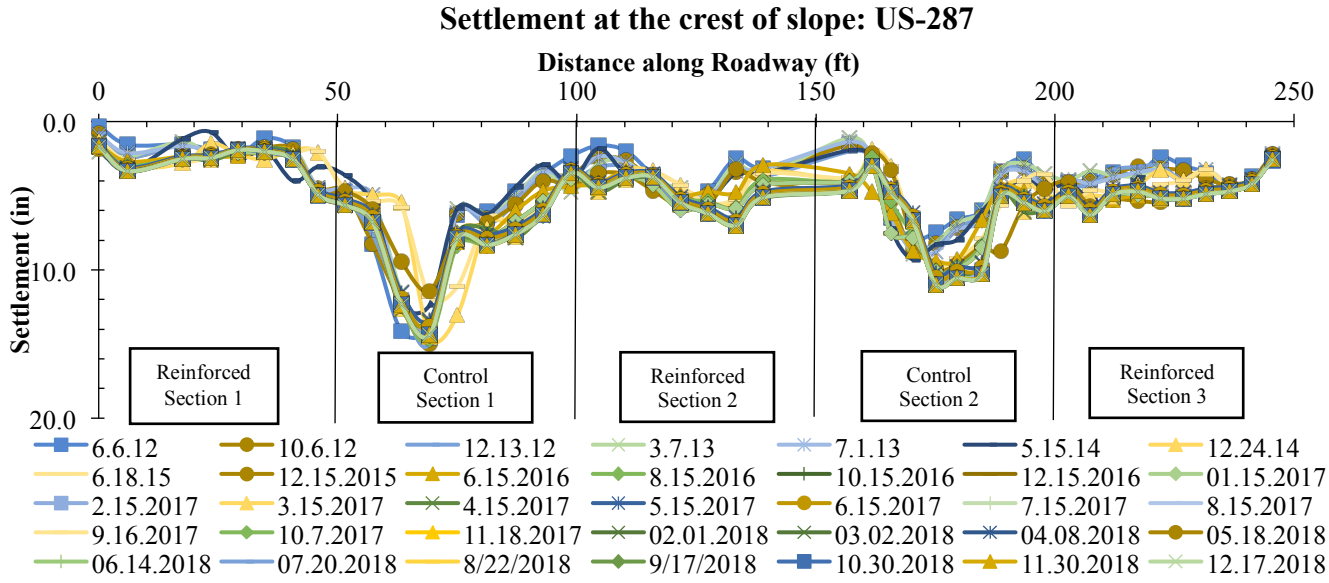

Figure 4- 2 Settlement at the crest of US-287

The largest total settlements measured each year from Figure 4-2 are presented, numerically, in Table 4-1. The purpose in showing the maximum total measured settlement for each section is to display the RPP performance in the location of the crest of the slope that had initially experienced the most vertical deformation. Control Section 1 is not included in the table due to its reinforcement in 2017. As it was reinforced, the vertical deformation is not in good agreement to Control Section 2 performance.

Table 4- 1 Maximum total settlement on US-287 for reinforced sections and Control Section 2

	Maximum Total Settlement (in.)						
	2012	2013	2014	2015	2016	2017	2018
Reinforced Section-1	4.69	4.93	4.07	5.08	4.94	4.98	4.99
Reinforced Section -2	5.47	5.12	5.68	6.55	5.98	7.04	7.02
Reinforced Section -3	5.1	4.39	5.44	5.68	6.11	6.28	6.3
Control Section -2	8.68	8.93	10.09	10.18	10.1	10.99	11

Based on the data presented in Figure 4-2 and Table 4-1, the lowest total settlement measured was in Reinforced Section 1, measured as 5.08 in. in 2015, and reducing to 4.99 in at the end of 2018. Reinforced Section 1 is preceded by Reinforced Section 3 (6.30 inches) and concluded with Reinforced Section 2 (7.04 inches) in terms of maximum total settlement measured. Seen in Khan (2013), the sections performances have followed the same general trend as observed in the first few years of investigation. Despite fluctuations in the total slope settlement, the difference in total settlement from the first measurement in 2012 to the last measurement presented in this study in 2018 has shown that all reinforced sections performed better than non-reinforced sections. Table 4-2 displays the maximum change in total settlement from the beginning to end of measurements on the US-287 slope for all sections, reinforced and control.

Table 4- 2 Difference in maximum total settlement between 2012 and 2018

Difference in Total Settlement (in.)			
	2012	2018	Difference (2012, 2018)
Reinforced Section -1	4.69	4.99	0.3
Reinforced Section -2	5.47	7.02	1.55
Reinforced Section-3	5.1	6.03	1.2
Control Section -2	8.68	10.99	2.32

Comparing the performance of each reinforced section with respect to Control Section 2, it was observed that the seven-year difference in vertical deformation measured was only a percentage of the control. With respect to Control Section 2, Reinforced Section 1 experienced only 13% the settlement of the control section. Reinforced Section 3 experienced only 52% of the settlement of the control section and Reinforced Section 2 was only 67%. The results that were obtained for the performance of the reinforced sections are reasonable when analyzing the spacing that was implemented for the RPP. Reinforced Section 1 and 3 had the lowest RPP spacing (3 ft. c/c) at the crest of the slope while Reinforced Section 2 had an RPP spacing of 4 ft. c/c at the crest of the slope. Therefore, the spacing of the RPP at the crest of the slope could, potentially, be attributed with each reinforced sections performance.

4.1.1.1 Control Section 1

Control Section 1 experienced a decrease in incremental settlement after the sections reinforcement in 2017. Presented in Figures 4-3 (a) through (d), it can be observed that the settlement the control section is experiencing is negligible. While not associated with the long-term performance aspect of the present study, due to the study only compiling a years' worth of measurements, the contribution in the performance of the control section of the slope with RPP is

clear. Control Section 1, after reinforcement, experienced a maximum total settlement of 0.27 in. at the crest of the slope. Figure 4-4 presents the lines utilized for the topographic survey.

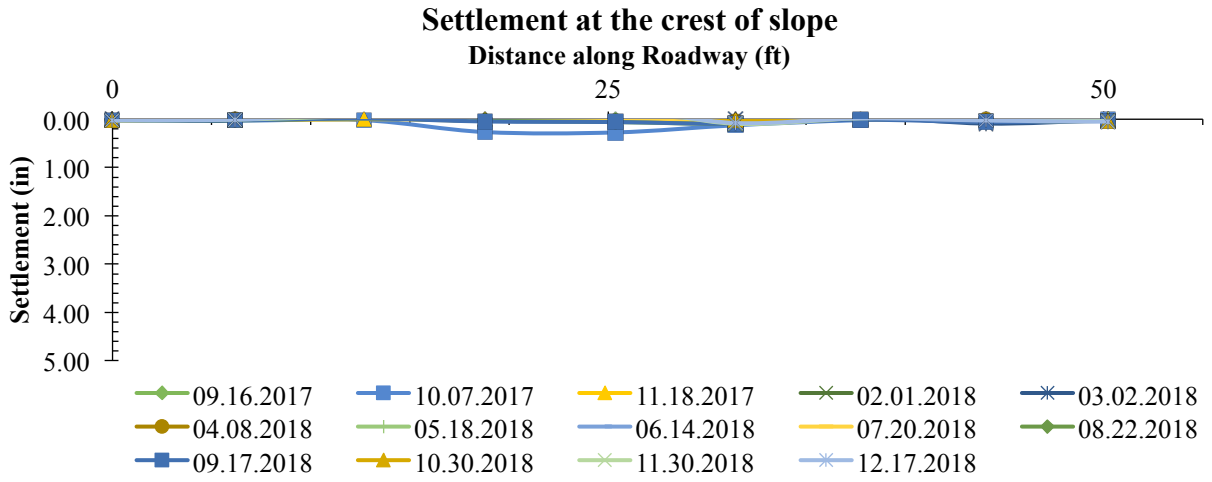

(a)

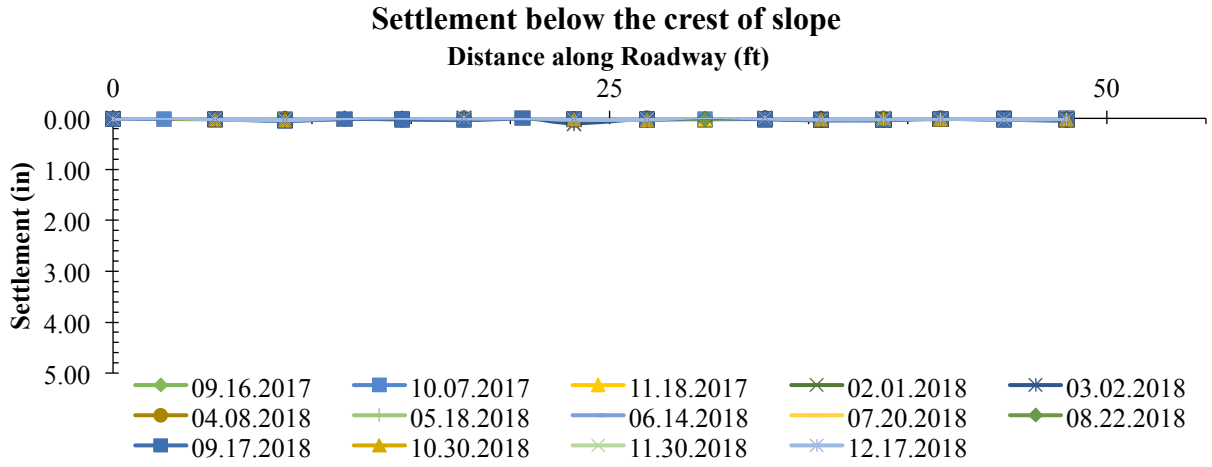

(b)

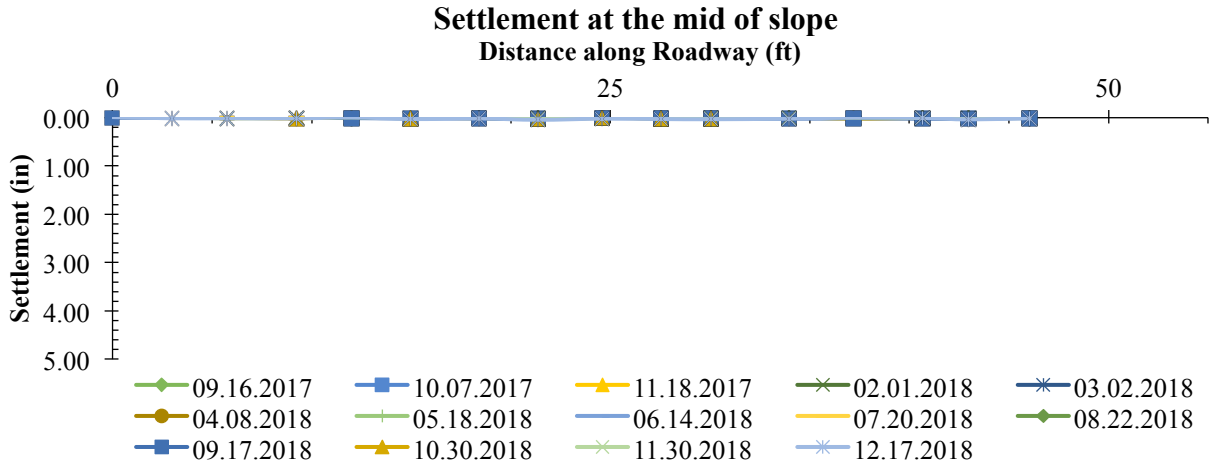

(c)

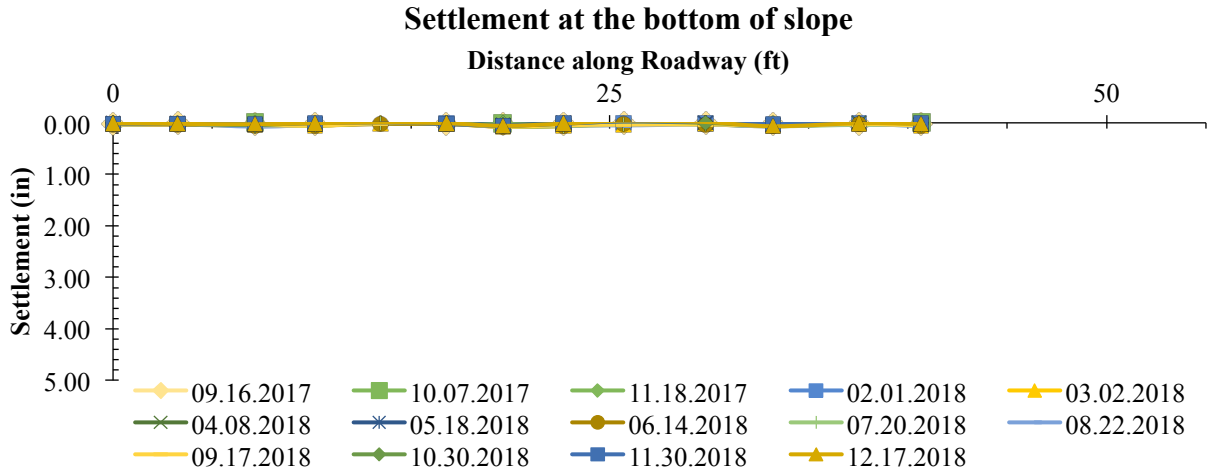

(d)

Figure 4- 3 Settlement diagrams at (a) Crest of slope, (b) Below the crest, (c) Mid slope, (d) Bottom of slope of US-287 slope

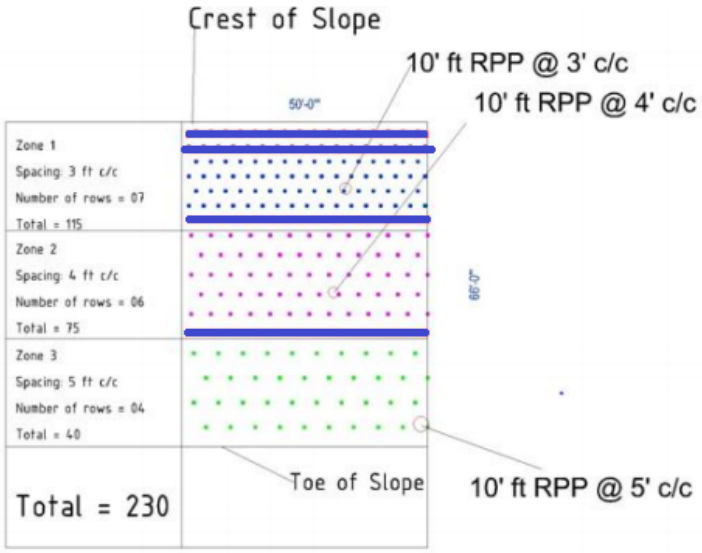

Figure 4- 4 Surveying rows in US-287 control section

4.1.2 Inclinometer

Installed at the US-287 slope site were three inclinometers denoted as Inclinometer 1, Inclinometer 2, and Inclinometer 3. Inclinometer 1 was installed at Reinforced Section 1, Inclinometer 2 was installed at Control Section 1, and Inclinometer 3 was installed at Reinforced Section 2. The depths of the inclinometer casings were 30 ft. each and were installed perpendicular to the slopes surface. The layout of the inclinometers is presented in Figure 4-5.

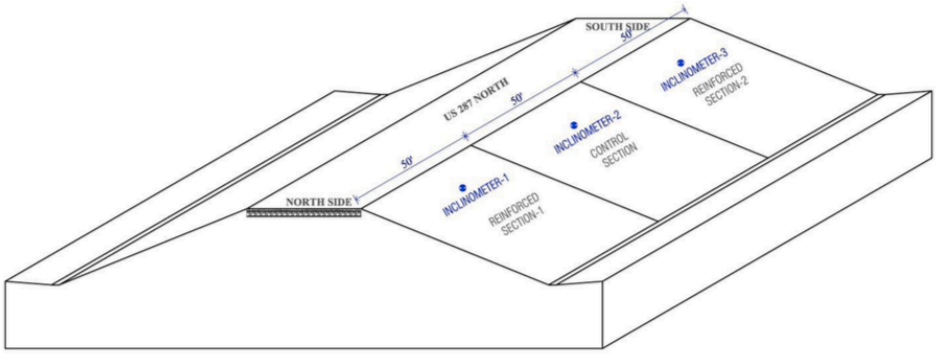

Figure 4- 5 Layout of inclinometer at US-287 slope (Tamrakar 2015)

The inclinometer monitoring was performed on a monthly basis along with the topographic survey. Despite the installment of three inclinometers, only Inclinometer 1 and

Inclinometer 3 are included in this study as Inclinometer 2 was blocked, not allowing for further readings. The cumulative displacement along with precipitation is presented in Figure 4-6 and Figure4-7.

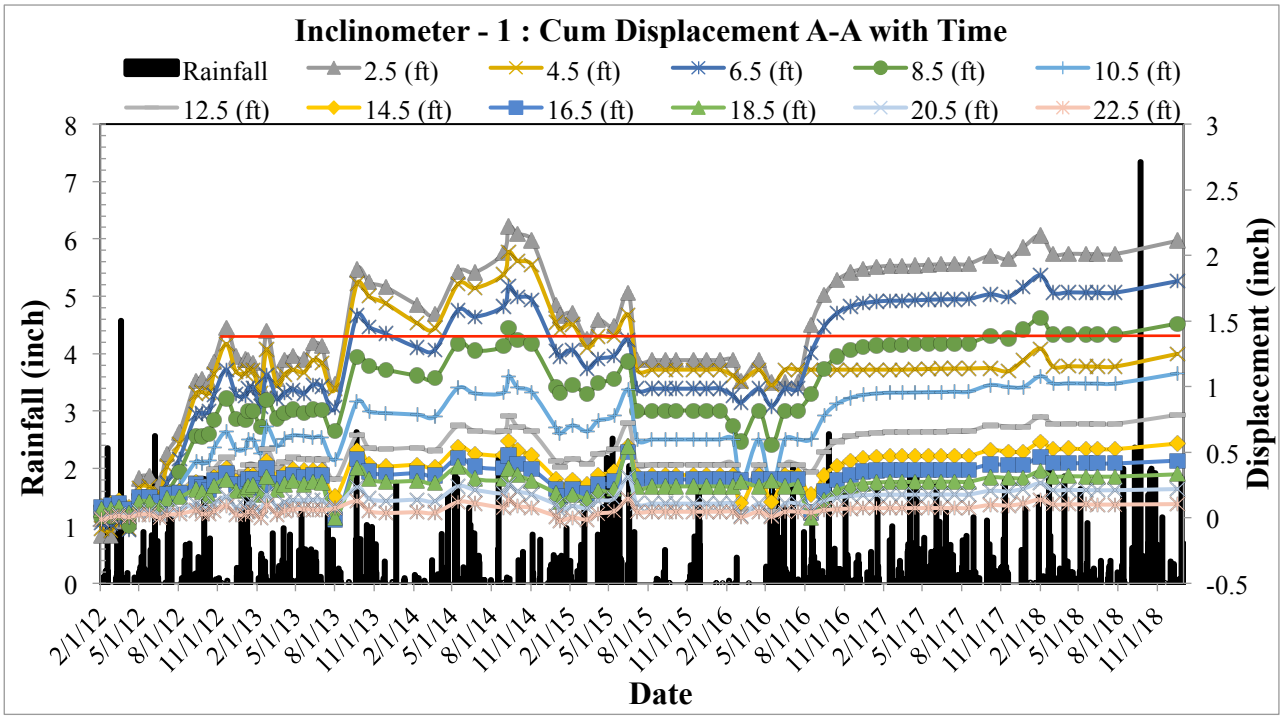

Figure 4- 6 Displacement in Inclinometer I-1 at US-287

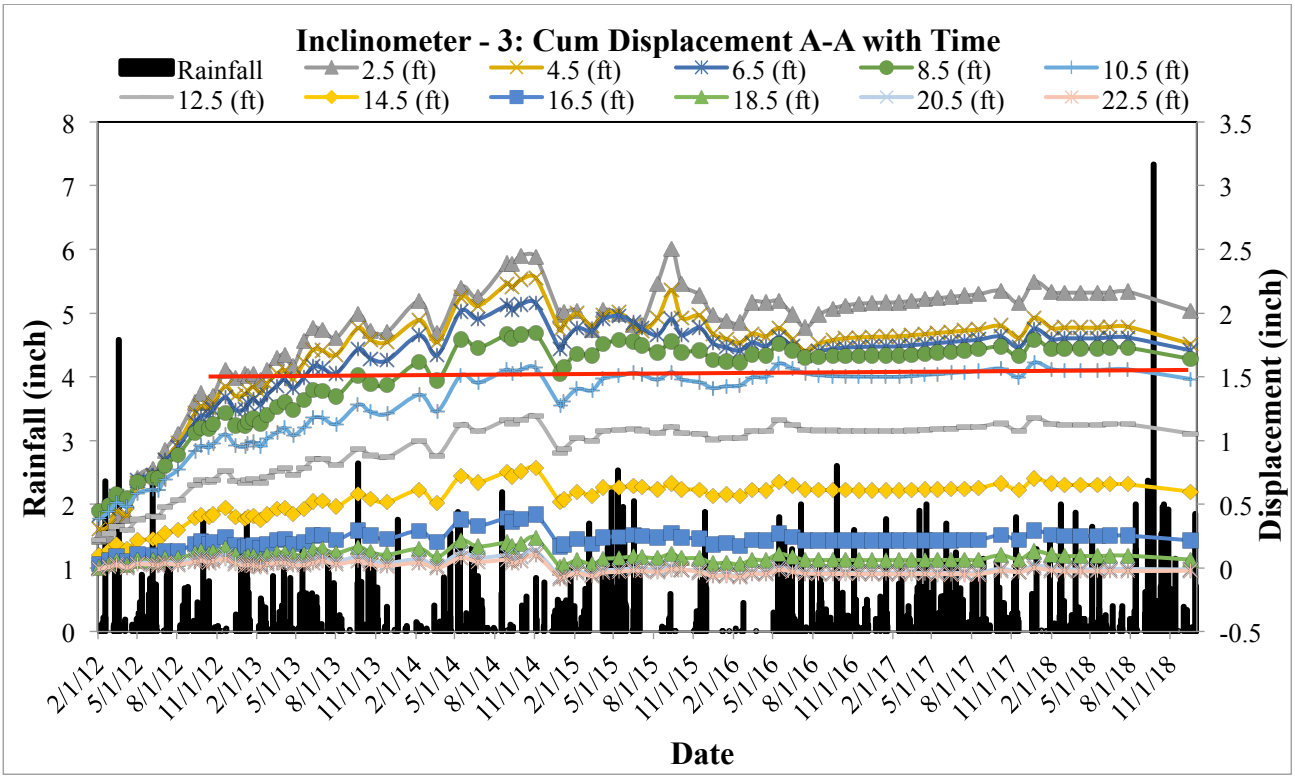

Figure 4- 7 Displacement in Inclinometer I-3 at US-287

From the results obtained from the plot for Inclinometer I-1, the maximum cumulative displacement was measured at 2.2 in., occurring near the surface of the slope at a depth of 2.5 ft. As the depth of inclinometer readings increased, the displacement experienced decreased. After a depth of 16.5 ft., the displacement measured is nearly negligible. Additionally, despite fluctuations in the graph due to rainfall events, after the adjustment period it can be seen that the cumulative displacement remains in a range of 0.5 in. It should be noted that due to sending the inclinometer for recalibration, a gap between August 2018 and November 2018 is observed.

Inclinometer I-3 experienced a higher maximum cumulative displacement in comparison to Inclinometer I-1. Obtaining a maximum cumulative displacement of approximately 2.5 in., the displacement occurred near the surface of the slope at a depth of 2.5 ft. Similar to results obtained from Inclinometer I-1, after a depth of 16.5 ft., the displacement measured were nearly negligible. Despite the fluctuations in readings from rainfall events, comparable to Inclinometer

I-1, the cumulative maximum displacement measured after the adjustment period stayed within a range of 1 in., often being approximately 0.5 in. Due to the inclinometers recalibration, a gap is additionally experienced for Inclinometer I-3.

The top 2.5 ft. readings were taken from Inclinometer I-1 and I-3 in order to compare the results with rainfall, shown in Figure 4-8. Based on the results, it can be observed that Inclinometer I-1 typically performed better. Throughout the measurements for the two inclinometers, it can be observed that Inclinometer I-1 generally displayed a displacement value of approximately 0.25 to 0.5 in. less in comparison to Inclinometer I-3. It should be noted that Inclinometer I-1 was installed in Reinforced Section 1 with a RPP spacing of 3 ft. c/c, while Inclinometer I-3 was installed in Reinforced Section 2 with an RPP spacing of 4 ft. c/c. Therefore, it is possible that the closer spacing is what can be attributed to the success of Inclinometer I-1 in comparison to Inclinometer I-3.

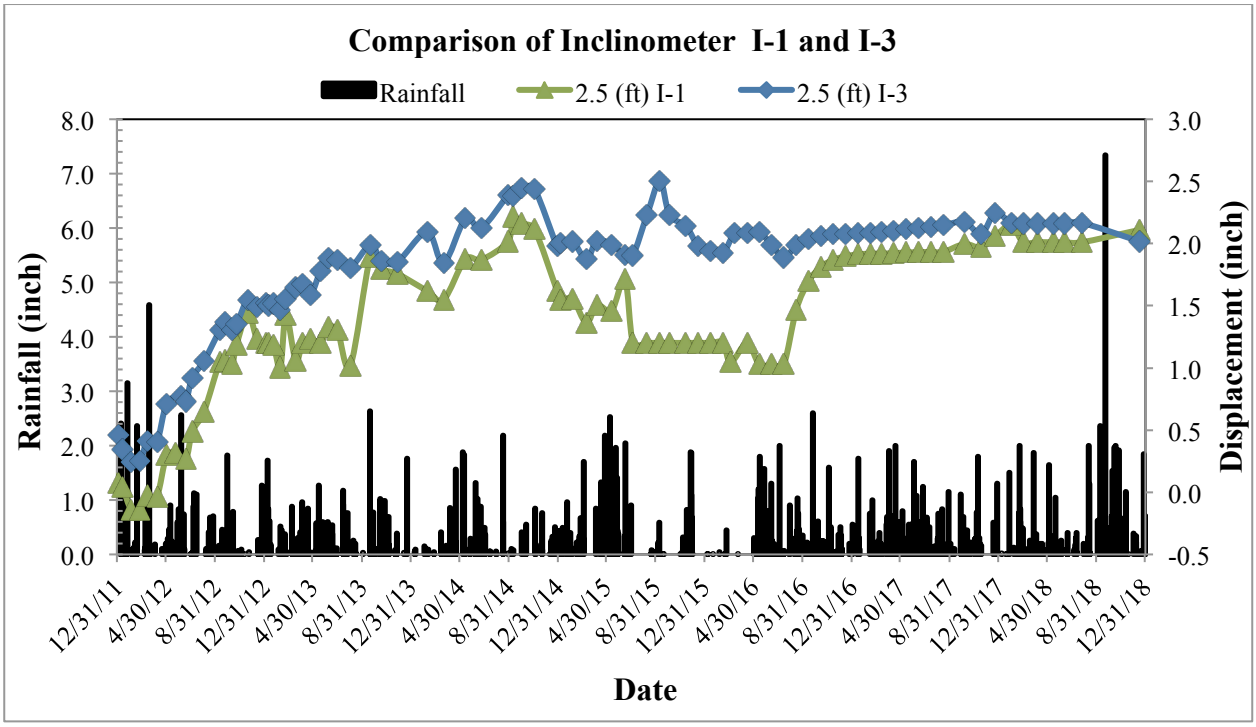

Figure 4- 8 Comparison at 2.5 ft. depth of Inclinometers I-1 and I-3 at US-287 slope

4.2 Performance Monitoring of I-35 Slope

The performance monitoring of the I-35 slope included a monthly site visit using a total station for the topographic survey and an inclinometer to measure the displacement. The results obtained for the Mockingbird slope are summarized in the subsequent sections.

4.2.1 Topographic Survey

The crest of the Mockingbird slope was routinely measured on a monthly basis during each site visit. In order to observe the performance of the RPP, the cracks that had developed on the shoulder prior to installation were left intact and unsealed. Figure 4-9 displays the total settlement at the crest of the I-35 slope while Table 4-3 displays the yearly maximum total settlement experienced.

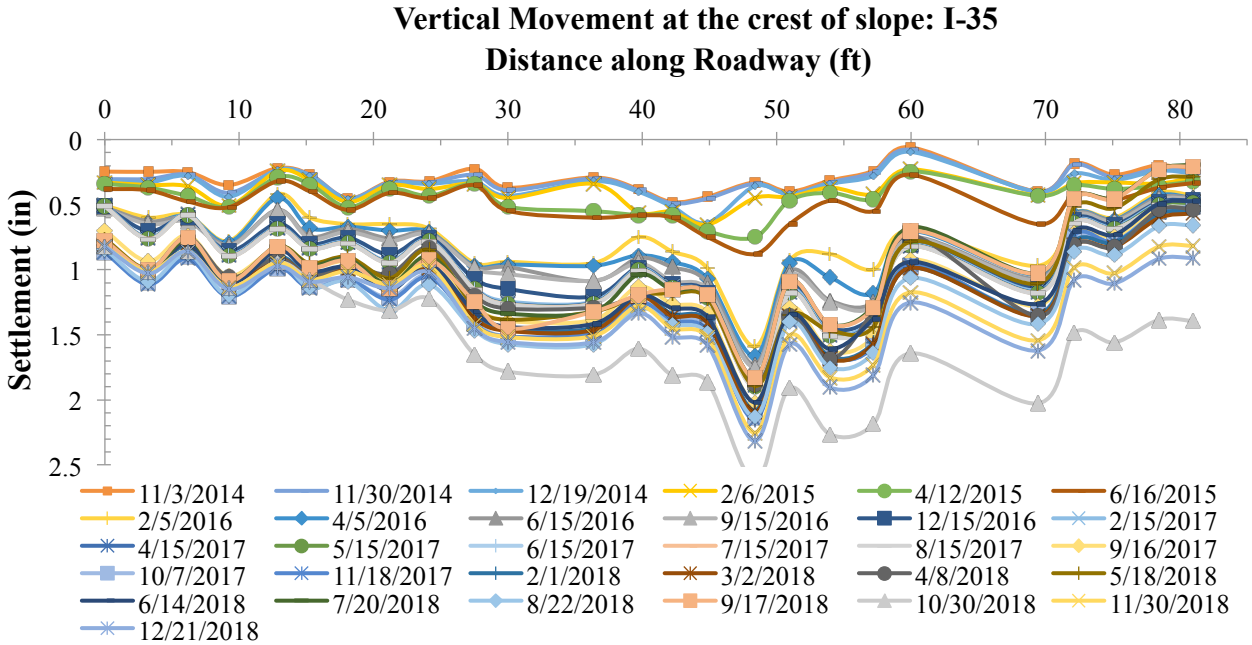

Figure 4- 9 Settlement at the crest of I-35 Slope

Table 4- 3 Maximum total settlement experienced at I-35 slope

	Maximum Total Settlement (in.)				
	2014	2015	2016	2017	2018
I-35 Slope	0.67	1.46	1.84	2.15	2.63

Based on Figure 4-9, the maximum total settlement experienced by the reinforced section of the slope does not exceed 2.65 in. over the 5-year span. Despite October 2018 displaying a trend with incremental settlement from the previous month approaching 0.75 in. at certain locations, it could potentially be related to human error in the input of the height of the total station used. While the maximum settlement experienced each year is around 0.5 in., after prolonged rainfall in the Fall 2018, the egregious crack that was left unsealed further expanded and began to shift. Figure 4-10(a) through (c) displays the settlement and bulging of the slope in particular locations from August 2018 to November 2018.

(a)

(b)

(c)

Figure 4- 10 Gradual settlement experienced at the crest (a) August 2018, (b) September 2018 and (c) November 2018

Figure 4-11 (a) through (c) views the shoulder crack from the position of the overpass on I-35 near the bridge abutment.

(a)

(b)

(c)

Figure 4- 11 Settlement of shoulder in successive months (a) August 2018, (b) September 2018 and (c) November 2018

The crack that was observed from the beginning of installment of the RPP at the I-35 slope experienced both an increase in width and depth with multiple wetting and drying cycles. In reference to the time frame depicted in Figures 4-11(a) through (c), the Dallas area experienced two distinct rainfall events in which the precipitation was in excess of 13 in. For the months of September and October 2018, the rainfall experienced in the Dallas area was 15.30 in. and 13.39 in., respectively. The recent influx of heavy rainfall, seen in the increase of yearly precipitation in 2018 as compared to previous years in Table 4-4, as well as the degradation of the shoulder crack itself could be linked with the steady increase in settlement measured. With the increase in crack depth and width on the shoulder, it is possible that the amount of runoff that would be experienced on the slope has decreased, with the precipitation infiltrating into the slope by means of the crack acting as a conduit. The potential increase of water in the slope can reduce the shear strength of the soil, causing an increase in the settlement experienced over time.

Table 4- 4 Yearly precipitation for Dallas Area

	Yearly Precipitation (in.)				
	2014	2015	2016	2017	2018
I-35 Site	3.88	68.02	38.48	33.23	55.29

The location of the crack on the shoulder, where the highest settlement was experienced on the slope, is local to the removal of where a drilled shaft was previously located. While more pins were added once removed, voids could have been created leading to increased settlement as well as slight bulging on the slope from continual water infiltration. A depth of nearly 2 ft., reaching the subgrade, expresses the extent of the crack condition and a width of nearly 1 ft. as can be seen in Figure 4-12(a) and (b).

(a) (b)

Figure 4- 12 Characteristics of crack on shoulder of I-35 (a) crack 2 ft. depth and (b) crack 1 ft. length

Although the cracks on the shoulder are excessive, the overall settlement experienced by the slope has not been representative. With the RPP reinforcement, the maximum total settlement experienced was 2.65 in. near the mid-span of the slope, while the majority of the settlement rests in the 1.5 in. to 2 in. range.

At the location of Inclinometer 2, the soil around local RPP had begun to separate. With loss of soil contact nearly at a foot, the pins are still offering enough resistance against sliding to keep the slope intact. Figure 4-13 shows the condition of the pins relative to Inclinometer 2.

(a) (b)

Figure 4- 13 Condition of slope on I-35 displaying (a) loss of contact between RPP, inclinometer and soil and (b) 1 ft. loss of contact soil on RPP

It could be inferred that without the slope reinforcement from the RPP, the high intensity rain experienced, and the further deterioration of the crack at the crest, the slope may have experienced failed.

4.2.2 Inclinometer

The inclinometers were measured on a monthly basis along with the topographic survey site visits. The cumulative displacements with time for Inclinometer I-1 through I-3 are presented in Figures 4-14, 4-15, and 4-16.

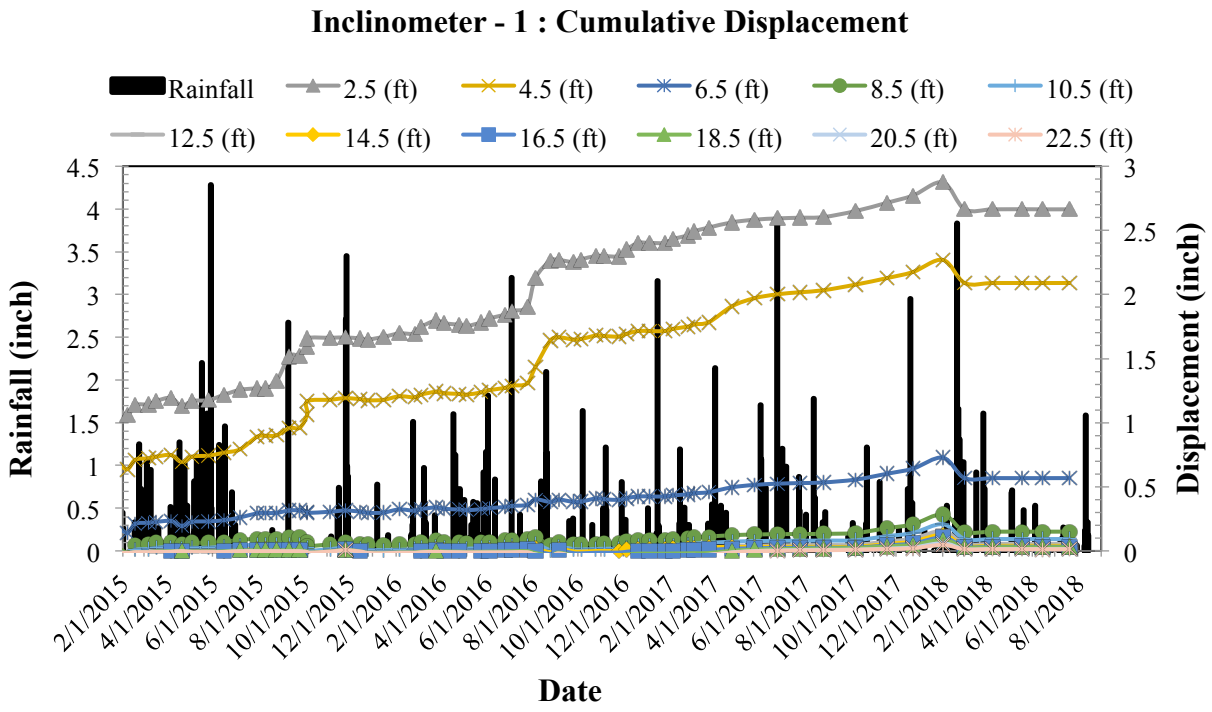

Figure 4- 14 Displacement in Inclinometer I-1 at I-35

Inclinometer I-1 (Figure 4-14) displayed an increasing trend in the displacement experienced in the top 4.5 ft. of measurement. At a depth of 2.5 ft., the maximum displacement was approximately 2.80 in. Looking at the displacement values each year, beginning in February 2015, the inclinometer saw an average yearly increase of 0.6 in. Table 4-5 shows the yearly incremental change for Inclinometer I-1.

Table 4- 5 Yearly incremental change in displacment Inclinometer I-1

	Incremental Displacement (in.)		
	2015-2016	2016-2017	2017-2018
I-1	0.63	0.74	0.44

The reduction seen after February 2018 can potentially be explained by the overall movement the slope had experienced and the loss of contact between the soil and the inclinometer casing. The data presented in the Inclinometer I-1 graph ends after August 2018 due

to the exacerbation of the shoulder crack near the crest of the slope at the location of Inclinometer I-1. Due to the movement of the slope from an increase in rainwater infiltration, the inclinometer will no longer take readings for the depth of the inclinometer casing, stopping at a depth of approximately 8 ft. Figure 4-15 displays the current condition of Inclinometer I-1.

Figure 4- 15 Condition of I-35 slope near Inclinometer 1

Inclinometer 2 (Figure 4-16) displayed a jump in displacement after the removal of the drilled post in the Fall 2015. After the maximum displacement, approximately 0.97 in., the cumulative displacement did not fluctuate much. Past the top 2.5 ft., the displacement measured is negligible. Inclinometer 3 (Figure 4-17), located at the toe of the slope, experienced a maximum cumulative displacement of approximately 2 in. at a depth of 2.5 ft. Similar to the trend seen by Inclinometer 1, for the depth of 2.5 ft., there is a gradual increase in the displacement measured however it remains generally within a range of 0.25 in. Additionally, the readings after a year showed an increase in the displacement felt at a depth of 4.5 ft. while all other depths displacements were negligible.

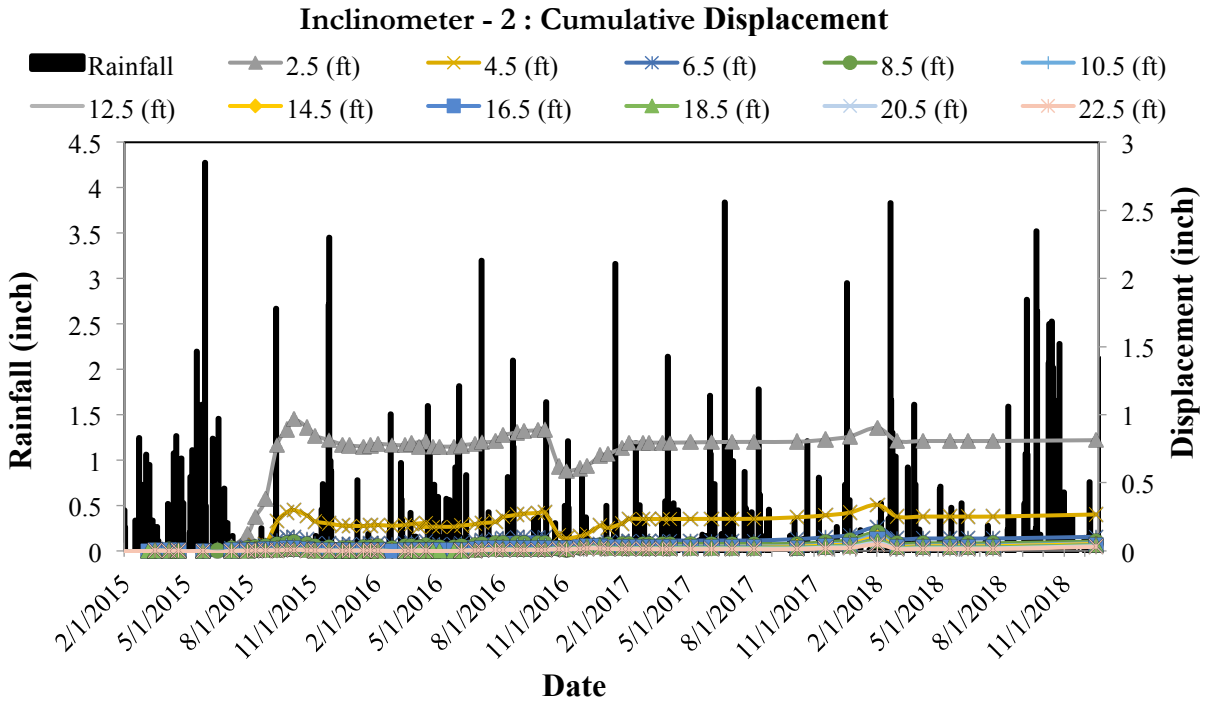

Figure 4- 16 Displacement in Inclinometer I-2 at I-35

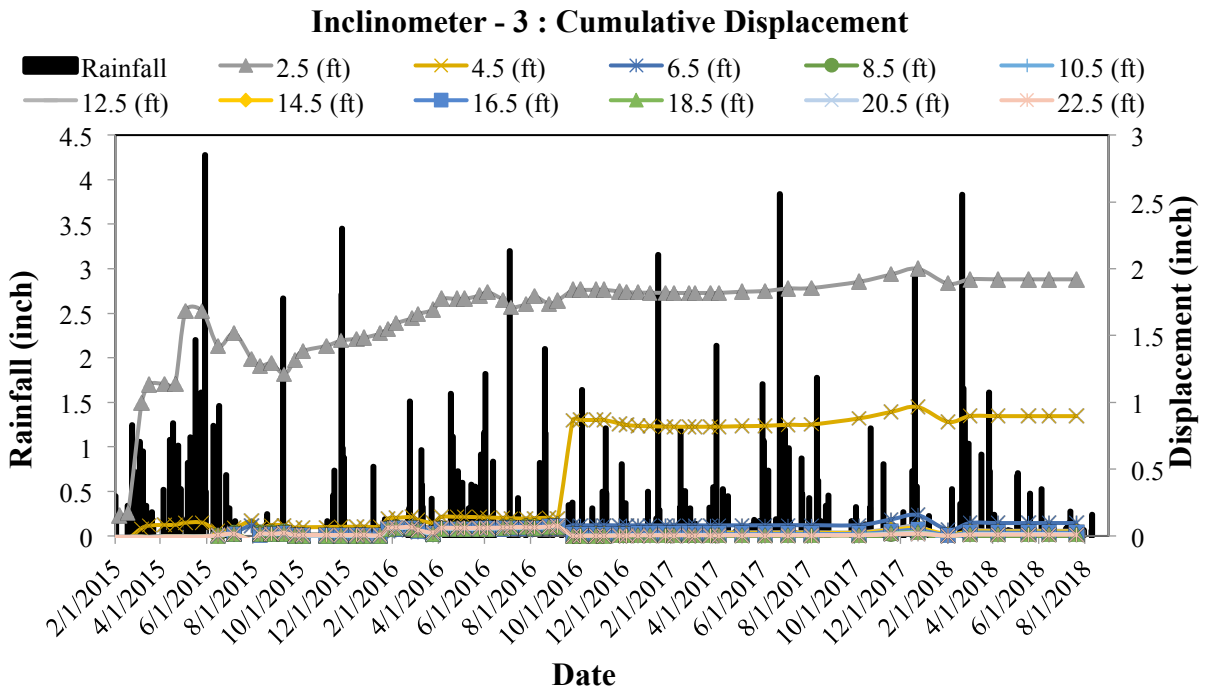

Figure 4- 17 Displacement in Inclinometer I-3 at I-35

4.3 Performance Monitoring of SH-183 Slope

The performance monitoring of the SH-183 slope included a monthly site visit using a total station for the topographic survey. Due to the steepness of the slope, no inclinometers were installed.

4.3.1 Topographic Survey

The total settlement over the crest of the slope was measured on a monthly basis and is presented in Figure 4-18.

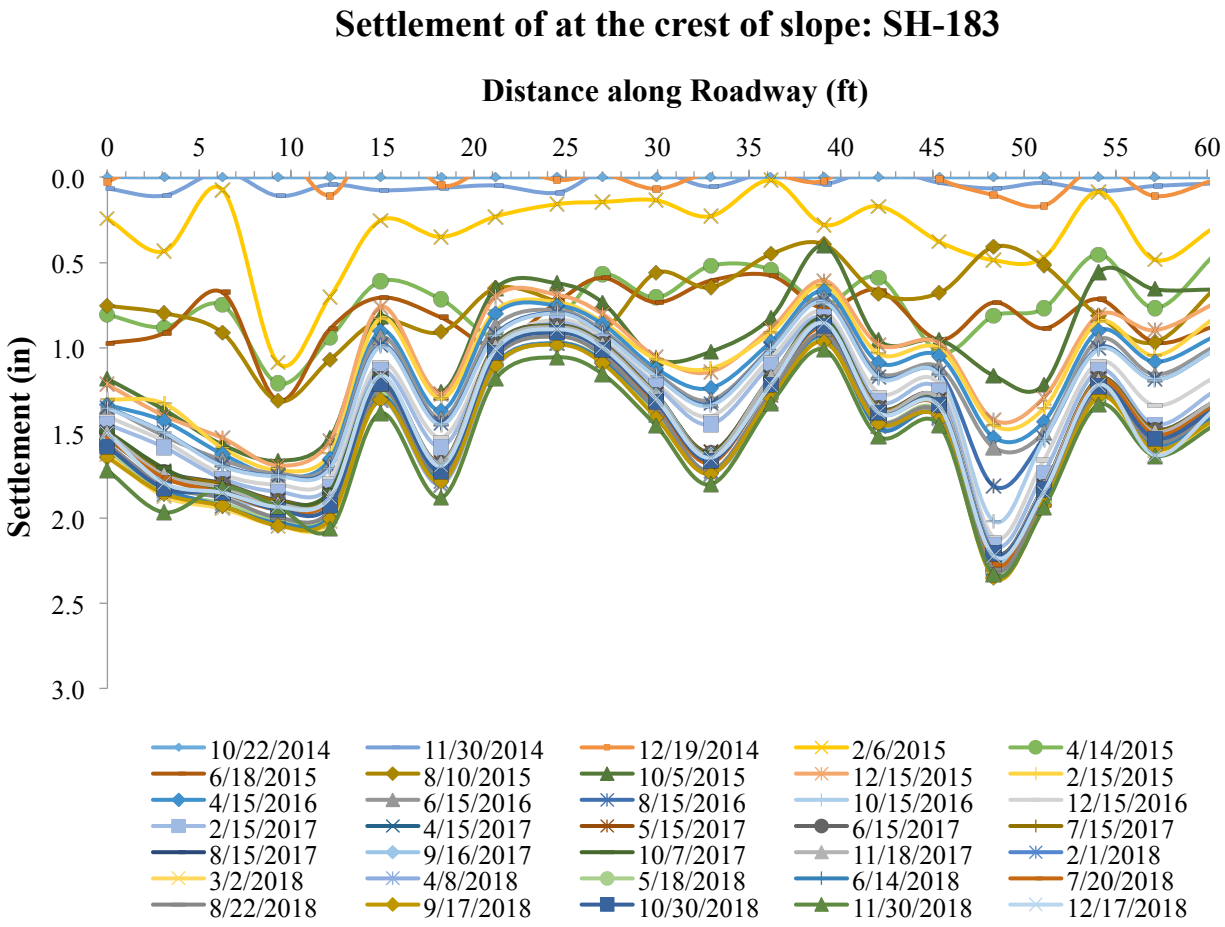

Figure 4- 18 Settlement at the crest of SH-183 slope

The maximum total settlement measured on the slope was measured at 2.35 in. Although 2015 to 2016 saw an incremental settlement of approximately 0.5 in., from 2016 until 2018, incremental settlement has reduced, measuring at approximately 0.1 in. The maximum total settlement of the slope each year is presented in Table 4-6.

Table 4- 6 Maximum total settlement for SH-183 slope

Maximum Total Settlement (in.)				
	2015	2016	2017	2018
SH-183 Slope	1.69	2.11	2.25	2.35

The performance of the slope can potentially be linked with the rainfall experienced in the region. During 2015, the slope location experienced approximately 68 in. worth of precipitation, with May, October, and November seeing the accumulation of rainfall being 14.98 in., 11.83 in., and 10.35 in., respectively. With the large influx of precipitation infiltrating the slope, the soil may have attained a state close to fully softened, weakening the soil and making it more prone to particle reorientation (Skempton A. W., 1985). This particle reorientation could potentially be attributed to the decrease in settlement experienced on the slope.

Chapter 5: Comparison of Site Performance

5.1 Comparison of US-287 Sections

The performance of the RPP reinforcement on the US-287 slope was observed to be beneficial in limiting the surficial movement of the slope. Despite the soil being susceptible to repeated wetting and drying cycles, as the cracks were left unsealed on the shoulder of the highway, the slope experienced limited settlement. Though it was previously discussed which reinforced sections had experienced the lowest maximum settlement, it is still important to understand the overall performance of each section in comparison to one another for future recommendations on projects. In order to better analyze each section, Figures 5-1 through 5-3 present enlarged plots of Reinforced Section 1, Reinforced Section 2, and Reinforced Section 3, respectively.

Beginning with Reinforced Section 1, Figure 5-1 displays a larger maximum settlement plot than previously displayed in the performance monitoring section. Approximately 50 ft. in length, Reinforced Section 1 was designed with various combinations of RPP lengths and spacing's. At the crest, however, 10 ft. long RPP were utilized at 3 ft. c/c spacing for the top third of the slope. It should be noted that for Reinforced Section 1, the shoulder cracks observed were not as severe as those present further along the roadway.

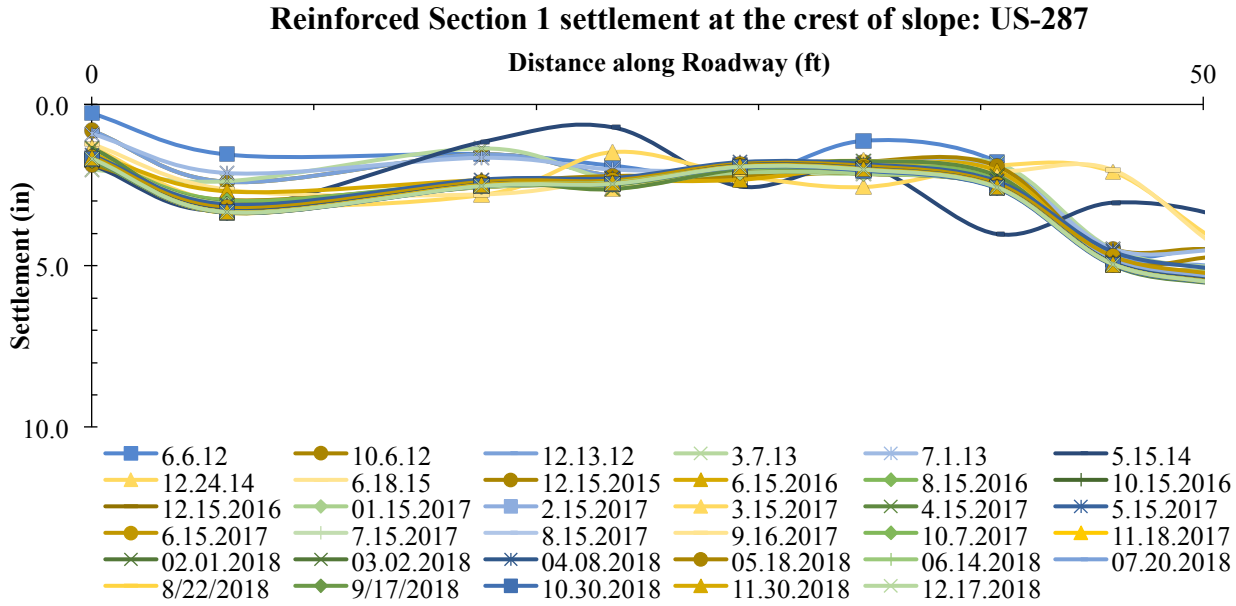

Figure 5- 1 Settlement along the crest of US-287 for Reinforced Section 1 (Distance along roadway from 0 ft. - 50 ft.)

Proceeding to Reinforced Section 2, Figure 5-2 presents the larger settlement plot from the performance monitoring section. Similar to Reinforced Section 1, Reinforced Section 2 was approximately 50 ft. in length. In contrast, however, Reinforced Section 2 possessed a simpler design scheme for the slope section, utilizing only two varying lengths at a constant spacing throughout. At the crest of the slope, 10 ft. long RPP were installed at 4 ft. c/c spacing for the top third of the slope. The shoulder cracking observed at the second reinforced section exhibited cracks far more extensive than those of the first reinforced section.

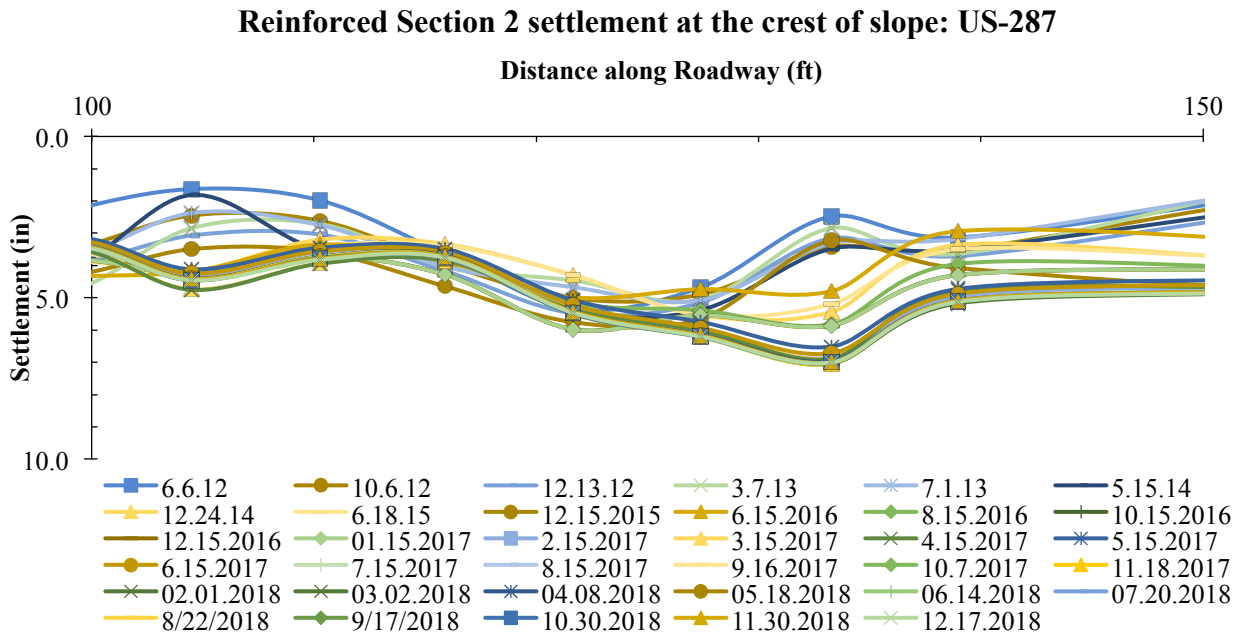

Figure 5- 2 Settlement along the crest of US-287 for Reinforced Section 2 (Distance along roadway from 100 ft. – 150 ft.)

Lastly, Reinforce Section 3 is presented in Figure 5-3. Still approximately 50 ft. in length as both Reinforced Section 1 and 2, Reinforced Section 3 contains a relatively constant reinforcement pattern, utilizing 10 ft. RPP at 4 ft. c/c spacing. At the crest, however, the top two lines of reinforcement are 10 ft. RPP at 3 ft. c/c spacing. The cracks that are observed at the crest of the slope in the third reinforcement location are similar those present in Reinforced Section 2.

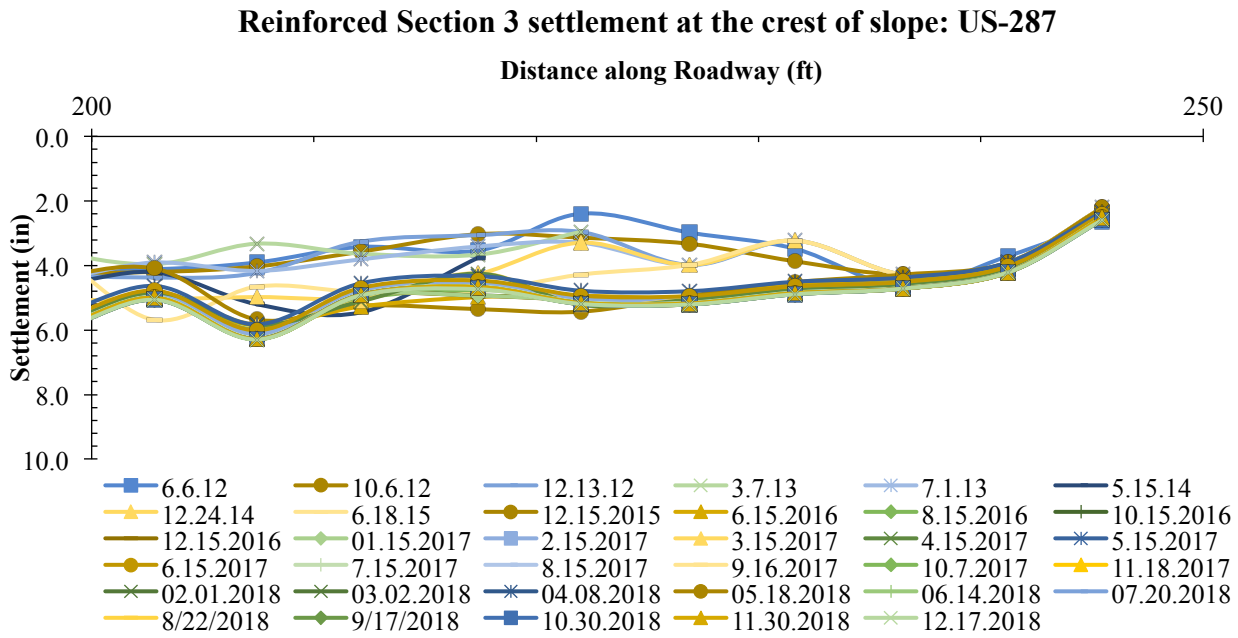

Figure 5- 3 Settlement along the crest of US-287 for Reinforced Section 3 (Distance along roadway from 200 ft. – 250 ft.)

As noted in the performance monitoring chapter, Reinforced Section 1 possessed the lowest maximum total settlement at 5.08 in., followed by Reinforced Section 3 with 6.30 in., and concluded with Reinforced Section 2 with 7.04 in. While these settlements are attributed to the maximum within each section (i.e. a single reference point), it does not adequately compare how each section, on average, is performing. Figure 5-4 presents the average incremental settlement of the three reinforced sections. Additionally, Table 5-1 presents the comparison between the three reinforced sections average incremental settlement.

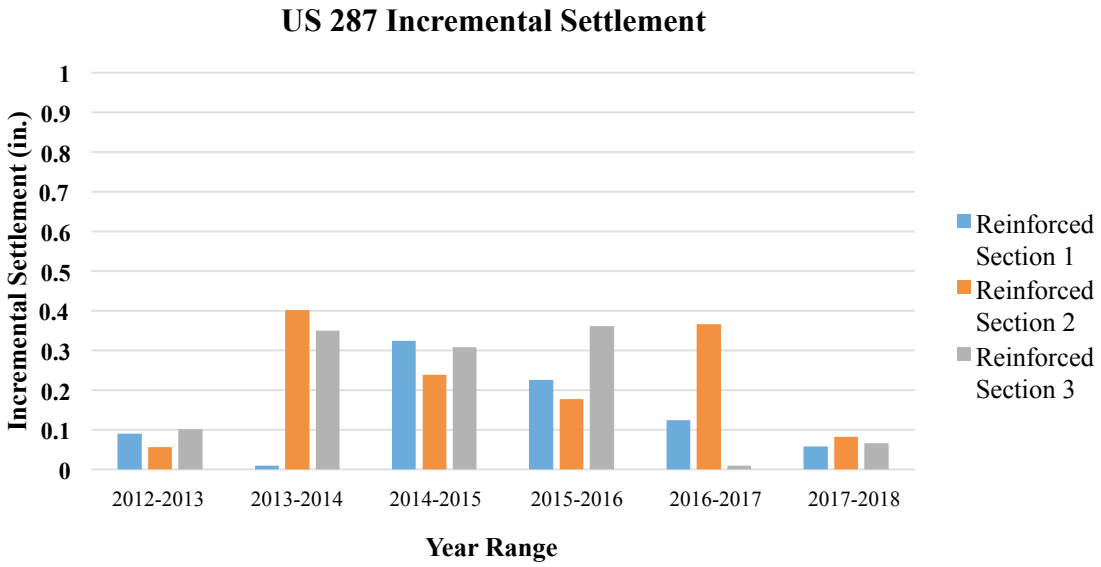

Figure 5- 4 Incremental settlement between reinforced sections of US-287

Table 5- 1 Incremental settlement values of reinforced sections of US-287

US-287 Slope			
Year	Reinforced Section 1	Reinforced Section 2	Reinforced Section 3
	Average Incremental Settlement (in.)	Average Incremental Settlement (in.)	Average Incremental Settlement (in.)
2012-2013	0.09	0.06	0.10
2013-2014	0.01	0.40	0.35
2014-2015	0.32	0.24	0.31
2015-2016	0.23	0.18	0.36
2016-2017	0.12	0.37	0.01
2017-2018	0.06	0.08	0.07

From both Figure 5-4 and Table 5-1, it can be observed that the incremental settlement experienced in the three sections has generally shown a decrease. While each reinforced section experienced a fluctuation in the general trend, the overall settlement experienced for each of the three sections was not in excess of 2 in. on average for a time span of 7 years of monitoring. Similar to the comparison of the maximum settlements recorded, the order in which the reinforced sections experienced the lowest total incremental settlement was Reinforced Section 1 (0.83 in.), Reinforced Section 3 (1.20 in.) and lastly Reinforced Section 2 (1.33 in.), respectively.

Reinforced Section 1 presented the lowest overall incremental settlement. The sections performance could be related to the relative spacing implemented in the section, including multiple rows of RPP spaced at 3 ft. c/c, as well as the lower prevalence of cracking on the shoulder. Reinforced Section 3 performed similar to Reinforced Section 2 on average. Despite having the first two lines reinforced at a spacing of 3 ft. c/c, similar to Reinforced Section 1, Reinforced Section 3 also had prevalent cracking on the shoulder of the US-287 highway similar to Reinforced Section 2. In addition, after the two lines of reinforcement at 3 ft. c/c, the spacing then increased similar to Reinforced Section 2 at 4 ft. c/c. The closer spacing may have attributed to the sections slightly better performance in comparison to Reinforced Section 2, however with the cracks present, the infiltration of precipitation could have affected the performance due to soils repeated shrinking and swelling.

5.1.1 Cost Analysis of US-287 Sections

The installment of RPP in the US-287 slope site was performed by a crawler-type drilling rig that included a mast-vibrator hammer (Model: Klemm 802 drill rig along with KD 1011 percussion head drifter) (Khan, 2013). The drilling rig was chosen after Bowders et al. (2003) deemed the mounted hammering system maintained the alignment of the hammer while restricting additional lateral load during the driving process of the RPP. First observed in the schematic of the design grid of RPP for US-287, Table 5-2 presents the amount of RPP, size ratios, and the total cost associated with the material of the RPP for each reinforced section.

Table 5- 2 Total RPP and cost per reinforced section

	Reinforced Section 1		Reinforced Section 2		Reinforced Section 3	
	RPP (4"x4"x10')	RPP (4"x4"x8')	RPP (4"x4"x10')	RPP (4"x4"x8')	RPP (4"x4"x10')	RPP (4"x4"x8')
Total RPP in Section	141	51	125	88	246	0
Cost per RPP ($)	75	50	75	50	75	50
Total Cost RPP ($)	13125		13775		18450	

The average driving time of RPP for each reinforced section was recorded by Khan (2013). It was determined, that on average, a total of 100 to 120 RPPs would be capable of being installed in a single day. Table 5-3 presents the average driving times recorded by Khan (2013) study.

Table 5- 3 Average driving time of RPP at US-287 slope (Khan, 2013)

Location of RPP	Length of RPP (ft.)	RPP Spacing (ft.)	Average RPP Driving Time (min)
	10	3	3.55
	10	6	4.76
	8	6	3.65
Reinforced Section 1	8	5	2.63
	10	4	2.76
Reinforced Section 2	8	4	3.08
Reinforced Section 3	10	4	4.65

Taking into account a mobilization fee and an average daily installment fee, based on previous projects quotations, it is then possible to create a simple cost benefit analysis of each reinforced section. The cost benefit analysis will consider the average cost associated with the slopes reinforcement based on the quotations that were obtained for each project. The findings of the costs associated with the reinforced sections are presented in Table 5-4.

Table 5- 4 Total cost of installment of RPP in each reinforced section

	Reinforced Section 1	Reinforced Section 2	Reinforced Section 3
Mobilization Fee ($)	6500	6500	6500
Daily Installment Fee ($)	3000	3000	4500
Days for Section Completion	2	2	3
Total Cost of Installment ($)	12500	12500	20000
Total Cost of Material ($)	13125	13775	18450
Total Cost of Section ($)	25625	26275	38450

From the average costs associated with the completion of the project, it can be seen that Reinforced Section 1 had the lowest cost of completion (approximately 25,700 USD), followed by Reinforced Section 2 (approximately 26,300 USD) and Reinforced Section 3 (approximately 38,500 USD), respectively. As the cost associate with mobilization and installation are constant, the variables present in the cost benefit analysis are the days necessary to complete the section and the amount of RPP needed to reinforce the slope. Reinforced Section 1 not only experienced the lowest incremental settlement of the three reinforced sections, it was also the most economical grid design. The benefit that was observed for Reinforced Section 1 in terms of settlement is explained, in part, due to reduced presence of shoulder cracking, but also the close spacing for the approximately 17 ft. of the slope face. With the spacing of the RPP being closest at the crest of the slope, where rainfall can potentially infiltrate deeper into the slope, it was not necessary to heavily reinforce the middle and toe of the slope, reducing the amount of pins needed to obtain an adequate factor of safety. This benefit, in the reduction of pins, in comparison to Reinforced Sections 2 and 3 yielded a lower material cost and on occasion a

reduction in the days necessary to complete installation. Table 5-5 presents the associated cost per square foot of the three reinforced sections.

Table 5- 5 Cost per square foot of reinforcement for US-287 sections

	US-287		
	Reinforced Section 1	Reinforced Section 2	Reinforced Section 3
Total Cost ($)	25625	26275	38450
Area Covered	50 ft. x 73 ft.	50 ft. x 73 ft.	50 ft. x 73 ft.
Cost/Sq. Ft. ($)	7.02	7.20	10.55

5.2 Comparison of I-35 Sections

While the I-35 slope was composed of a single reinforcement scheme, it is possible to analyze the slope into three sections also. Broken into sections denoted S1, S2 and S3, Figure 5-6 displays the distance along the roadway associated with each taken section. S1 is the section closest to the bridge abutment, spanning 0 ft. to 30 ft. along the I-35 highway. This section possesses cracks along the shoulder approximately 1 in. in width for the 30 ft. section, with larger cracks becoming prevalent nearing section S2. S2 was denoted as the section 30 ft. to 60 ft. along the roadway and is local to the removal of a drilled shaft in the slope. As previously mentioned, the removal of the drilled shaft potentially could have led to the development of voids in the slope causing additional settlement, this settlement was observed on the crest as the cracks that had previously been present were exacerbated, widening and deepening further into the slope. S3 is the section of the slope furthest from the bridge abutment, spanning a length along the roadway of 60 ft. to approximately 80 ft. For section S3, similar to S1, cracks were prevalent however only approximately 1 in. to 2 in. in width. Figures 5-5 through 5-7 present the three sections individually.

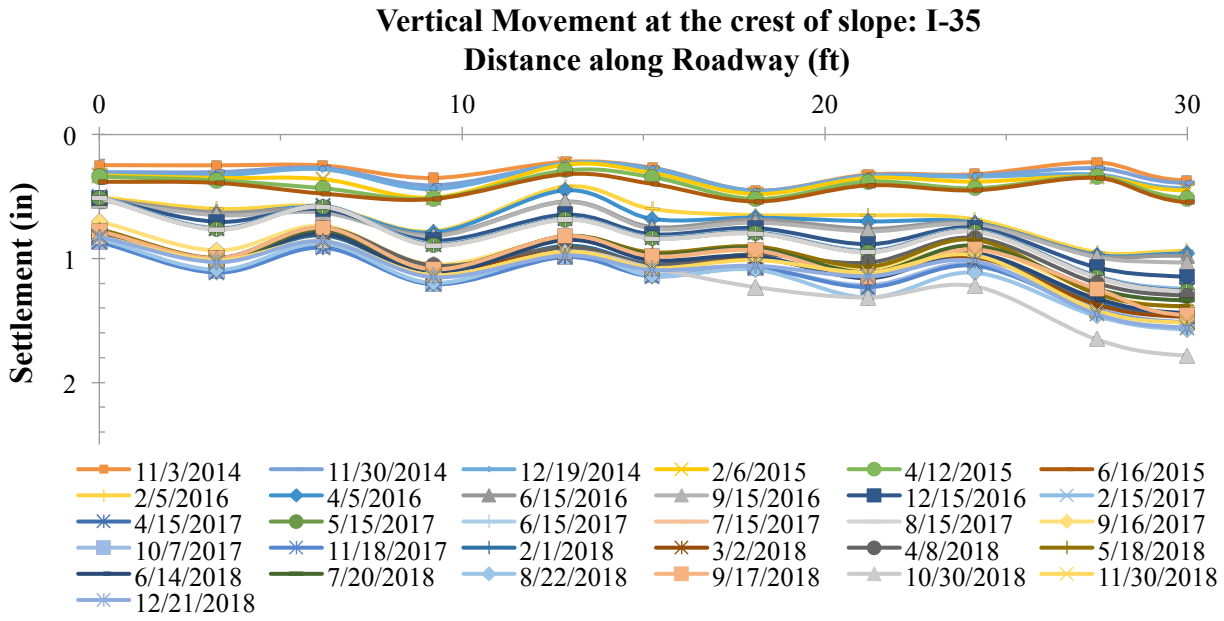

Figure 5- 5 Settlement at crest for I-35 slope Section S1

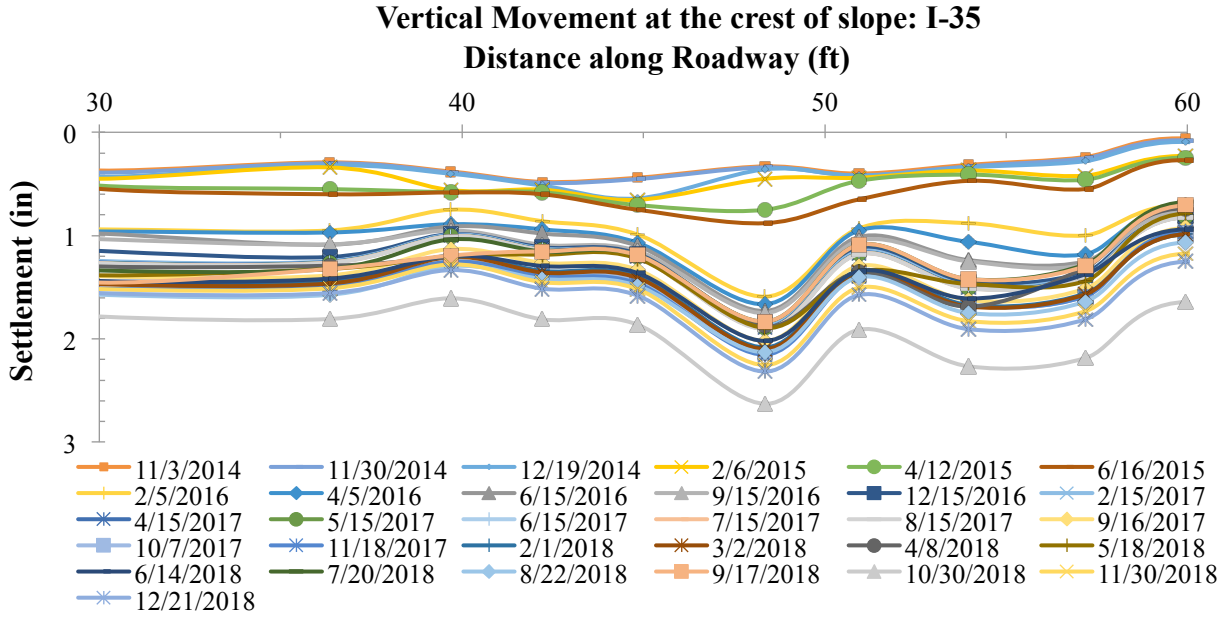

Figure 5- 6 Settlement at crest for I-35 slope Section S2

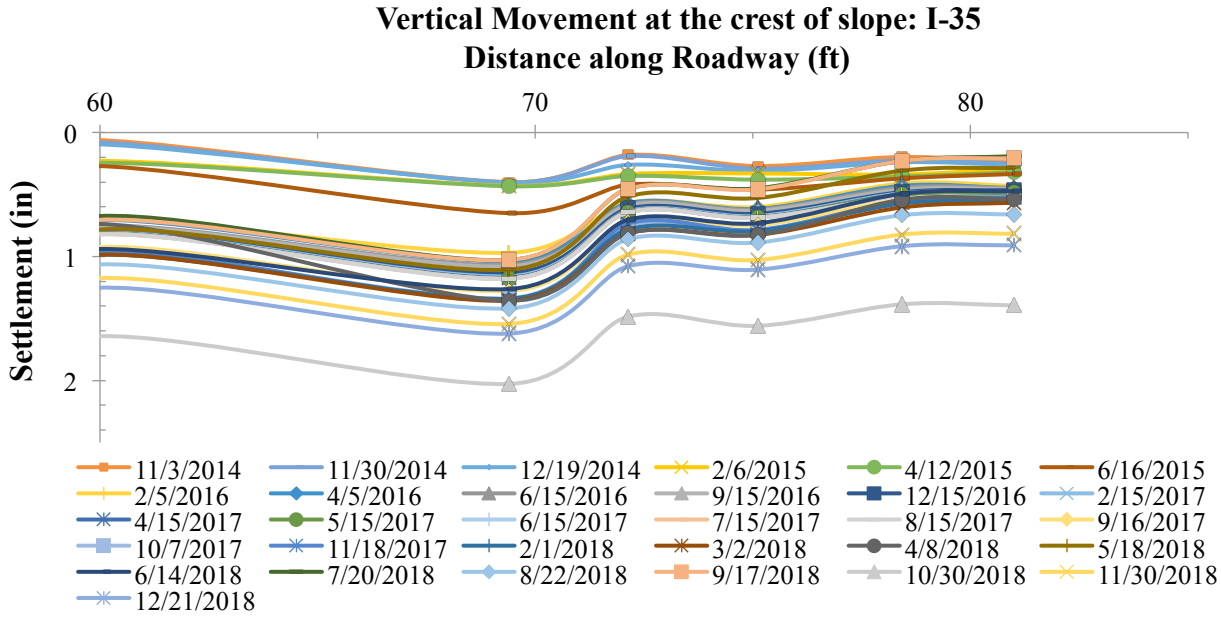

Figure 5- 7 Settlement at crest for I-35 slope Section S3

All three of the sections possess a crest reinforcement spacing of 3 ft. c/c, however it is the influence of the crack that is the purpose of the section breaks. Presented in Figure 5-8, Sections S1 and S3 performed similarly in contrast with Section S2. Both Section S1 and S2 contain cracks on the shoulder of the highway, however they are not to the extent of Section S2. From Figure 5-6, the crack can be observed in the total settlement plot occurring approximately around the 45 ft. to 50 ft. length along the roadway section. The removal of a drilled post during the 2015-2016 year transition affected the slopes performance within the section due to the potential voids created after its removal. While the section was reinforced, the potential void and rainwater infiltration could be linked with the cracks worsening. Table 5-6 presents the impact of the removal of the drilled post on the incremental settlement of the reinforced section. The average incremental settlements for sections S1, S2 and S3 are 0.19 in., 0.28 in., and 0.15 in., respectively.

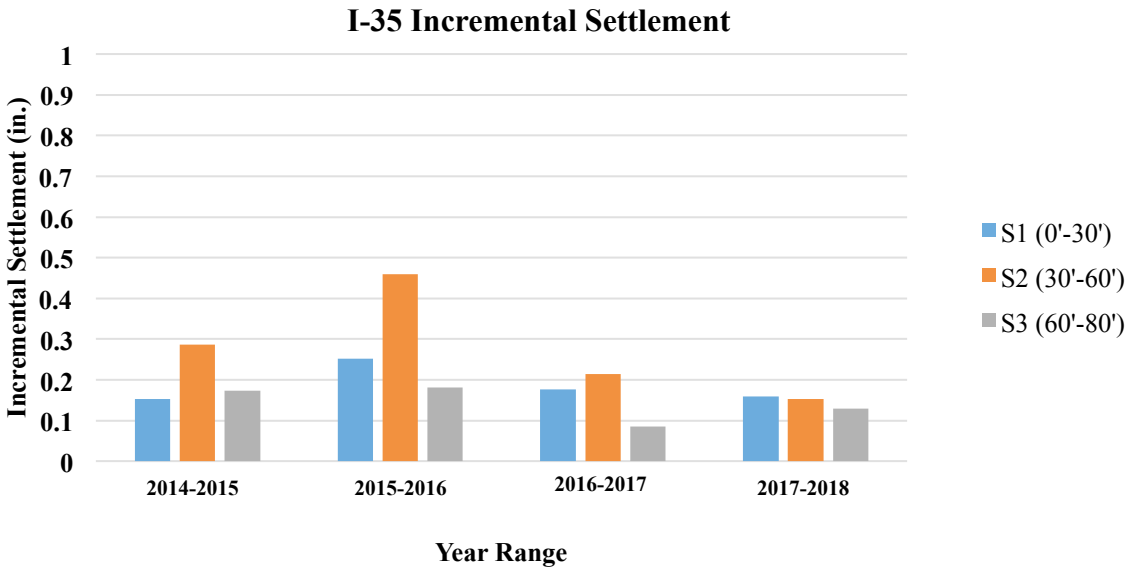

Figure 5- 8 I-35 Incremental settlement

Table 5- 6 I-35 Average incremental settlement of slope sections

I-35 Average Incremental Settlement (in.)				
	2014-2015	2015-2016	2016-2017	2017-2018
S1 (0'-30')	0.153	0.252	0.177	0.159
S2 (30'-60')	0.286	0.46	0.215	0.153
S3 (60'-80')	0.174	0.182	0.086	0.129

5.2.1 Cost Analysis of I-35 Sections

Tamrakar (2015) recorded the installation process for the RPP installment at the I-35 slope. For the installment of RPP in the I-35 slope, a crawler mounted rig with pseudo vibratory hammer (Model: Casagrande M9-1) was initially utilized. While in other studies the crawler mounted rig worked well, due to the steepness of the I-35 slope near the crest, installation was halted and a change in machinery was necessary due to safety issues. The installment of the RPP resumed with an excavator equipped with Hydraulic breaker (Model: deer 200D with FRD, F22

hydraulic hammer). The excavator worked well with the slope and the installment was able to be completed after two days. The second phase of the installation utilized a Caterpillar rig with the hydraulic hammer CAR H130S (Model: CAT 32D LLR). Due to the stiffness of the soil, based on previous soils stabilization measures and the time of year the installment occurred, 251 pins were installed in the slope. Table 5-7 presents the amount of RPP, size ratio, and the total cost associated with the material for the RPP of the section.

Table 5- 7 Total RPP and material cost for I-35 slope

I-35 Reinforced	
	4"x4"x10'
Total RPP in Section	251
Cost per RPP ($)	75
Total Cost RPP ($)	18825

While the average driving times of the RPP were not recorded, the time necessary for the slope reinforcement was approximately 4 days (2 different installment dates). Similar to US-287, the cost associated with the slopes reinforcement includes a mobilization fee, an average daily installment fee, based on previous quotations of projects, as well as the total cost of material. With this information, Table 5-8 presents the average cost associated with the slope reinforcement.

Table 5- 8 Total cost of installment of RPP in I-35 slope

I-35 Slope		
	Phase 1	Phase 2
Mobilization Fee ($)	6500	6500
Daily Installment Fee ($)	4500	4500
Days for Completion	2	2
Total Cost of Installment ($)	15500	15500
Total Cost of Material ($)	9750	9075
Total Cost ($)	49825	

Based on the average costs associated with the completion of the I-35 slope project, it can be seen that the total cost is approximately 50,000 USD. The slight increase in cost can be attributed to the difficulty of the slope. As the slope has failed in the past, the lime stabilization measure that occurred in the past, presented difficulties in the RPP installment as some pins encountered a stiff zone (Tamrakar, 2015). Additionally, the lack of space in comparison to US-287 and the steepness of the crest of the slope also played a role as the change of machinery necessitated an additional installation phase.

5.3 Comparison between US-287 and I-35 slopes

Comparing the US-287 slope and the I-35 slope, there are some noticeable similarities. Based on the average incremental settlement of each slopes sections, it was found that Reinforced Section 1 from the US-287 slope had performed the best, having an average incremental settlement of approximately 0.14 in. While other sections had not performed as well as Reinforced Section 1, Reinforced Section 2 from the US-287 slope performed similar to the S2 section developed for the I-35 slope and Reinforced Section 3 of the US-287 slope performed similar to S1 and S3 section of the I-35 slope. Figures 5-9 and 5-10 present the incremental settlement between the three reinforced sections of US-287 and the I-35 section as a whole as well as the incremental settlement difference between the three reinforced sections of US-287 and the three developed sections of I-35. Similarly, Table 5-9 presents the numerical values associated with the plots in Figures 5-9 to 5-10.

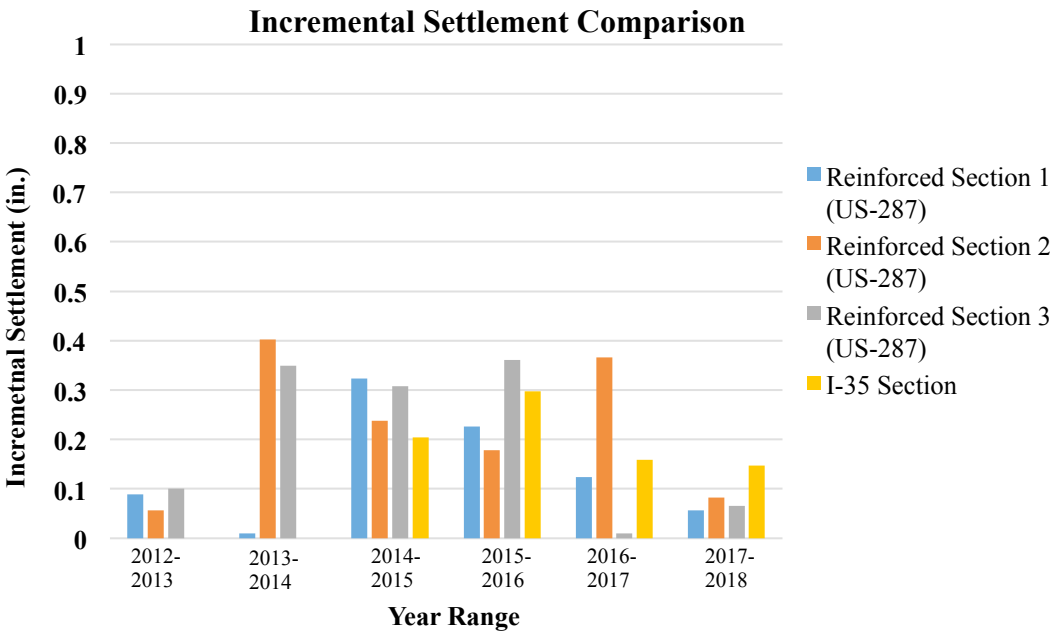

Figure 5- 9 Incremental settlement of US-287 slope reinforced sections 1, 2 and 3 and I-35 slope

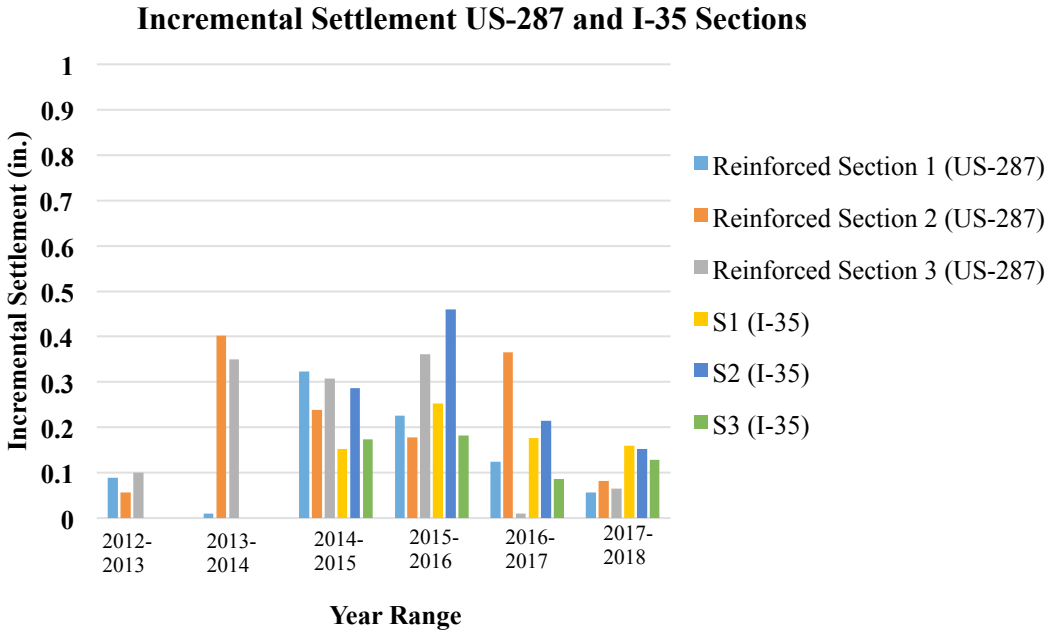

Figure 5- 10 Incremental settlement comparison of US-287 reinforced sections 1, 2 and 3 and I-35 slope reinforced sections S1, S2, and S3

Table 5- 9 Comparison of average incremental settlement between US-287 and I-35 slope sections

	Average Incremental Settlement (in.)					
	2012-2013	2013-2014	2014-2015	2015-2016	2016-2017	2017-2018
R1 (3' c/c)	0.09	0.01	0.32	0.23	0.12	0.06
R2 (4' c/c)	0.06	0.40	0.24	0.18	0.37	0.08
R3 (3' c/c)	0.10	0.35	0.31	0.36	0.01	0.07
S1 (0'-30')			0.15	0.25	0.18	0.16
S2 (30'-60')			0.29	0.46	0.22	0.15
S3 (60'-80')			0.17	0.18	0.09	0.13

As previously stated, Reinforced Section 1 for the US-287 slope performed the best in terms of an incremental settlement standpoint. Reinforced with RPP at a spacing of 3 ft. c/c for approximately the top 17 ft., the section had the greatest reinforcement on the crest of the slope in comparison to the other sections. In addition, the slope section possessed limited cracking on the shoulder of the US-287 highway, which potentially could have led to less water infiltration into the slope in comparison to other sections. Excluding the performance of Reinforced Section 1 in the comparison of all other sections, there are similarities in the performances of US-287 and I-35. Both slopes possessing a slope geometry of 3 (H): 1 (V), it is possible to investigate the shoulder cracks influence on the settlement of each slope as both slopes also possess high plastic clay. Looking first into the comparison between Reinforced Section 3 of US-287 and Sections S1 and S3 of I-35, the average incremental settlement settlements for the three sections were within the range of 0.20 in. Despite Reinforced Section 3 having only the top two lines of RPP spaced at 3 ft. c/c and then widening to 4 ft. c/c thereafter, the performance is still similar to I-35 sections S1 and S3, which are reinforced for the top six lines with RPP spaced at 3 ft. c/c. While cracks are well observed in Reinforced Section 3, as it was shown in the performance monitoring graph Figure 4-2 that the difference between the shoulder elevations was initially 5 in., the width of the crack is not excessive. For the I-35 section S1 and S3, the cracks are also well observed, and

while they are continuous throughout the designated section, the widths, also, are not excessive. The narrow cracks of S1, S3, and Reinforced Section 3 are in contrast to S2 and Reinforced Section 2, where the cracks have widened as well as being continuous. With the possibility of the cracks that are wider acting as a preferential flow path for water infiltration, it could potentially lead to why the two sections saw an increase of incremental settlement (approximately 0.25 in.).

In addition to looking at the performance, it is also necessary to look at the comparison of the sections in terms of cost. While it was noted which sections performed similarly, looking at the cost breakdown, it further helps to identify which sections performance is desirable for future projects design schemes. Tables 5-10 and 5-11 present the cost breakdown between the three reinforced sections of US-287 and I-35 as well as the entire US-287 and I-35 slope, respectively.

Table 5- 10: Cost per square foot of reinforcement for sections of US-287 and I-35

	US-287			I-35
	Reinforced Section 1	Reinforced Section 2	Reinforced Section 3	
Total Cost ($)	25625	26275	38450	49825
Area Covered	50 ft. x 73 ft.	50 ft. x 73 ft.	50 ft. x 73 ft.	50 ft. x 85 ft.
Cost/Sq. Ft. ($)	7.02	7.20	10.55	11.73

Table 5- 11 Cost per Square Foot of Reinforcement for Slopes US-287 and I-35

	US-287	I-35
Total Cost ($)	90350	49825
Area Covered	150 ft. x 73 ft.	50 ft. x 85 ft.
Cost/Sq. Ft. ($)	8.25	11.73

Based on the tables, it can be observed that Reinforced Section 1 utilized the RPP best in the stabilization measure as the section observed the lowest settlement while still being cost effective. While the I-35 slope (85 ft. x 50 ft.) encompassed an area approximately 15% more than that of the US-287 reinforced sections (50 ft. x 73 ft.), the average incremental settlement observed for Reinforced Section 1 was only 62% of the I-35 slope. Even comparing the entire section of US-287 to I-35, the cost per square foot of installation of RPP for slope stabilization is more than 3 USD for I-35. Comparing the average incremental settlement of US-287 with I-35, US-287 averaged among all sections approximately 0.19 in. while I-35 averaged 0.23 in.

5.4 Comparison of SH-183 Sections

Similar to I-35, SH-183 was a slope reinforcement project that consisted of a single section of reinforcement. For comparison purposes of the SH-183 slope, the slope was split into two sections of 30 ft. The two sections, denoted as S1 and S2, are presented in Figures 5-11 and 5-12. The top 30 ft. of reinforcement for the slope utilizes 10 ft. RPP at a 3 ft. c/c spacing grid. The slope geometry of the SH-183 slope is 2.5 (H): 1 (V).

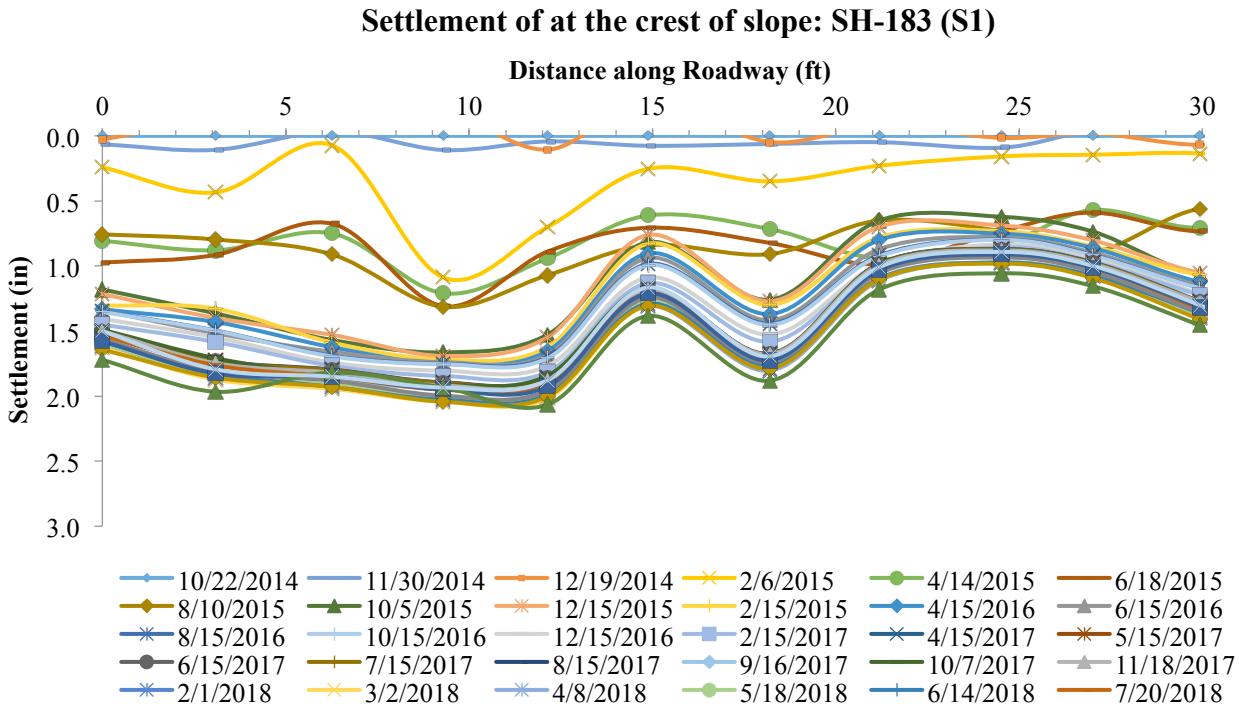

Figure 5- 11 Settlement at the crest of SH-183 slope (S1 Section)

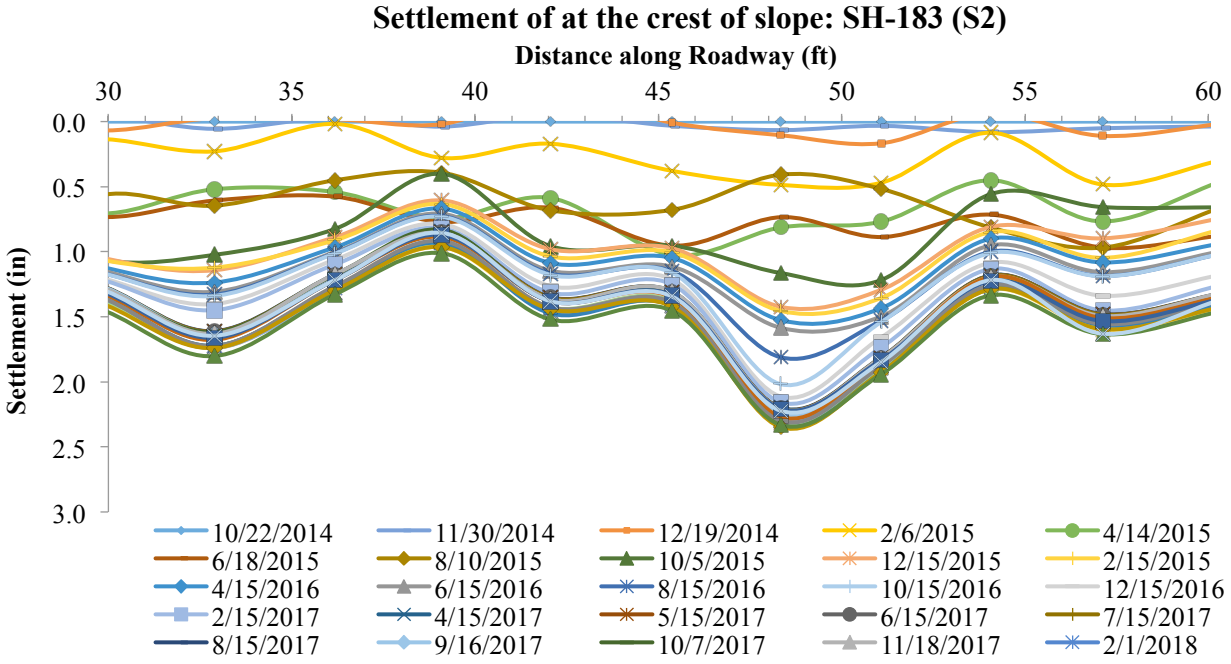

Figure 5- 12 Settlement at the crest of SH-183 slope (S2 Section)

From the graphs presented in Figures 5-11 and 5-12, it can be observed, on average, that the incremental settlement for the two sections performed nearly identical. This is portrayed in Figure 5-13 comparing sections S1 and S2 incremental settlements. From the figure, while the initial adjustment time for the RPP experienced higher measurements of settlement, on average approximately 0.70 in. during 2014 to 2015, the settlement observed decreased over time. After each yearly transition, it can be observed that the incremental settlement is reduced by half, approximately, in the next year transition.

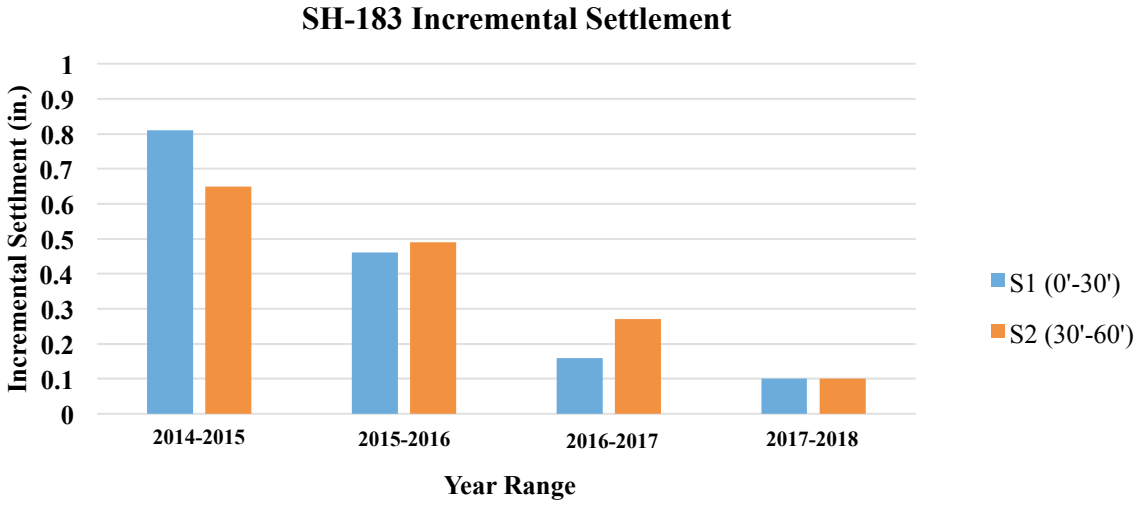

Figure 5- 13 SH-183 incremental settlement

5.4.1 Cost Analysis of SH-183 Section

Tamrakar (2015) additionally monitored the installment of the SH-183 slope. Similar to I-35, the SH-183 slope utilized a Caterpillar rig with a hydraulic hammer CAT H130S (Model: CAT 32D LLR). In order to more easily install the RPP into the soil, an iron nail was hammered into the ground initially. The iron nail was utilized due to the regions experience of a drought and dry summer, causing the soil conditions to be very stiff to hard in consistency. Table 5-12 presents the amount of RPP, size ratio, and the total cost associated with the material of the RPP

for each reinforced section. Table 5-13 presents the average drive time of the RPP with and without the use of the iron nail.

Table 5- 12 Total RPP and material cost for SH-183 slope

SH-183 Reinforced	
	4"x4"x10'
Total RPP in Section	425
Cost per RPP ($)	75
Total Cost RPP ($)	31875

Table 5- 13 Average RPP driving time (Tamrakar, 2015)

Location of RPP	Length of RPP (ft.)	RPP Spacing (ft.)	Average Iron Nail Hammering Time (mins.)	Average RPP Driving Time (mins)	Final Average Pin Installation Time (mins.)
W/O using Iron Nail	10	4	0	22.33	22.33
Using Iron Nail	10	3 to 4	2.92	2.71	5.64
			1.4	1.6	3
			0.93	1.23	2.16
			0.49	1.32	1.81
			1.31	1.36	2.67

For the SH-183 slope, approximately 100 RPP were able to get installed in a day's work without the disturbances of mechanical breakage, weather permitting. Taking into account a mobilization fee and an average daily installment fee, based on previous quotations of projects, a cost projection of the project can be done as the amount of days necessary to reinforce the slope can be concluded. Table 5-14 presents the total cost associated with the reinforcement of SH-183 slope.

Table 5- 14 Total cost of installment of RPP in SH-183 slope

SH-183 Section	
Mobilization Fee ($)	6500
Daily Installment Fee ($)	5500
Days for Completion	5
Total Cost of Installment ($)	27500
Total Cost of Material ($)	31875
Total Cost ($)	59375

Based on the table, a slight increase can be observed in the cost due to the condition of the soil. Similar to I-35, the condition of the soil caused an increase in cost due to the additional work necessary to properly push the pins into the ground. Having a very stiff to hard consistency, the holes that the RPP were to be placed in needed to first be pushed with an iron nail. Constantly nailing the soil led to a slight decrease in the number of pins that could be installed in a day.

5.5 Comparison between US-287, I-35, and SH-183 slopes.

Looking at the incremental settlement observed on the crest of the three reinforced slopes on US-287, I-35, and SH-183, certain similarities and comparisons can be made. Figure 5-14 presents the incremental settlement of the three slopes, with US-287 being broken up into its own individual three reinforced sections. From the plot, certain similarities are presented such as an increase in incremental settlement observed in the transition years 2014-2015 and 2015-2016. This could be attributed to the immense rainfall that occurred in both the Midlothian and Dallas/Fort Worth region of Texas during 2015. Plotted in Figures 5-15 and 5-16 are the precipitation graphs that display the daily, average, and monthly sum of precipitation experienced in the Midlothian and Dallas/Fort Worth area, respectively.

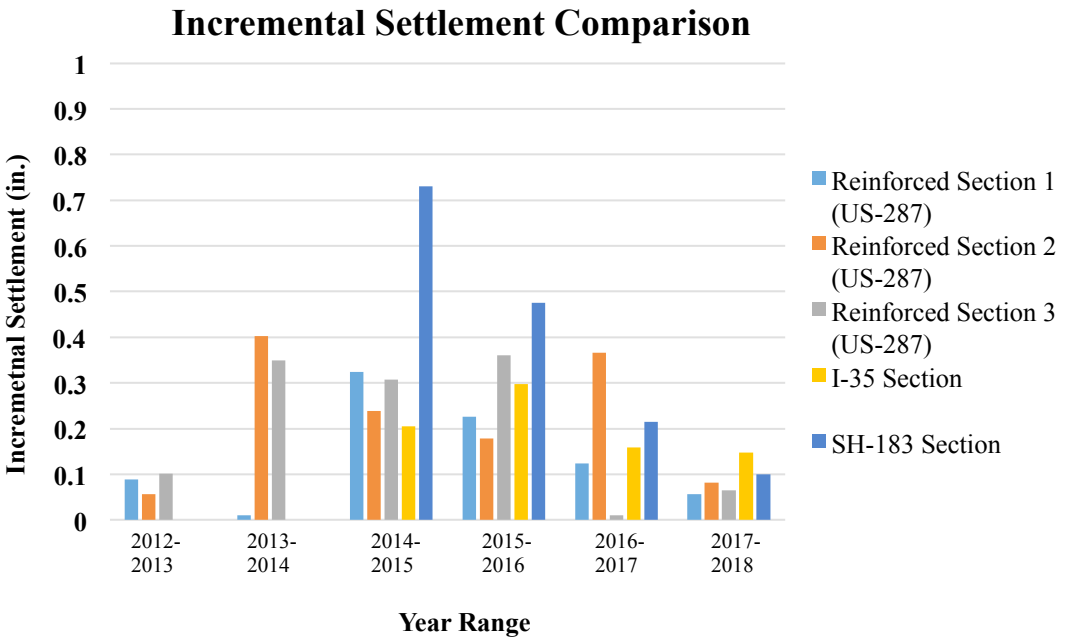

Figure 5- 14 Comparison of incremental settlement between US-287, I-35 and SH-183 reinforced sections

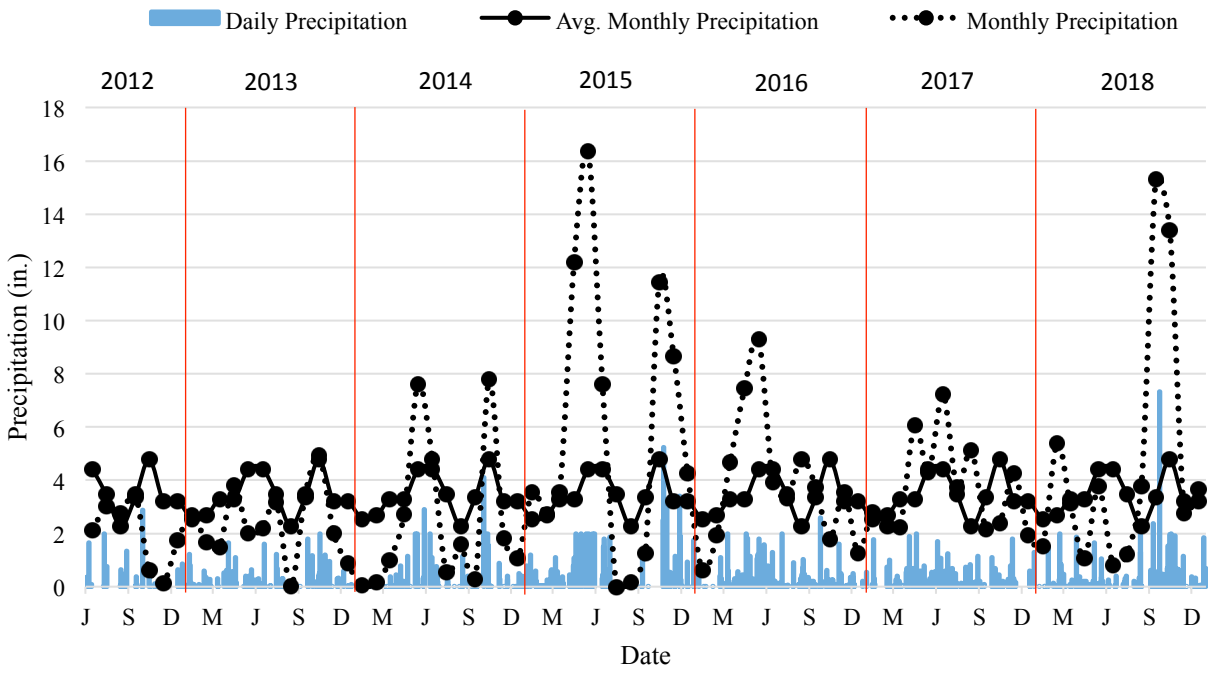

Figure 5- 15 Precipitation data for Midlothian, Texas (US-287 Slope Site General Location)

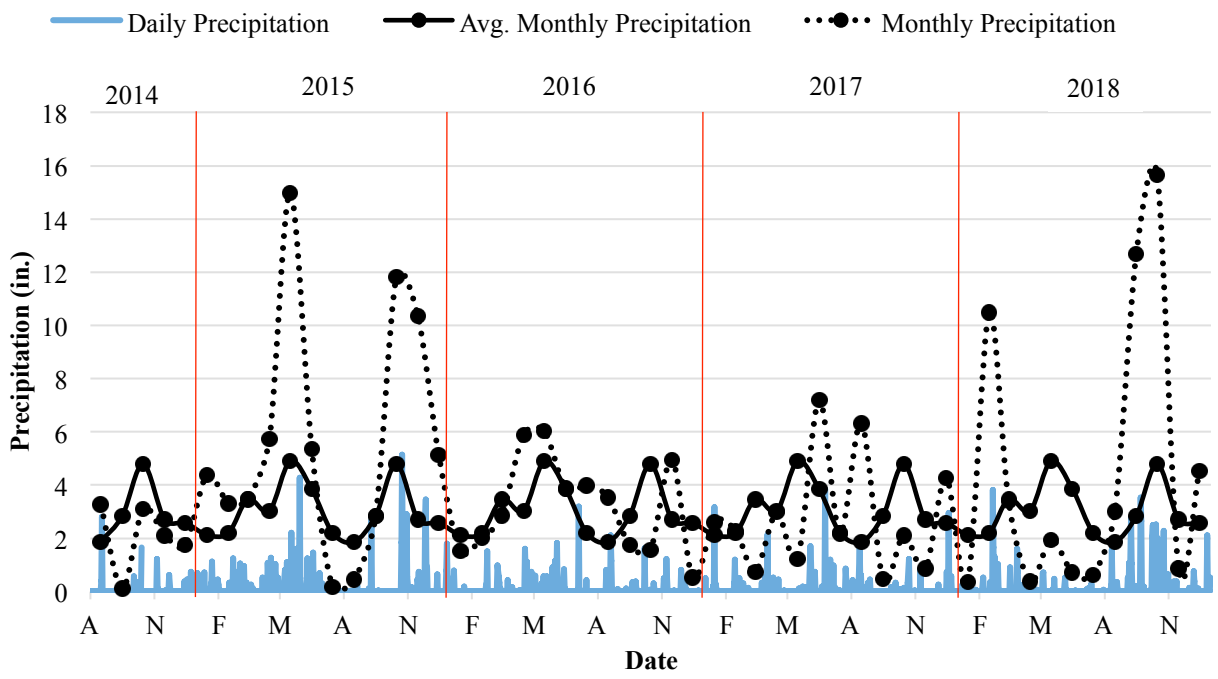

Figure 5- 16 Precipitation data for Dallas/ Fort Worth Area, Texas (General Location of I-35 and SH-183)

With such a high amount of rainfall observed in the regions where the slopes are located, the slopes would have experienced swelling initially, as the soil for the three slopes are either high plastic or low plastic clayey soils. After the swelling however, with the addition of higher temperatures, the soil could eventually lead the soil to a fully softened state, making the soil prone to more settlement. As 2016 experienced more normal levels of rainfall, the settlement for most sections saw in increase during the 2015-2016 transition year.

While all of the sections experienced certain increases in incremental settlement during one year transition or another, all three slope sections, US-287, I-35 and SH-183, all generally display a decrease in the incremental settlement over the five or seven year monitoring period. It can also be noted that during the monitoring period of 2017-2018, the three slope sections generally performed identical, having an incremental settlement less than 0.15 in. Additionally, while US-287 and I-35 experienced a gradual decrease in incremental settlement from year to

year, SH-183 experienced a more rapid decrease in incremental settlement, generally reducing by nearly half from year to year.

Being that the settlements for the three slopes generally merged to performing similar, with certain sections performing slightly better than others in the 2017-2018 monitoring period, it then is important to analyze the economic impact of the reinforced sections. In order to analyze the economic impact on the slopes, Table 5-15 presents the cost per square foot of the installation process of RPP for each section.

Table 5- 15 Cost per square foot of reinforcement for US-287, I-35 and SH-183

	US-287	I-35	SH-183
Total Cost ($)	90350	49825	31875
Area Covered	150 ft. x 73 ft.	50 ft. x 85 ft.	60 ft. x 90 ft.
Cost/Sq. Ft. ($)	8.25	11.73	5.90

Based on the associated cost, the SH-183 section recorded the lowest cost of total installation of RPP, followed by US-287 and concluded with I-35. While the cost of SH-183 is the lowest initially, when comparing the sections, US-287 provided the best cost benefit. Encompassing an area twice that of SH-183, the total cost per square foot for US-287 is only 40% more than SH-183, while having the sections that performed the best during the monitoring period. Additionally, the average incremental settlement for US-287 was approximately 0.2 in. in comparison to the average incremental settlement of 0.35 in. for SH-183.

Chapter 6: Conclusions and Future Recommendations

6.1 Summary and Conclusion

The current study observed the long-term performance of three slopes, US-287, I-35 and SH-183, utilizing RPP as a slope stabilization method. The US-287 highway slope, located over US-287 near the St. Paul overpass in Midlothian, Texas, was stabilized in three sections while maintaining two control sections. Denoted as Reinforced Section 1, Reinforced Section 2 and Reinforced Section 3, the 50 ft. sections were each reinforced utilizing different RPP gird patterns and spacing's to alleviate the massive settlement that was occurring due to cracks that had opened and expanded on the shoulder of the highway. Additionally, Control Section 1 and Control Section 2 were 50 ft. un-reinforced sections, though Control Section 1 was later reinforced in 2017. The field performance monitoring of the slope was performed on a monthly basis and incorporated the use of inclinometers for horizontal displacement and a topographic survey for vertical displacement or settlement,

The site investigation of the US-287 slope indicated that the slope was constructed primarily of high plastic clayey soil, therefore being susceptible to shrinking and swelling. With cracks prevalent on the shoulder of the US-287 slope, water infiltration into the slope could potentially have a preferential flow path through the cracks. Taking the site investigation into consideration, three distinct soil reinforcement grid patterns were established for the site. Reinforced Section 1 utilized a closer spacing pattern at the crest of the slope (3 ft. c/c) while Reinforced Sections 2 and 3 generally utilized a wider spacing pattern (4ft. c/c, except for Reinforced Section 3 utilizing 2 lines at the crest of 3 ft. c/c). Based on the results obtained from the topographic survey, Reinforced Section 1 experienced the least amount of incremental settlement, followed by Reinforced Section 3 and concluded with Reinforced Section 3. In terms of the inclinometer readings, the results generally performed similar, with both inclinometers

observing a reading of approximately 2 in. at the conclusion of the monitoring data presented in this study. The prevalence of cracks on the shoulder and the spacing at the crest could potentially be linked with each sections performance.

The site investigation of the I-35 slope indicated that the slope was also primarily constructed of high plastic clayey soil, therefore being susceptible to shrinking and swelling, similar to US-287. Also possessing a 3 (H): 1 (V) slope geometry, the I-35 slope was reinforced as a whole, not broken up into individual sections like US-287. Similar to US-287, the I-35 slope had observed cracking on the shoulder of the I-35 highway. The crack widened after rainfall, therefore causing swelling and later shrinking in the heat, as well as after the removal of a drilled post in the slope. The removal of the drilled post is visible in both the topographic survey measurements as well as in the inclinometers readings as a spike. While the slope was reinforced utilizing a 3 ft. c/c spacing at the crest of the slope, the section was subdivided into three separate sections based on the location of the crack. S1 was representative of the section before the crack, furthest away from the bridge abutment, followed by S2, which was the location of the excessive crack, concluded with section S3 which was the area closest to the bridge abutment. While S2 is denoted as the section that included an excessive crack, S1 and S3 still observed smaller cracks on the shoulder of the highway. It was found that the influence of the crack was observed in the incremental settlement. While S1 and S3 generally performed similar in the experienced incremental settlement, S2 saw an increase in comparison during the monitoring period. This could have potentially been observed in the data presented in Inclinometer 1, located in close proximity to the removal of the drilled post, as the cumulative displacement saw a gradual increase in successive months.

The site investigation of SH-183 slope indicated the presence of both low plastic and high plastic clay. Possessing a slope geometry of approximately 2.5 (H): 1 (V), the slope is steeper than the previous two described. Similarly utilizing a 3 ft. c/c reinforcement scheme at the crest of the slope, SH-183 experienced the highest incremental settlement the year after installation. While the section was broken into two sections, basically in half with one section being closer to the bridge abutment (S1) and one being 30 ft. from it (S2), both sections performed nearly identical. From year to year, the incremental settlement measured decreased by nearly half the next year transition. By the 2017-2018 monitoring year, all three slopes were generally performing the same, with Reinforced Section 1 of US-287 performing the best.

When interpreting the cost of each section, it was found that while SH-183 presented the lowest cost per square foot of reinforcement with RPP, US-287 as a whole saw the best value. Encompassing an area twice that of SH-183, the cost associated with the US-287 reinforcement was only 40% more in price. Regardless, the performance presented in the analyses show that RPP is a suitable reinforcement method for shallow slope stability. Therefore, based on the results obtained through years of continual research monitoring, the slope sites stabilized with RPP have shown promise to be an alternative to simply recompacting the slope as a routine maintenance for department of transportations. Additionally it provides an economic, environmental, and sustainable alternative for shallow slope stabilization and repair.

6.2 Recommendation of Future Research

The following recommendations are presented for future studies with respect to RPP.

1. Continued monitoring of sites to further analyze the performance the long-term performance of the RPP in stabilizing the slope.

2. For future sites, adding resistivity imaging at the crest of the slope might be beneficial to see the fluctuations of moisture throughout a certain depth.
3. Increased site visits to bi-weekly to better observe the variations in the settlement with the soil shrinking and swelling.

References

Abramson, L. W., Lee, T. S., Sharma, S., and Boyce, G. M. (1996). *Slope Stability and Stabilization Methods*, Wiley, New York.

Abramson, L., Lee, T., Sharma, S., and Boyce, G., (2002). Slope Stability and Stabilization Methods, John Wiley, New York, 712 p.

Ahmed, Faisal S. "Engineering Characteristics Of Recyled Plastic Pin, Lumber And Bamboo For Soil Slope Stabilization." ResearchCommons Home, Civil & Environmental Engineering, 1 Jan. 2012, rc.library.uta.edu/uta-ir/handle/10106/11638.

Bergado, D. T., Anderson, L. R., Miura, N., and Balasubramaniam, A. S. (1996). *Soft ground improvement in lowland and other environment*, ASCE, New York

Bowders, J. J., Loehr, J. E., Salim, H., & Chen, C. W. (2003). Engineering properties of recycled plastic pins for slope stabilization. Transportation Research Record: Journal of the Transportation Research Board, 1849(1), 39-46.

Breslin, V.T., Senturk, U., Berndt, C.C. (1998) "Long-term engineering properties of recycled plastic lumber in pier construction". *Resources, Conservation and Recycling 23* (1998), 243–258.

Bruce, D.A., Juran, I., 1997. Drilled and Grouted Micropiles: State-of-Practice Review. US Federal Highway Administration. Publication FHWA-RD-96-017, Washington, DC.

Chen, C. W., Salim, H., Bowders, J., Loehr, E., and Owen, J. (2007). "Creep Behavior of Recycled Plastic Lumber in Slope Stabilization Applications" *J. Mater. Civ. Eng.*, 19(2), 130-138

Chen, C. W., Salim, H., Bowders, J., Loehr, E., and Owen, J. (2007). "Creep Behavior of Recycled Plastic Lumber in Slope Stabilization Applications" J. Mater. Civ. Eng., 19(2), 130-138.

Day, R. W., & Axten, G. W. (1989). Surficial stability of compacted clay slopes. J. of Geotech. Engg., 115(4), 577-580.

Day, R. W. (1996). Design and Repair for Surficial Slope Failures. Practice Periodical on Structural Design and Construction, 1(3), 83-87.

Evans, D. A. (1972). Slope Stability Report. Slope Stability Committee, Department of Building and Safety, Los Angeles, CA.

Fay, L., Akin, M., & Shi, X. (2012). Cost-Effective and Sustainable Road Slope Stabilization and Erosion Control (Vol. 430). Transportation Research Board, Washington, D.C.

Gray, D.H. and Sotir, R. B. (1996). "Biotechnical and Soil Bioengineering Slope Stabilization: A Practical Guide for Erosion Control", John Wiley & Sons, New York, N.Y.

Hejazi, Sayyed Mahdi, et al. "A Simple Review of Soil Reinforcement by Using Natural and Synthetic Fibers." *Construction and Building Materials*, vol. 30, 2012, pp. 100–116., doi:10.1016/j.conbuildmat.2011.11.045.

Khan, S. (2013) "Sustainable Slope Stabilization Using Recycled Plastic Pin in Texas". Ph.D. Dissertation, The University of Texas at Arlington, Arlington, Texas

Khan, M. S., Hossain, S., Ahmed, A., and Faysal, M. (2017). "Investigation of a shallow slope failure on expansive clay in Texas." Engineering Geology, 219, 118-129.

Krishnaswamy, P., and Francini. R., (2000), "Long term durability of recycled plastic lumber in structural application", http://www.environmental-expert.com/Files/0/articles/2183/2183.pdf accessed May 22, 2013.

Lade, Poul V. "The Mechanics of Surficial Failure in Soil Slopes." *Engineering Geology*, vol. 114, no. 1-2, 5 May 2010, pp. 57–64., doi:10.1016/j.enggeo.2010.04.003.

Loehr, J. E., Bowders, J., Owen, J., Sommers, L., & Liew, L. (2000). Stabilization of slopes using recycled plastic pins. *Transportation Research Board : Transportation Research Record*, 1-8.

Loehr, J. E., and Bowders, J. J. (2007). "Slope stabilization using recycled plastic pins – phase III", Final Report: RI98-007D, Missouri Department of Transportation, Jefferson City, Missouri

Loehr, J. E., and Bowders, J. J. (2007). "Slope Stabilization using Recycled Plastic Pins – Phase III", Final Report: RI98-007D, Missouri Department of Transportation, Jefferson City, Missouri.

Loehr, J. E., Fennessey, T. W., & Bowders, J. J. (2007). Stabilization of surficial slides using recycled plastic reinforcement. Transportation Research Record: Transportation Research Record, 1989(1), 79-87.

Lynch, J. K., Nosker, T. J., Renfree, R. W., Krishnaswamy, P., & Francini, R. (2001). Weathering effects on mechanical properties of recycled HDPE based plastic lumber. Proc. ANTEC 2001, Dallas, Texas, May 6-10.

Malcolm, G. M. (1995). "Recycled plastic lumber and shapes design and specifications." In Proc. Structures Congress (Vol. 13, pp. 2-5).

McCormick, W., and Short, R. (2006). "Cost effective stabilization of clay slopes and failures using plate piles." Proc., IAEG2006, Geological Society of London, London, 1-7

Parra, J., Loehr, J., Hagemeyer, D., and Bowders, J. (2003). "Field performance of embankments stabilized with recycled plastic reinforcement." Transportation Research Record: Journal of the Transportation Research Board, (1849), 31-38

Peron, Hervé, et al. "Desiccation Cracking of Soils." *Mechanics of Unsaturated Geomaterials*, 2013, pp. 55–86., doi:10.1002/9781118616871.ch3.

Short, R. and Collins, B.D., (2006), "Testing and Evaluation of Driven Plate Piles in Full-Size Test Slope: New Method for Stabilizing Shallow Landslides", TRB 85th Annual Meeting Compendium of Papers CD-ROM, January 22-26, Washington D.C.

Saleh, A A, and S G Wright. *Shear Strength Correlations and Remedial Measure Guidelines for Long-Term Stability of Slopes Constructed of High Plastic Clay Soils*. 1997, pp. 1–156, *Shear Strength Correlations and Remedial Measure Guidelines for Long-Term Stability of Slopes Constructed of High Plastic Clay Soils*.

Skempton, A W. "Residual Strength of Clays in Landslides, Folded Strata and the Laboratory." *Geotechnique*, vol. 22, no. 4, 1985, p. 111., doi:10.1016/0148-9062(85)92980-8.

Sun, Shu-Wei, et al. "Design Method for Stabilization of Earth Slopes with Micropiles." *Soils and Foundations*, vol. 53, no. 4, 29 July 2013, pp. 487–497., doi:10.1016/j.sandf.2013.06.002.

Tamrakar, Sandip. "Slope Stabilization and Performance Monitoring of I-35 and SH-183 Slopes Using Recycled Plastic Pins." *The University of Texas at Arlington* , 2015.

Taquinio, F. and Pearlman, S.L. (1999). "Pin Piles for Building Foundations," presented at the 7th Annual Great Lakes Geotechnical and Geoenvironmental Conference, Kent, Ohio, May 10.

Titi, H., & Helwany, S. (2007). Investigation of Vertical Members to Resist Surficial Slope Instabilities (No. WHRP 07-03). Wisconsin Department of Transportation, Madison, WI.

Turner, John P., and Wayne G. Jensen. "Landslide Stabilization Using Soil Nail and Mechanically Stabilized Earth Walls: Case Study." *Journal of Geotechnical and Geoenvironmental Engineering*, vol. 131, no. 2, 2005, pp. 141–150., doi:10.1061/(asce)1090-0241(2005)131:2(141).

U.S. Department of Agriculture (USDA), (1992). Natural Resources Conservation Service, National Engineering Handbook, Part 650, Engineering Field Handbook, Chapter 18, "Soil Bioengineering for Upland Slope Protection and Erosion Reduction," USDA, Washington, D.C.,

Wu, Jason Y., et al. "Remediation of Slope Failure by Compacted Soil-Cement Fill." *Journal of Performance of Constructed Facilities*, vol. 31, no. 4, 15 Feb. 2017, p. 04017022., doi:10.1061/(asce)cf.1943-5509.0000998.

Zeng, Zhao Tian, et al. "Wetting-Drying Effect of Expansive Soils and Its Influence on Slope Stability." *Applied Mechanics and Materials*, vol. 170-173, 2012, pp. 889–893., doi:10.4028/www.scientific.net/amm.170-173.889.5